

# ICRR *ANNUAL REPORT*

APRIL 2004 – MARCH 2005

Institute for Cosmic Ray Research  
University of Tokyo



**INSTITUTE**  
**FOR**  
**COSMIC RAY RESEARCH**  
**UNIVERSITY OF TOKYO**

**ANNUAL REPORT**  
**(APRIL 2004 – MARCH 2005)**

## **Editorial Board**

TAKEUCHI, Yasuo

MIYOKI, Shinji

©**Institute for Cosmic Ray Research, University of Tokyo**

5-1-5, Kashiwanoha, Kashiwa, Chiba 277-8582 Japan

Telephone: (81)4-7136-3102

Facsimile: (81)4-7136-3115

WWW URL: <http://www.icrr.u-tokyo.ac.jp>

Printed by  
Universal Academy Press, Inc.

Postal Address: C.P.O. Box 235, Tokyo 100-91, JAPAN  
Address for Visitors: BR-Hongo-5 Bldg., 6-16-2, Hongo,  
Bunkyo-ku, Tokyo 113, JAPAN

Telephone: + 81 3 3813 7232

Facsimile: + 81 3 3813 5932

E-Mail: [general@uap.co.jp](mailto:general@uap.co.jp)

WWW URL: <http://www.uap.co.jp>

# TABLE OF CONTENTS

Preface	
Research Divisions	1
Neutrino and Astroparticle Division	
High Energy Cosmic Ray Division	
Astrophysics and Gravity Division	
Observatories and a Research Center	40
Norikura Observatory	
Akeno Observatory	
Kamioka Observatory	
Research Center for Cosmic Neutrinos	
Appendix A. ICRR International Workshops	49
Appendix B. ICRR Seminars	50
Appendix C. List of Publications — 2004 fiscal year	51
(a) Papers Published in Journals	
(b) Conference Papers	
(c) ICRR Report	
Appendix D. Doctoral Theses	55
Appendix E. Public Relations	55
(a) ICRR News	
(b) Public Lectures	
(c) Visitors	
Appendix F. Inter-University Researches	57
Appendix G. List of Committee Members	58
(a) Board of Councillors	
(b) Executive Committee	
(c) Advisory Committee	
Appendix H. List of Personnel	59

## PREFACE

Starting from April 2004, Japanese national universities have become independent corporations and were set up outside of the government organizations. We therefore are supposed to have much more autonomy. However the new mechanism of the budget allocation from the government to the universities is inadequate to initiate big and long term scientific projects to be conducted in the universities. It is also known to be difficult to increase the number of scientific staffs for the long term programs. A new contrivance for the budget allocation from the government is urgently needed in order to keep activities in basic science in Japanese universities and institutions.

The Institute for Cosmic Ray Research, the inter-university institute, is closely associated with Japanese universities and foreign institutes. The experimental facilities located at the institute are jointly established and used by about 350 physicists. We hope that we will continue to keep good collaborations and to keep providing important results on cosmic rays physics and related subjects although the university system has been drastically changed.

The institute has been re-organized into three research divisions; Neutrino and Astroparticle Division, High Energy Cosmic Ray Division, and Astrophysics and Gravity Division. In each division, a few different experiments are conducted.

The next big project of the institute is the gravitational wave detector (LIGO), by which the direct detection of the gravitational wave (GW) is aimed. The detection of the GW will prove the correctness of the Einstein's theory of general relativity and can provide the details of the dynamic feature of the universe.

The study of the cosmic ray had often played a leading role when the particle physics had made a significant development. The pions and muons were discovered in the cosmic rays and those discoveries had brought a fruitful study of the elementary particles using particle accelerators. The discovery of the neutrino mass has again brought a triumph to the cosmic ray research and it has opened up a new field.

At Kamioka underground observatory, the Super-Kamiokande experiment is continuously producing interesting results. There are some other projects in Kamioka, for example, dark matter experiments and geo-physics experiments, which make use of advantages of the underground environments. The construction of the prototype gravitational wave antenna is also in progress.

In 2003, the long-awaited Telescope Array project has been approved and its construction has begun. The existence of the highest energy cosmic rays beyond the ZGK cut-off indicated by the AGASA group is a big puzzle. If it is confirmed, it may suggest a new physics. There is a steady flow of data from the experiment at Yangbajing (Tibet), and from the cosmic gamma-ray telescope (CANGAROO) deployed over the desert of Woomera (Australia).

The underground physics and the ground based cosmic ray measurements overseas are the back-born of the institute.



Yoichiro Suzuki,  
Director of ICRR



Fig. 1. The ICRR building at Kashiwa, Chiba, Japan.

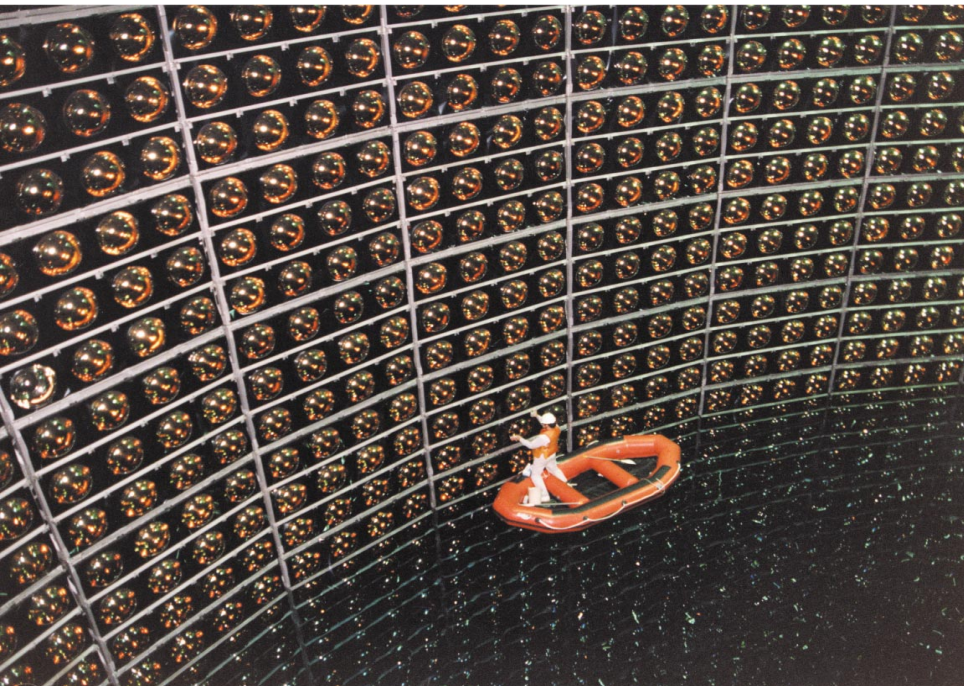


Fig. 2. The inner detector of Super-Kamiokande-I during the initial construction. The purified water is under filling. One can clearly see the 20-inch diameter photomultiplier tubes and a person working on a boat.



Fig. 3. The system of four imaging atmospheric Cherenkov telescopes of 10 m diameter of CANGAROO project for detection of very high energy gamma-rays. The whole system is in operation since March 2004 in Woomera, South Australia..



Fig. 4. Tibet-III air shower array (37000 m<sup>2</sup>) at Yangbajing, Tibet (4300 m in altitude).

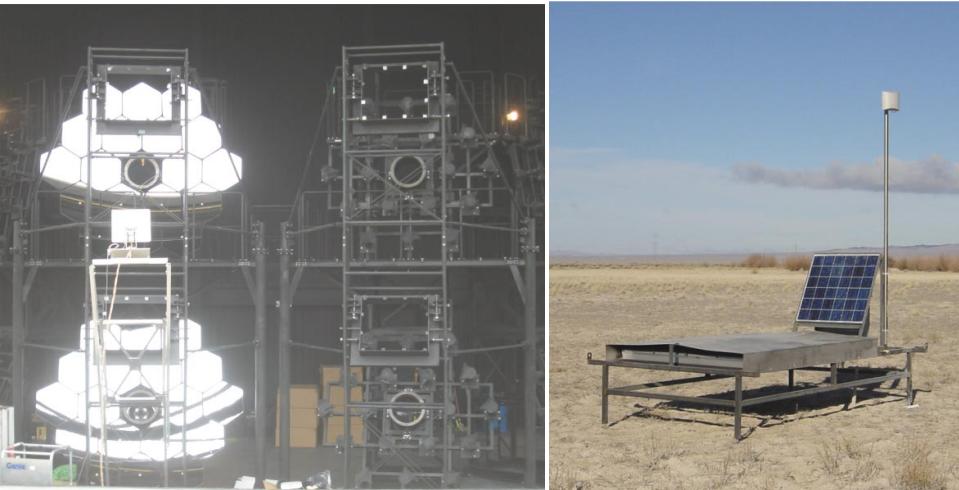


Fig. 5. Air fluorescence telescopes (left) and a scintillator surface detector (right) of the Telescope Array experiment under construction in Utah, USA for the study of extremely high energy cosmic rays.

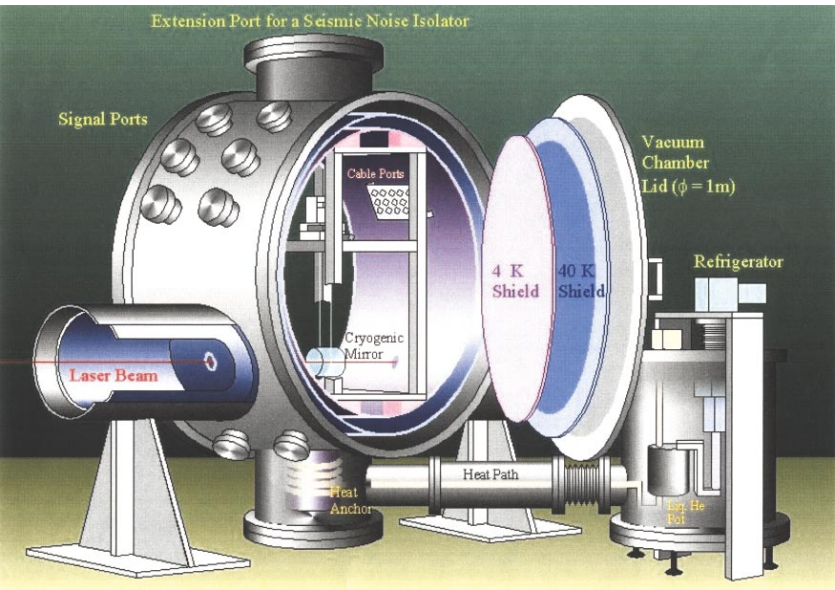


Fig. 6. Cryogenic mirror suspension system for Large Scale Cryogenic Gravitational Wave Telescope.



Fig. 7. Wide-view telescope of 2.5 m diameter (left telescope) in Arizona, USA for the Sloan Digital Sky Survey project.

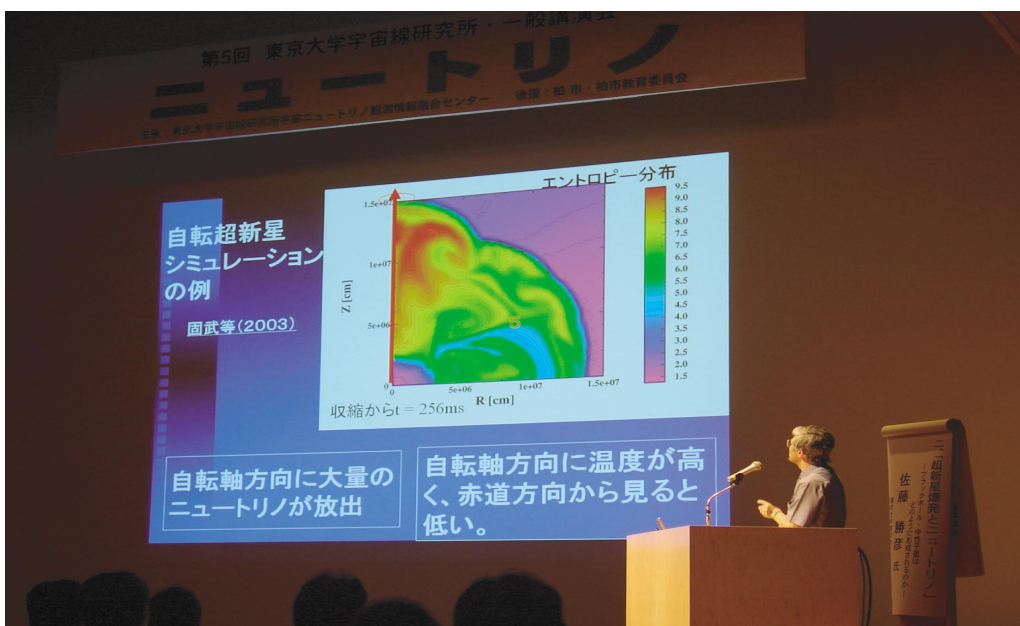
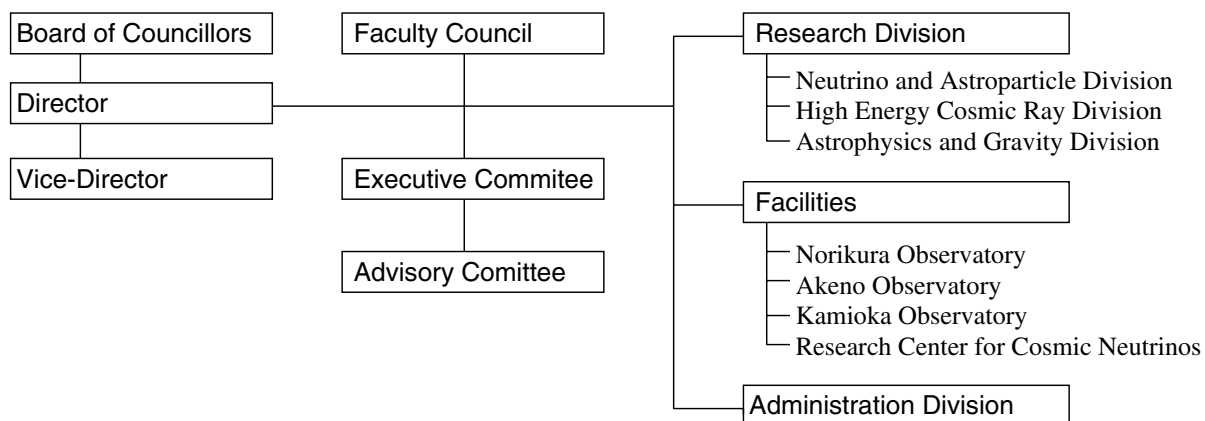


Fig. 8. A public lecture held by Research Center for Cosmic Neutrinos.

## Organization



### Number of Staff Members in 2004

	Professor	Associate Professor	Research Associate	Technical Staff	Research Fellows	Administrators and Secretaries	
	Neutrino and Astroparticle Div.	3	4	7	3	8	
High Energy Cosmic Ray Div.	2	5	6	13	17	3	46
Astrophysics and Gravity Div.	3	3	2	1	8	0	17
Administration	0	0	0	0	0	11	11
<b>Total</b>	<b>8</b>	<b>12</b>	<b>15</b>	<b>17</b>	<b>33</b>	<b>22</b>	<b>107</b>

### FY 1999–2004 Budget

	1999	2000	2001	2002	2003	2004
Personnel expenses	569 050	589 879	418 475	460 332	434 874	444 498
Non-personnel expenses	1 411 063	1 423 789	1 518 584	1 518 065	1 785 449	2 054 950
<b>Total</b>	<b>1 980 113</b>	<b>2 013 668</b>	<b>1 937 059</b>	<b>1 978 397</b>	<b>2 220 323</b>	<b>2 499 448</b>

(in 1 000 yen)

# RESEARCH DIVISIONS

## Neutrino and Astroparticle Division

### Overview

**Super-Kamiokande Experiment**

**K2K Experiment**

**XMASS Experiment**

## High Energy Cosmic Ray Division

### Overview

**CANGAROO-II & -III Project**

**Study of the Most Energetic Cosmic Rays — AGASA Collaboration**

**Seeking for an Origin of Super-GZK Events — Telescope Array Experiment**

**Experimental Study of High-energy Cosmic Rays by the Tibet Air Shower Array  
in the Tibetan Highlands (The Tibet AS $\gamma$  Collaboration)**

**Development of Wide Angle High Resolution Detector**

**Chacaltaya Observatory of Cosmic Physics**

## Astrophysics and Gravity Division

### Overview

**TAMA Project**

**LCGT Project**

**Construction of CLIO at Kamioka**

**Sloan Digital Sky Survey**

**Theory Group**

**Implications of the Curvaton on Inflationary Cosmology**

**Spacetime Symmetries on the Supermanifolds**

**EWIMP Dark Matter Detections**

**Significant Effects of the Second KK Particles on LKP Dark Matter Physics**

**Hadronic Electric Dipole Moments in Supersymmetric Grand Unified Theories**

**Big-Bang Nucleosynthesis and Hadronic Decay of Long-Lived Massive Particles**

# NEUTRINO AND ASTROPARTICLE DIVISION

## Overview

The Neutrino and Astroparticle division consists of Kamioka Observatory and Research Center for Cosmic Neutrinos (RCCN) and performs neutrino physics and astroparticle physics. Kamioka Observatory is located at Kamioka, Hida-shi, Gifu prefecture. The observatory has underground experimental sites at 1000 m underground and research facilities on the ground.

The main experiment at Kamioka Observatory is Super-Kamiokande (SK). The SK detector was built from 1991 to 1995 and data taking was started in 1996. In 1998, the SK collaboration announced the discovery of neutrino oscillations using atmospheric neutrinos. Another evidence for neutrino oscillations was found in 2001 using solar neutrinos by comparing solar neutrino data from SK and SNO. The SK detector has been used as the far detector of the artificial neutrino beam experiment (K2K) performed from 1999 and neutrino oscillation was confirmed in 2002. After the discovery of neutrino oscillations, detailed studies of neutrino oscillations have been performed at SK. In the analysis of atmospheric neutrinos, oscillation parameters, oscillation mode (whether  $\nu_\mu$  oscillates to  $\nu_\tau$  or  $\nu_{sterile}$ ) and  $L/E$  dependence of oscillation have been studied. In the solar neutrino analysis, oscillation parameters has been determined in 2002 and now searching for energy spectrum distortion and day/night time variation expected from the obtained solution. SK has been monitoring neutrinos from supernova burst. If a supernova burst occurs at the distance to the center of our galaxy, SK is able to detect about 8,000 neutrino events. SK is also searching for nucleon decay as the direct evidence of Grand Unified Theories. A high intensity neutrino beam experiment using J-PARC (T2K) is expected to start in 2009 and SK detector will be the far detector of the experiment. High precision measurement of oscillation parameters and the third oscillation pattern (from the third neutrino mass eigenstate to the first eigenstate) will be investigated by T2K.

Another activity of the Neutrino and Astroparticle division is a multi-purpose experiment using liquid xenon aiming at the detection of cold dark matter, neutrino absolute mass using neutrinoless double beta decay, and low energy solar neutrinos. An R&D study for the liquid xenon detector is being performed at Kamioka observatory.

Recent progress of research activities in the Neutrino and Astroparticle division is presented.

## Super-Kamiokande Experiment

[Spokesperson : Yoichiro Suzuki]

Kamioka Observatory, ICRR, Univ. of Tokyo, Gifu, 506-1205

In collaboration with the members of:

Kamioka Observatory, ICRR, Univ. of Tokyo, Japan; RCCN, ICRR, Univ. of Tokyo, Japan; Boston Univ., USA; BNL,

USA; Univ. of California, Irvine, USA; California State Univ., Dominguez Hills, USA; Chonnam National Univ., Korea; Duke Univ., USA; George Mason Univ., USA; Gifu Univ., Japan; Univ. of Hawaii, USA; Indiana Univ., USA; KEK, Japan; Kobe Univ., Japan; Kyoto Univ., Japan; LANL, USA; Louisiana State Univ., USA; Univ. of Maryland, USA; Univ. of Minnesota, USA; Miyagi Univ. of Education, Japan; SUNY, Stony Brook, Japan; Nagoya Univ., Japan; Niigata Univ., Japan; Okayama Univ., Japan; Osaka Univ., Japan; Seoul National Univ., Japan; Shizuoka Seika College, Japan; Shizuoka Univ., Japan; Sungkyunkwan Univ., Korea; Tohoku Univ., Japan; Univ. of Tokyo, Japan; Tokai Univ., Japan; Tokyo Inst. of Tech., Japan; Inst. of Experimental Physics, Poland; Univ. of Washington, USA.

## Introduction

Super-Kamiokande(SK) is a large water Cherenkov detector, located 1000 m underground in Kamioka mine, Japan. 50 kton of pure water is contained in a stainless steel tank of 39.3 meters in diameter and 41.4 m in height. SK took data from April 1996 to July 2001 (SK-I phase) using 11,146 20-inch photomultipliers(PMTs) for inner detector and 1,885 8-inch PMTs for outer detector. After the accident in November 2001, the detector was reconstructed in 2002 using about 5200 20-inch PMTs. The detector has been running as the second phase of the experiment(SK-II) since December 2002.

In this report, those results are described.

## Atmospheric neutrinos

Cosmic ray interactions in the atmosphere produce neutrinos. The prediction of the absolute flux has an uncertainty of at least  $\pm 20\%$ . However, the flavor ratio of the atmospheric neutrino flux,  $(\nu_\mu + \bar{\nu}_\mu)/(\nu_e + \bar{\nu}_e)$ , has been calculated to an accuracy of better than 5%. Another important feature of atmospheric neutrinos is that the fluxes of upward and downward going neutrinos are expected to be nearly equal for  $E_\nu > (\text{a few GeV})$  where the geomagnetic effect on primary cosmic ray is negligible.

SK-I observed 12,180 fully-contained (FC) events and 911 partially-contained (PC) events during 1489 days of data taking. FC events deposit all of their Cherenkov light in the inner detector, while PC events have exiting tracks which deposit some Cherenkov light in the outer detector. The neutrino interaction vertex was required to have been reconstructed within the 22.5 kiloton fiducial volume, defined to be  $> 2$  m from the PMT wall.

The FC events were classified into "sub-GeV" ( $E_{vis} < 1330$  MeV) and "multi-GeV" ( $E_{vis} > 1330$  MeV) samples. The numbers of observed and predicted events for sub- and multi-GeV energy regions in SK are summarized in Table 1. The prediction is based on the recent precise measurements of

Table 1. Summary of the atmospheric  $(\mu/e)_{data}/(\mu/e)_{MC} (\equiv R)$  ratio measurement.

	Data	MC
Sub-GeV		
$e$ -like	3353	2879.8
$\mu$ -like	3227	4212.8
$R = 0.658 \pm 0.016 \pm 0.035$		
Multi-GeV		
$e$ -like	746	680.5
$\mu$ -like(FC+PC)	1562	2029.5
$R = 0.702^{+0.032}_{-0.030} \pm 0.101$		

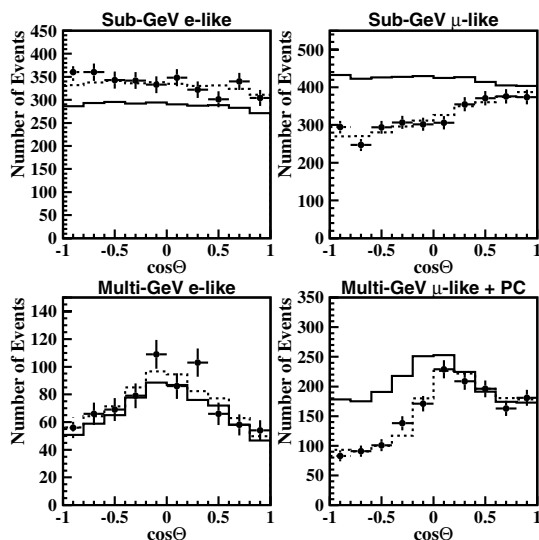


Fig. 1. The zenith angle distributions for sub-GeV  $e$ -like, sub-GeV  $\mu$ -like, multi-GeV  $e$ -like and multi-GeV (FC+PC)  $\mu$ -like events.  $\cos\Theta = 1$  means down-going particles. The solid histograms show the MC prediction for the no neutrino oscillation case. The dashed histograms show the Monte Carlo prediction for  $\nu_\mu \leftrightarrow \nu_\tau$  oscillations with  $\sin^2 2\theta = 1.0$  and  $\Delta m^2 = 2.1 \times 10^{-3} \text{eV}^2$ .

primary cosmic rays by BESS and AMS and a three dimensional calculation of the neutrino flux by Honda et al. The hadronic interaction model of cosmic rays is also improved in the calculation.

Among FC events, single-ring events are identified as  $e$ -like or  $\mu$ -like based on a Cherenkov ring pattern. All the PC events were assigned to be multi-GeV  $\mu$ -like. Using the number of  $e$ -like and  $\mu$ -like events, the ratio of  $(\mu/e)$  was obtained and it is significantly smaller than the expectation as shown in the table.

The zenith angle distributions for the sub- and multi-GeV samples are shown in Fig. 1. The  $\mu$ -like data from SK exhibited a strong up-down asymmetry in zenith angle ( $\Theta$ ) while no significant asymmetry was observed in the  $e$ -like data. The data were compared with the Monte Carlo expectation without neutrino oscillations and the best-fit expectation for  $\nu_\mu \leftrightarrow \nu_\tau$  oscillations. The oscillated Monte Carlo reproduced well the zenith angle distributions of the data. Some fraction of the multi-ring events is also subdivided into  $e$ -like and  $\mu$ -like

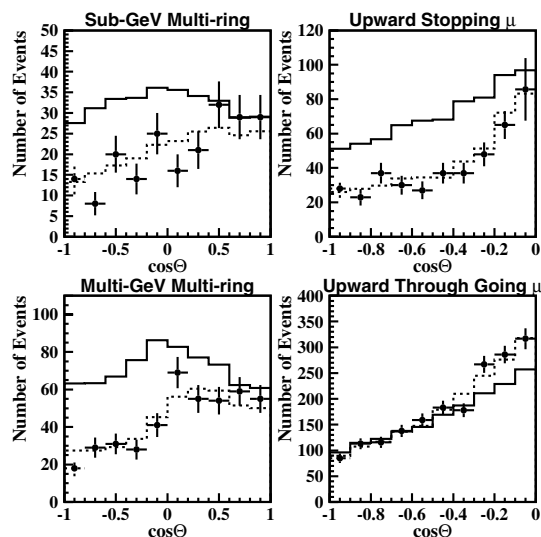


Fig. 2. The zenith angle distributions for multi-ring sub-GeV  $\mu$ -like (upper left) and multi-ring multi-GeV  $\mu$ -like (lower left) samples. The zenith angle distributions of upward stopping muons (upper right) and upward through-going muons (lower right). The solid histograms show expectations without neutrino oscillations. The dashed histograms show the expected flux for the  $\nu_\mu \leftrightarrow \nu_\tau$  oscillation with  $\sin^2 2\theta = 1.0$  and  $\Delta m^2 = 2.1 \times 10^{-3} \text{eV}^2$ .

events using the event pattern of the most energetic Cherenkov ring in each event. Fig. 2 shows the zenith angle distribution of multi-ring events and they also agree well with the expectations from neutrino oscillations.

Energetic atmospheric  $\nu_\mu$ 's passing through the Earth interact with rock surrounding the detector and produce muons via charged current interactions. These neutrino events are observed as upward going muons. Upward going muons are classified into two types. One is ‘‘upward through-going muons’’ which have passed through the detector, and the other is ‘‘upward stopping muons’’ which come into and stop inside the detector. The mean neutrino energies of upward through-going muons and upward stopping muons are  $\sim 100$  GeV and  $\sim 10$  GeV, respectively. SK has observed 1856 upward through-going muons and 458 upward stopping muons during 1646 days’ live time. Fig. 2 shows the zenith-angle distributions of those upward muons. They agree with the expectations assuming neutrino oscillations.

We carried out a neutrino oscillation analysis using the entire SK-I atmospheric neutrino data. Fig. 3 shows the allowed neutrino oscillation parameter regions for  $\nu_\mu \leftrightarrow \nu_\tau$  oscillations. The best fit oscillation parameters are  $\sin^2 2\theta = 1.0$  and  $\Delta m^2 = 2.1 \times 10^{-3} \text{eV}^2$ . The allowed oscillation parameter range is obtained to be  $\sin^2 2\theta > 0.92$  and  $\Delta m^2 = (1.5 - 3.4) \times 10^{-3} \text{eV}^2$  at 90% C.L. [1].

The atmospheric neutrino data is well described by the neutrino oscillations shown above. In this case, the survival probability of  $\nu_\mu$  is given by a sinusoidal function of  $L/E$ , where  $L$  is the travel distance,  $E$  is the neutrino energy. However, the sinusoidal  $L/E$  dependence of the survival probability of  $\nu_\mu$  has not yet been directly observed. We used a selected sample of these atmospheric neutrino events, those with good resolution in  $L/E$ , to search for an oscillation max-

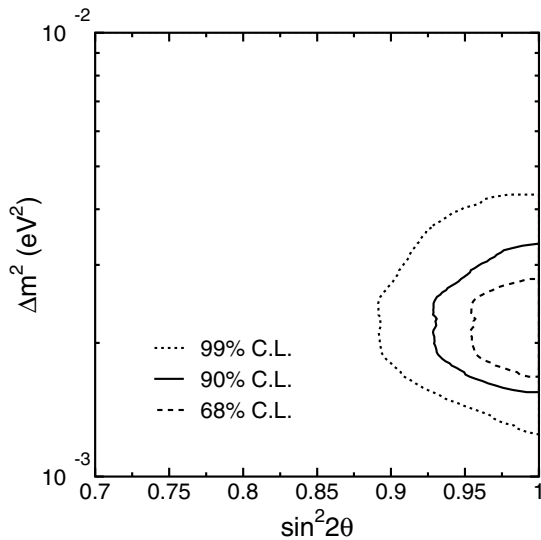


Fig. 3. Allowed region of  $\nu_\mu \rightarrow \nu_\tau$  neutrino oscillation parameters obtained by SK by using contained atmospheric neutrino events and the upward-going muon events.

imum in the  $L/E$  distribution.

The neutrino energy,  $E$ , was estimated from the total energy of charged particles observed in the inner detector. The flight length of neutrinos,  $L$ , which ranges from approximately 15 km to 13,000 km depending on the zenith angle, was estimated from the reconstructed neutrino direction. The neutrino direction was taken to be along the total momentum vector from all observed particles. Since the correlation between neutrino directions and the directions of observed particles are taken into account in Monte Carlo simulations, we applied same analysis both for real events and Monte Carlo events. We applied a cut to reject low energy or horizontal-going events since they have either large scattering angles or large  $dL/d\Theta_{\text{zenith}}$ .

Fig. 4 shows the observed  $L/E$  distribution after taking ratio to the Monte Carlo events without neutrino oscillations. In the figure, a dip, which should corresponds to the first oscillation maximum, is observed around  $L/E = 500 \text{ km/GeV}$ . The distribution was fit assuming  $\nu_\mu \leftrightarrow \nu_\tau$  oscillations. The best-fit expectation shown in the figure corresponds to  $(\sin^2 2\theta, \Delta m^2) = (1.00, 2.4 \times 10^{-3} \text{ eV}^2)$ . Fig. 5 shows the contour plot of the allowed oscillation parameter regions. The result is consistent with that of the oscillation analysis using zenith angle distributions. The observed  $L/E$  distribution gives the first direct evidence that the neutrino survival probability obeys the sinusoidal functions as predicted by neutrino flavor oscillations [2].

Another interest is an observation of  $\nu_\tau$  in the atmospheric neutrinos since there has not been apparent evidence for the appearance of  $\nu_\tau$  charged current interactions due to  $\nu_\mu \leftrightarrow \nu_\tau$  oscillations. We have performed a search for the  $\nu_\tau$  appearance by using the SK-I atmospheric neutrino data. The analysis is based on two statistical methods: a likelihood analysis and a neural network. Since  $\tau$ 's produced in the Super-K detector would immediately decay into many hadrons, the event pattern would be similar to that of high-energy multi-ring  $\nu_e$

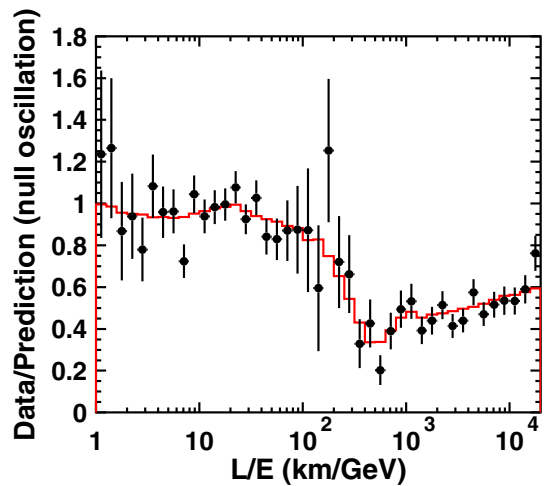


Fig. 4. Ratio of the data to the MC events without neutrino oscillation (points) as a function of the reconstructed  $L/E$  together with the best-fit expectation for 2-flavor  $\nu_\mu \leftrightarrow \nu_\tau$  oscillation (solid line). The error bars are statistical only.

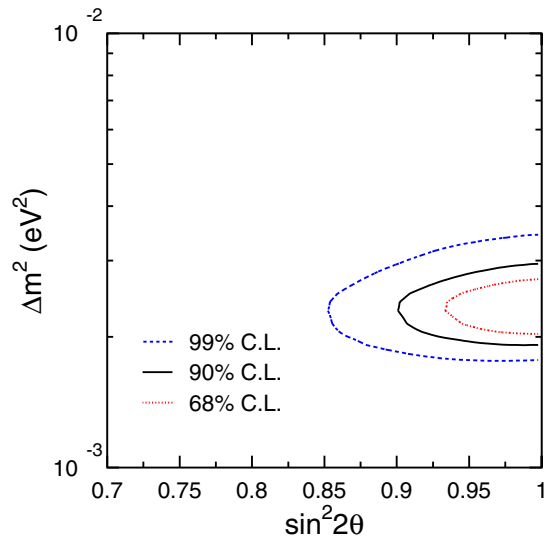


Fig. 5. 68, 90 and 99% C.L. allowed oscillation parameter regions for 2-flavor  $\nu_\mu \leftrightarrow \nu_\tau$  oscillations obtained in the  $L/E$  analysis.

events. Using the statistical difference in  $\tau$ -like and background events, we have derived the variables to select an enriched sample of  $\nu_\tau$  charged current events in the atmospheric neutrino data. The differences appear in the energy spectrum, the number of charged pions in the final state, the fraction of lepton energy with respect to neutrino energy and so on. We optimized a combination of the variables and defined a likelihood function so that the signal to noise ratio becomes the maximum. We also use the neural network for the analysis. Before these analyses, we applied a pre-selection: (1) fiducial events, (2) multi-GeV, and (3) the most energetic ring is  $e$ -like.

After the pre-selection and cuts based on the likelihood and neural network, we fit the zenith angle distribution of a  $\nu_\tau$  enriched sample to a combination of the expected  $\nu_\tau$  and the atmospheric neutrinos ( $\nu_\mu$  and  $\nu_e$ ) including oscillations with the oscillation parameter,  $\sin^2 2\theta = 1.0$  and  $\Delta m^2 = 2.1 \times$

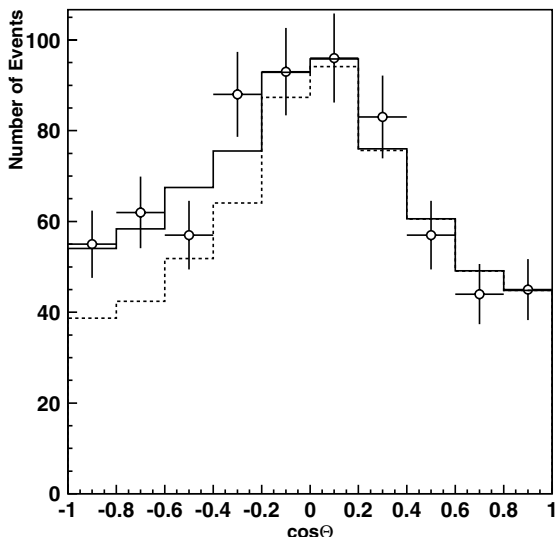


Fig. 6. The zenith angle distribution for tau candidate events in the likelihood analysis. The dashed histogram (background neutrinos) and the solid line (excess by  $\nu_\tau$ ) show the best fit for the data.

$10^{-3}\text{eV}^2$ . Fig. 6 shows the fitted zenith angle distribution. Using  $\tau$  selection efficiencies estimated by Monte Carlo study, we concluded the number of tau events with SK-I exposure is  $155 \pm 50^{+12}_{-72}$  for the likelihood analysis and  $155 \pm 50^{+0}_{-53}$  for the neural network while  $79 \pm 30$  and  $79 \pm 29$  are expected for each analysis. Thus the fitted results are found to be consistent with pure  $\nu_\mu \leftrightarrow \nu_\tau$  oscillations and  $\nu_\tau$  appearance.

The two flavor neutrino oscillations successfully described the SK-I atmospheric neutrino data. However, any contributions by electron neutrinos have not been observed yet. We extended our neutrino oscillation analysis in order to treat three neutrino flavors. For the analysis,  $\Delta m_{23}^2 \sim \Delta m_{13}^2 \equiv \Delta m^2 \gg \Delta m_{12}^2$  was assumed. If the parameter  $\theta_{13}$  in the mixing matrix of lepton sector (MNS matrix) is finite, neutrino oscillations among  $\nu_\mu \leftrightarrow \nu_e$  may be observed. Moreover, the mixing parameter is affected by potentials caused by matter and oscillations are expected to have a resonance around 5 GeV. Therefore, we can expect an increase at upward-going Multi-GeV  $e$ -like samples. Fig. 7 shows the result of the three-flavor neutrino oscillation analysis. Though there was no significant excess of electrons, we set an upper limit on  $\theta_{13}$ . More statistics is needed to have better sensitivity.

Atmospheric neutrino events are being accumulated during SK-II. A preliminary analysis has already shown the distortion of the zenith angle distribution and consistency with SK-I results.

## Solar neutrinos

The observed flux by the solar neutrino experiments (Homestake, Kamiokande, Super-Kamiokande, Gallium experiments, and SNO charged current) were lower than the expectations from the Standard Solar Model (SSM), which has been known as ‘‘solar neutrino problem’’. The precise measurements of solar neutrinos by SK and SNO established that the solar neutrino problem is due to neutrino oscillations.

SK detects  $^8\text{B}$  solar neutrinos through neutrino-electron

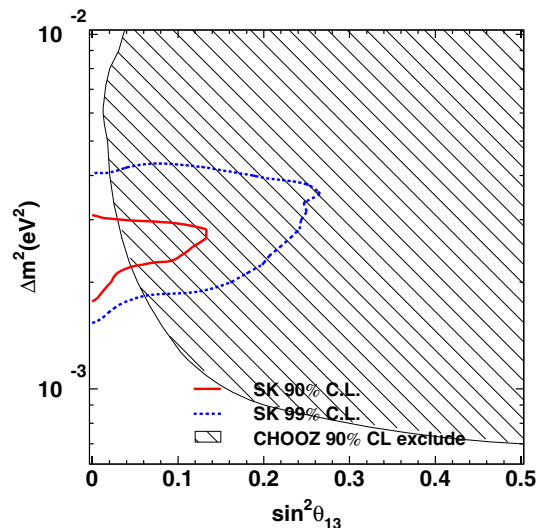


Fig. 7. The allowed region for  $(\Delta m^2, \sin^2 \theta_{13})$ . We assumed positive  $\Delta m^2$ . The solid and dotted contours correspond to allowed regions obtained by this analysis. The hatched region corresponds to 90% C.L. excluded area by CHOOZ experiment.

scattering,  $\nu + e \rightarrow \nu + e$ . The electron energy, direction and the time of the events are measured. The  $\nu + e \rightarrow \nu + e$  method of the solar neutrino detection is sensitive not only to  $\nu_e$  but also to  $\nu_\mu$  and  $\nu_\tau$ . The cross section of  $\nu_\mu + e$  and  $\nu_\tau + e$  scatterings are about  $\frac{1}{7}$  of the  $\nu_e + e$  cross section.

In order to perform precise solar neutrino measurement, the energy scale, the energy resolution, the angular resolution and the vertex position resolution were precisely calibrated using LINAC system and  $^{16}\text{N}$  events generated by a DT neutron generator. The absolute energy scale was calibrated with an accuracy of  $\sim 0.6\%$ .

SK-I has observed about 22,400 solar neutrino events above 5 MeV during 1496 days of live time from May 1996 to July 2001. This number corresponds to the  $^8\text{B}$  solar  $\nu$  flux of  $2.35 \pm 0.02$  (stat.)  $\pm 0.08$  (sys.)  $\times 10^6 \text{ cm}^{-2} \text{ s}^{-1}$ , which is  $40.6 \pm 0.4$  (stat.)  $^{+1.4}_{-1.3}$  (sys.)% of the BP04 SSM prediction. Sudbury Neutrino Observatory (SNO) observes solar neutrinos by using the charged current (CC), neutral current (NC) interactions, and electron scattering (ES). The CC flux, to which only  $\nu_e$  contributes, was  $1.68^{+0.10}_{-0.11} \times 10^6 \text{ cm}^{-2} \text{ s}^{-1}$  from the 391-day Salt Phase SNO data set. Figure 8 shows flux of  $\nu_e$  and  $\nu_\mu + \nu_\tau$  obtained by SK flux, SNO CC flux and SNO NC flux. The measured total neutrino flux was consistent with the SSM prediction as shown in the figure. It also indicated a non-electron type neutrino flux, though all the solar neutrinos should be generated in electron type. This comparison of the flux results between SK and SNO was initially done in 2001 when the first SNO data was published, then this comparison became the first strong experimental evidence of the solar neutrino oscillation among active neutrinos.

The measured energy spectrum and day/night difference in SK-I were used to constrain neutrino oscillation parameters. We have adopted a binning free method for day/night variation. Since the direction of the sun is precisely known by the time of each event, the expected oscillation probab-

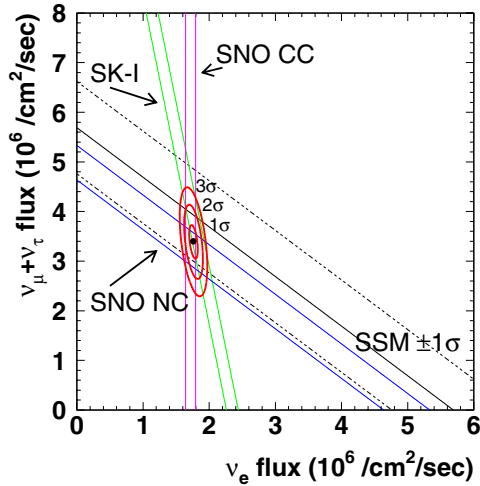


Fig. 8.  $\nu_e$  flux and  $\nu_\mu + \nu_\tau$  flux contour obtained by SK and SNO data.

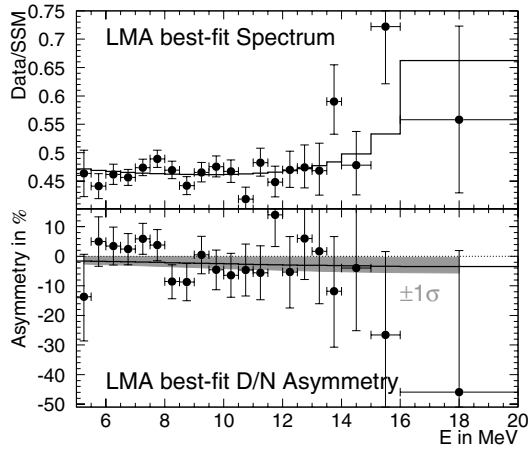


Fig. 9. SK-I energy spectrum compared with the expected Spectrum from LMA(top) and D/N Asymmetry (bottom). The predictions (solid lines) are for  $\tan^2 \theta = 0.55$  and  $\Delta m^2 = 6.3 \times 10^{-5} \text{eV}^2$  with  $\phi_{8B} = 0.96 \text{SSM}$  and  $\phi_{hep} = 3.6 \text{SSM}$ . The gray bands are the  $\pm 1\sigma$  ranges corresponding to the fitted value over the entire range 5-20 MeV:  $A = -1.8 \pm 1.6\%$ .

ity through the earth can be calculated on an event by event basis. Using a maximum likelihood method to accommodate this day/night variation and combining the energy spectrum shape information, we have done the new oscillation analysis. The energy range of the solar neutrino spectrum is divided into 21 energy bins and the day/night asymmetry value for each energy bin is shown in Fig.9. Assuming the total  $^8\text{B}$  flux predicted by SSM, the best fit oscillation parameters in the LMA region is obtained at  $\tan^2 \theta = 0.55$  and  $\Delta m^2 = 6.3 \times 10^{-5} \text{eV}^2$ . Using the expected energy and time dependence of the event rate, a fitted day/night asymmetry value is obtained to be  $-1.8 \pm 1.6(\text{stat})_{-1.2}^{+1.3}(\text{syst})\%$  using the binning free maximum likelihood method. It is statistically improved from the simple day/night difference described above. The obtained day/night asymmetry value is consistent with the expected asymmetry of  $-2.1\%$  for the best fit oscillation parameters.

Figure 10 shows results of oscillation analysis. The dark

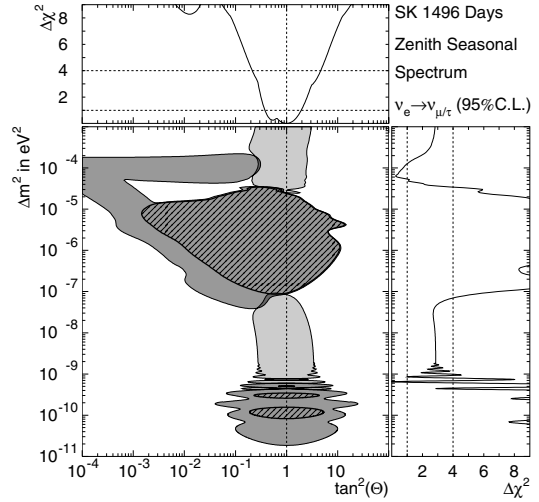


Fig. 10. Dark gray region shows the excluded region by SK-I spectrum and time variation analysis. The light gray region shows an allowed region assuming SSM flux prediction. Overlaid are the areas excluded just by the day/night and seasonal variation (hatched regions inside thick black lines). The graphs at the top (and right) show the  $\chi^2$  difference as a function of  $\tan^2 \theta$  ( $\Delta m^2$ ) along where the  $\Delta m^2$  ( $\tan^2 \theta$ ) is chosen to minimize  $\chi^2$ .

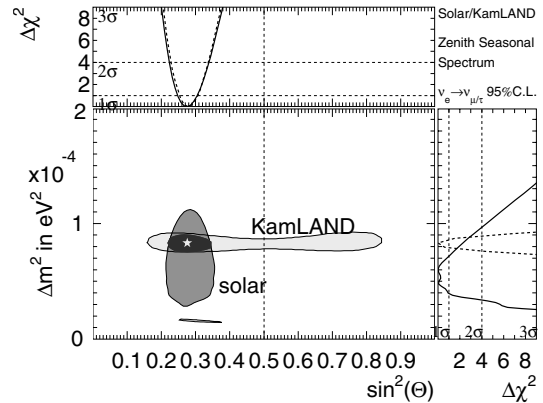


Fig. 11. Allowed areas at 95% C.L. of all the solar data and KamLAND. The combined area and the best-fit point are also shown. The graphs at the top (and right) show the  $\chi^2$  difference as a function of  $\sin^2 \theta$  ( $\Delta m^2$ ) only.

gray region in the figure shows an excluded region by SK spectrum and time variation without using absolute flux. The light gray region shows an allowed region assuming SSM prediction. Taking into account the results of other solar neutrino experiments, a global oscillation analysis is performed. The combined fit to SK data and all the solar neutrino experiments shows that only the LMA region remains as the allowed region.

Figure 11 shows the allowed regions from all the solar neutrino experiments and KamLAND. The obtained allowed region by the global solar neutrino analysis overlaps quite well with the reactor  $\bar{\nu}_e$  oscillation results from KamLAND.

An extensive study to obtain the solar neutrino flux below 5.0 MeV in SK-I was done in this year. In this energy region, the main reason why these events weren't used so far, was a

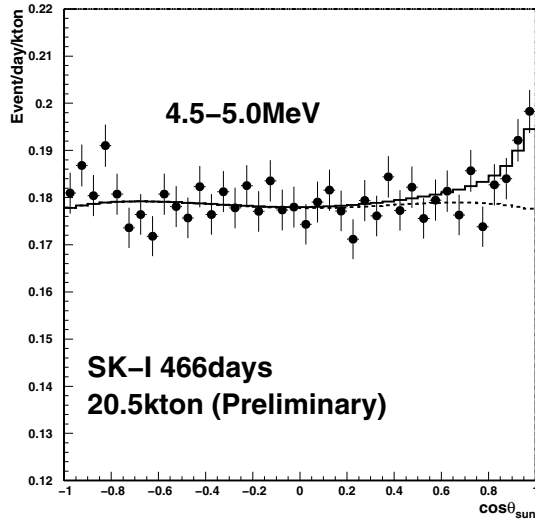


Fig. 12. Angular distribution of the special data sample below 5.0 MeV in SK-I. The dashed line is expected background shape in this analysis. The solid line is the best-fit.

high background level. Therefore, we have selected very stable and high trigger efficiency run periods, then applied new analysis tools to reject the remaining very low-energy background events. The live time and energy threshold of this analysis were 466 days and 4.5 MeV, respectively. Figure 12 shows the angular distribution of this special data sample between 4.5 MeV and 5.0 MeV. We obtained a clear signal in this energy region. The observed number of events were  $629+128-126(\text{stat.})$  events. This correspond to the  $^8\text{B}$  solar neutrino flux of  $3.13 \pm 0.63(\text{stat.})$ .

In this year, we also obtained the preliminary results from SK-II. The run period for this analysis was from Dec. 24, 2002 up to Oct. 1, 2004. The total live time in this period was 478 days. The analysis energy threshold was 8.0 MeV. The obtained solar neutrino flux was  $2.45 + 0.08 - 0.07(\text{stat.}) \times 10^6 \text{ cm}^{-2} \text{ s}^{-1}$ . This was consistent with the SK-I result. The systematic errors are under studying. The measured day-time and night-time fluxes are  $2.44 + 0.11 - 0.11(\text{stat.})$  and  $2.35 + 0.11 - 0.10(\text{stat.})$ , respectively. These are also consistent with SK-I. The preliminary energy spectrum was also obtained. Figure 13 shows the energy spectrum from the SK-II 478 days data. There was no significant distortion.

## Search for nucleon decay

Proton decays and bound neutron decays (nucleon decays in general) is a most dramatic prediction of Grand Unified Theories in which three fundamental forces of elementary particles are unified into a single force. Super-Kamiokande (SK) is the world largest detector to search for nucleon decays and it has accumulated data of 91.6 kt-yrs (SK-I) and 25.9 kt-yrs (SK-II) resulting in 117.5 kt-yrs data in total. Various nucleon decay modes have been looked for in the SK but we found no significant signal excess so far.

A proton decay into one positron and one neutral pion ( $p \rightarrow e^+ \pi^0$ ) is one of most popular decay mode. This decay

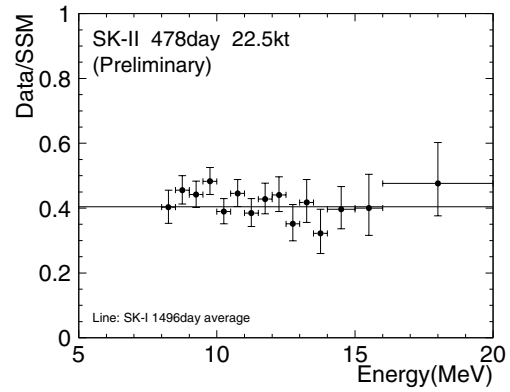


Fig. 13. Energy spectrum of the solar neutrino signal from SK-II 478 days data. The horizontal axis is the total energy of the recoil electrons. The vertical axis is the ratio of the event rates between the observation and the BP04 SSM prediction. The horizontal line shows the SK-I flux value.

mode is mediated by super-heavy gauge bosons and discovery of the signal would give us the information of the mass of the gauge mesons. To discriminate the signal from atmospheric neutrino background, we reconstruct the number of particles (Cherenkov rings) and reconstruct the total visible energy corresponding to parent proton mass and total momentum corresponding to proton's Fermi momentum. Even the photo coverage area is about half (19%) in SK-II, we achieved high detection efficiency of signals as 41% and low background levels as 0.1 events in 25.9 kt-yrs of SK-II. Because there are no candidate events in SK-I + SK-II data, we obtained lower limit on the partial lifetime of the proton,  $\tau/B_{p \rightarrow e^+ \pi^0} > 6.9 \times 10^{33}$  years at a 90% confidence level.

Moreover, we looked for SUSY favored decay modes which include K mesons in final state;  $p \rightarrow \bar{\nu} K^+$ ,  $n \rightarrow \bar{\nu} K^0$ ,  $p \rightarrow \mu^+ K^0$ , and  $p \rightarrow e^+ K^0$ . In  $p \rightarrow \bar{\nu} K^+$  search, we looked for 236 MeV/c monochromatic muons from the decay of  $K^+$ . Figure 14 shows the comparison between data and fitting results of muon momentum distribution for single-ring  $\mu$ -like events. We observed no excess of signal. In any other modes, there are no significant signal excess. Therefore we conclude that there is no evidence of nucleon decays and we calculated partial lifetime limits taking into account systematic uncertainties. Obtained limits are  $2.3 \times 10^{33}$ ,  $1.3 \times 10^{32}$ ,  $1.3 \times 10^{33}$ ,  $1.0 \times 10^{33}$ , years at 90% confidence level for  $p \rightarrow \bar{\nu} K^+$ ,  $n \rightarrow \bar{\nu} K^0$ ,  $p \rightarrow \mu^+ K^0$ , and  $p \rightarrow e^+ K^0$  modes, respectively. We have finalized this results using full SK-I data and submitted to a journal.

## Supernova neutrinos

Kamiokande and IMB observed neutrino burst from supernova 1987a. Those observations confirmed that the energy release by neutrinos is about several  $\times 10^{53}$  erg. Super-Kamiokande is able to detect several thousand neutrino events if it happens near the center of our galaxy.

During 1703.9 days of SK-I data taking period, there was no evidence of such supernova explosions, and the 90% C.L. upper limit on the rate of supernova explosions within 100 kpc

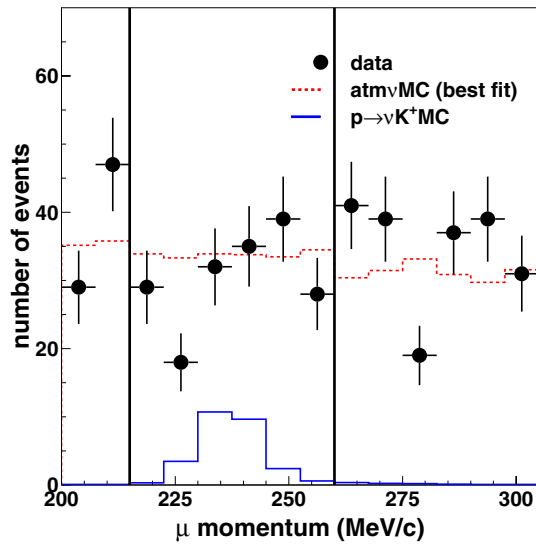


Fig. 14. The comparison between data and fitting results of muon momentum distribution for single-ring  $\mu$ -like events. The filled circles show data with statistical errors. The solid line shows  $p \rightarrow \bar{\nu}K^+$  MC. The dashed line shows the best fitted atmospheric neutrino MC with free normalization.

is obtained to be 0.49 explosions per year.

After the reconstruction of SK-II, the realtime supernova monitor system was restarted again as in SK-I. If a supernova is detected, this monitor reports it to shift persons in 5–10 minutes later. This monitor also sends a signal to SNEWS (the SuperNova Early Warning System) which takes coincidence of signals from SK, SNO, and LVD. Until now, no coincidence events were observed.

Due to the half photocoverage of SK-II, the energy threshold for the real time monitor was raised from 6.5 MeV to 8.5 MeV. However, since dominant signals of supernova neutrinos have around 15 MeV energy, the decrease of the detection efficiency is small, and SK-II still has 100% efficiency for galactic supernovae.

## Bibliography

- [1] Super-Kamiokande Collaboration, “A Measurement of Atmospheric Neutrino Oscillation Parameters by Super-Kamiokande I”, Submitted to Phys. Rev. D, hep-ex/0501064.
- [2] Super-Kamiokande Collaboration, “Evidence for an oscillatory signature in atmospheric neutrino oscillation”, Phys. Rev. Lett. 93 (2004) 101801.
- [3] K. Kobayashi *et al.* (Super-Kamiokande Collaboration), “Search for nucleon decay via modes favored by supersymmetric grand unification models in Super-Kamiokande-I”, Submitted to Phys. Rev. D, hep-ex/0502026.

## K2K Experiment

[Spokesperson : K. Nishikawa]  
Kyoto University, Kyoto 606-8502

In collaboration with the members of:

ICRR, University of Tokyo, Japan; Kyoto University, Japan; KEK, High Energy Accelerator Research Organization, Japan; Kobe University, Japan; Osaka University, Japan; Hiroshima University, Japan; Okayama University, Japan; Niigata University, Japan; Tokyo University of Science, Japan; Tohoku University, Japan; Miyagi Edu. University, Japan; Chonnam University, Korea; Seoul National University, Korea; Dongshin University, Korea; Korea University, Korea; University of California at Irvine, USA; State University of New York at Stony Brook, USA; Boston University, USA; University of Washington at Seattle, USA; Louisiana State University, USA; Massachusetts Institute of Technology, USA; University of Hawaii at Manoa, USA; Duke University, USA; TRIUMF, Canada; University of British Columbia, Canada; University of Barcelona, Spain; University of Valencia, Spain; INRM, Russia; CEA Saclay, France; University of Rome, Italy; University of Geneva, Swiss; University of Warsaw, Poland; A. Soltan Institute for Nuclear Studies, Poland

The discovery of the neutrino oscillation by Super-Kamiokande in 1998 has led to the conclusion that neutrino has a finite mass. The discovery implies the existence of new physics beyond the standard model of the elementary particles at a huge energy scale. Since the observed neutrino mass difference of  $\Delta m^2 \sim 3 \times 10^{-3} \text{eV}^2$  suggests the oscillation length is about a few hundred km for one GeV neutrinos, this phenomena can be experimentally tested by using the artificially created neutrino beam with the detector placed at a few hundred km away from the neutrino production point.

The k2k experiment was planned to detect such oscillation effect and to determine the oscillation parameters precisely. The neutrino beam created at KEK has a mean energy of 1.3 GeV and was sent to the Super-Kamiokande detector, 250 km west of KEK, every 2.2 seconds with the duration of 1.1  $\mu$  second. In the site of KEK, at the distance of 300 m from the target, we have prepared near detectors which mainly consist of 1 kt water Cherenkov detector, fine grained scintillation fiber detector (FGD), a lead glass calorimeter, and the muon ranger. The supplemental detectors are also placed. The ar-

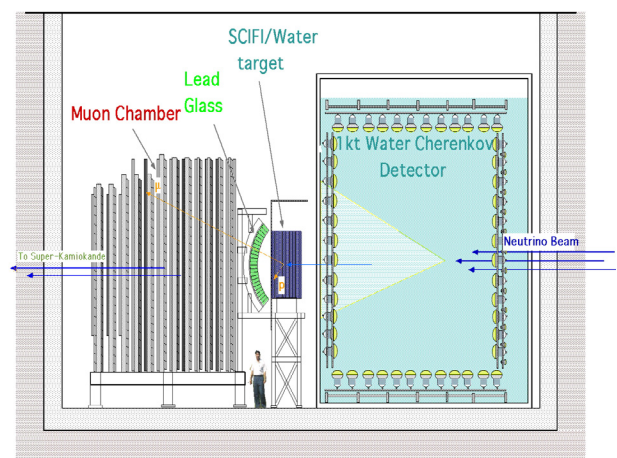


Fig. 1. The arrangement of the near detectors.

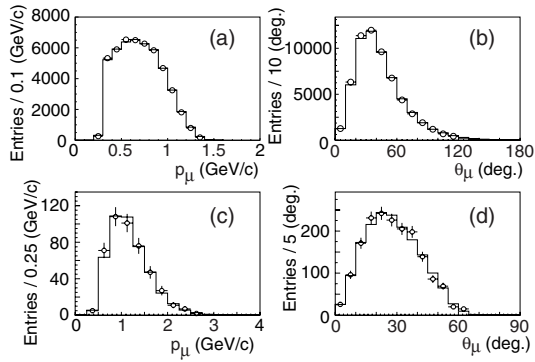


Fig. 2. Muon momentum ( $p_\mu$ ) and direction ( $\theta_\mu$ ) distributions: (a) the  $p_\mu$  distribution of 1KT fully contained 1-ring  $\mu$ -like sample, (b) 1KT  $\theta_\mu$  for the same sample, (c) SciFi  $p_\mu$  for 2-track QE sample, and (d) SciBar  $\theta_\mu$  for 2-track nonQE sample. Open circles represent data, while histograms are MC predictions using the best fit systematic uncertainties.

rangement of the front detectors at the beginning of the experiment is shown in Fig. 1. We have analyzed data taken from June 1999 to February 2004, which corresponds to  $8.9 \times 10^{19}$  protons on target (POT). The near detector data from this period include  $2.3 \times 10^{19}$  POT without the lead glass (K2K-IIa), and then  $1.9 \times 10^{19}$  POT (K2K-IIb) with a fully-active scintillator detector (SciBar) in its place.

There are several beam monitors, proton profile monitors, the muon monitor and the pion monitor, placed along the neutrino beam line. The decay length is about 200 m, therefore the beam is not scaled exactly by  $1/r^2$  law. The flux ratio of the near to the far detector was obtained by the beam Monte Carlo calculation by taking into account of the spread and emittance of the beam at the target, the production of the pions, the focusing effect by the HORN and the decay of pions to neutrinos. The beam calculation was validated by the pion monitor which measured the produced pion directions and momentum.

The beam flux and the spectrum were measured by the front detectors. ICRR group has a responsibility of providing the Super-Kamiokande data and the construction of the 1 kt front detector and the analysis of the data from those detector components. The coverage of PMT in the 1 kt front detector is same as the Super-Kamiokande detector with the 40% of the total inner detector surface. The 1kt detector provides information of the absolute neutrino flux and the spectrum of the neutrino beam. Figure 2 shows (a) the muon momentum spectrum and (b) the muon direction by using the single ring fully contained events at 1 kt detector. The observed spectrum is well reproduced by the Monte Carlo simulation in which beam energy spectrum and neutrino interaction in water are taken into account. Combining the 1 kt data and FGD data together with constraint of the pion monitor measurement, the expected neutrino energy spectrum was obtained for the far detector. All the systematic errors due to detector bias or uncertainty of neutrino interactions were carefully taken into account.

The synchronization of the timing between KEK 12 GeV Proton Synchrotron and Super-Kamiokande detector was performed using a GPS system. Figure 3 shows the timing distribution of the fully contained events observed at Super-

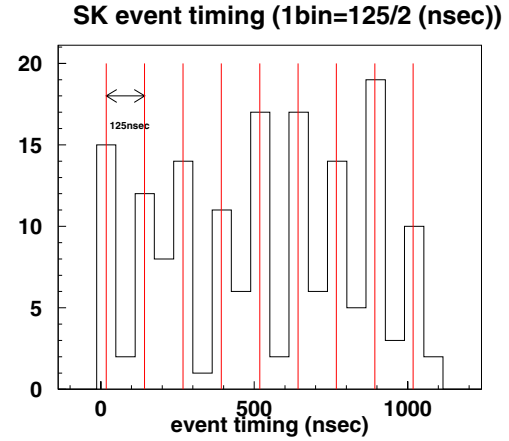


Fig. 3. The timing distribution of fully contained event observed at Super-Kamiokande with respect to the beam injection timing. Periodical structure coming from proton beam bunches is seen in the Super-Kamiokande, 250 km away from the accelerator.

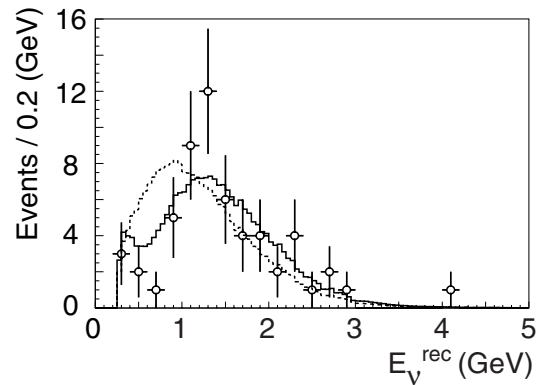


Fig. 4. The reconstructed  $E_\nu$  distribution from single ring fully contained events at SK. Points with error bars are data. The solid line is the best fit spectrum. The dashed line shows the expected spectrum without oscillation. Both histograms are normalized by the number of events observed(57).

Kamiokande with respect to the proton beam injection timing. The time of flight of neutrinos from KEK to Super-Kamiokande ( $\sim 830 \mu$  sec) is corrected in the figure.

Neutrino events were clearly observed near  $\Delta T=0$  and the spread in the timing was consistent with the duration of beam injection at KEK 12 GeV PS. In total, 107 events were identified as K2K beam induced events at Super-Kamiokande. Using the large number of observed neutrino events at front detectors, expected number of neutrino events at Super-Kamiokande was calculated to be  $151^{+12}_{-10}$ (syst) assuming no-oscillation.

57  $\mu$ -like single ring events were observed and the neutrino energy spectrum obtained from the energy and scattering angle of the observed muons is shown in Fig. 4. From the deficit of observed number of events together with the shape distortion of neutrino energy spectrum, we have concluded that probability of null oscillation is 0.0050% ( $4.0\sigma$ ). The allowed region of  $\Delta m^2$  and  $\sin^2 2\theta$  is shown in Fig. 5. The obtained result for neutrino oscillation parameters are consistent

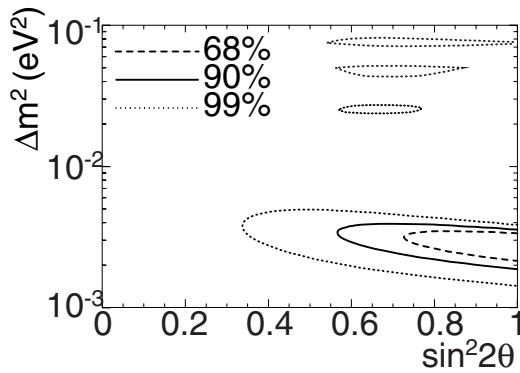


Fig. 5. Allowed regions of  $\nu_\mu$ - $\nu_\tau$  oscillation parameters. Dashed, solid and dot-dashed lines are 68.4%, 90% and 99% C.L. contours, respectively.

with that from atmospheric neutrino oscillations.

K2K is expected to finalize physics results using full K2K data in near future including  $\nu_\mu$  disappearance,  $\nu_e$  appearance, and detailed neutrino interaction studies.

## Bibliography

- [1] K2K collaboration, Detection of accelerator produced neutrinos at a distance of 250 km, *Phys. Lett. B*, 511, 178–184, 2001.
- [2] K2K collaboration, Indication of neutrino oscillation in a 250 km long baseline experiment, *Phys. Rev. Lett.*, 90, 041801, 2003.
- [3] K2K collaboration, Search for Electron Neutrino Appearance in a 250 km Long-baseline Experiment, *Phys. Rev. Lett.*, 93, 051801, 2004.
- [4] K2K collaboration, Measurement of single  $\pi^0$  production in neutral current neutrino interactions with water by a 1.3 GeV wide band muon neutrino beam, *submitted to Phys. Lett. B*, hep-ex/0408134.
- [5] K2K collaboration, Evidence for muon neutrino oscillation in an accelerator-based experiment *submitted to Phys. Rev. Lett.*, hep-ex/0411038.

## XMASS Experiment

[Spokesperson : Yoichiro Suzuki]

Kamioka Observatory, ICRR, Univ. of Tokyo, Gifu, 506-1205

In collaboration with the members of:

Kamioka Observatory, ICRR, Univ. of Tokyo, Japan; RCCN, ICRR, Univ. of Tokyo, Japan; Waseda Univ., Japan; Yokohama National Univ., Japan; Miyagi Univ. of Education, Japan; Nagoya Univ., Japan; Saga Univ., Japan; Gifu Univ., Japan; Seoul National Univ., Korea; INR-Kiev, Russia; Univ. of California, Irvine, USA; Sejon Univ., Korea.

## Overview

XMASS is a multi-purpose experiment using liquid xenon aiming at the detection of cold dark matter, neutrino absolute mass using neutrinoless double beta decay, and low energy solar neutrinos. An R&D study for the liquid xenon detector is being performed at Kamioka observatory.

Astronomical observations suggest that there is “dark matter” (non-luminous particles with mass) in the universe. One of the most likely candidates for dark matter is a weakly interacting massive particle (WIMP) like the lightest supersymmetry particle. A recoil of xenon by dark matter produces scintillation light in liquid xenon.

The Super-Kamiokande measurements show that neutrinos have masses. However, we do not know yet the absolute mass of neutrinos and the whether neutrino masses are Majorana type or Dirac type. Xenon nuclei with mass number 136 is one of the double beta nuclei which is best suited for this research.

The solar neutrino spectrum is measured only above 5 MeV by SK and SNO so far. The spectrum of low energy solar neutrinos ( $pp$  and  ${}^7\text{Be}$  neutrinos and etc.) are not measured yet. If a 10-ton class liquid xenon detector is constructed, it will be able to detect those neutrinos by  $\nu+e$  scattering with a rate of about 10 events/day.

Liquid xenon has the following advantages:

- A large light yield of 42,000 photons/MeV, which is as good as NaI(Tl) scintillator, enables detection of small energy signals like dark matter recoil.
- Because of the higher atomic number of xenon ( $Z=54$ ) and higher density of liquid xenon ( $\sim 3\text{g/cm}^3$ ), external gamma-ray background can be reduced in a short distance from the detector wall by self-shielding.
- 175 nm scintillation light of liquid xenon can be read out by typical PMTs of bi-alkaline photocathode with a quartz window.
- Purification is easier than other materials (e.g. distillation is possible).
- Isotope separation is possible. It is possible to enrich  ${}^{136}\text{Xe}$  for double beta decay and deplete  ${}^{136}\text{Xe}$  for solar neutrino measurements.

A 3 kg fiducial volume liquid xenon detector has been developed for the R&D study and test data was taken in 2003 and 2004.

We plan to make an 800 kg detector (Fig.1) aiming to search for dark matter down to  $10^{-45} \sim 10^{-44}\text{cm}^2$  in cross section which is more than two orders of magnitude better than the current best limits in the world.

## R&D study by a 3 kg fiducial volume detector

Figure 2 shows the 30 liter (3 kg fiducial volume) liquid xenon detector developed for the R&D study. It is a 30 cm cubic detector viewed by 54 2-inch PMTs. The PMTs are Hamamatsu R8778 which were developed by collaborating with Hamamatsu and can be used for low background purposes and also can be used at liquid xenon temperature ( $\sim 170\text{K}$ ). The detector is placed in a low background setup which consists of 5 cm-thick pure copper (OFHC), EVOH sheets, 15 cm-thick

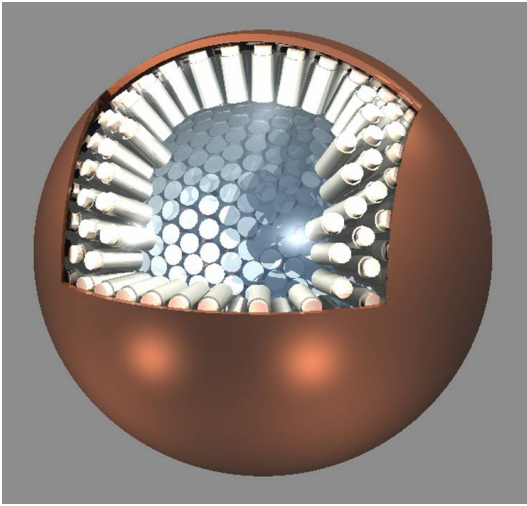


Fig. 1. Schematic view of the proposed 800 kg liquid xenon detector aiming at dark matter search. The detector has a sensitivity of  $10^{-45} \sim 10^{-44} \text{cm}^2$  in cross section which is more than two orders of magnitude better than the current best limits in the world.



Fig. 2. 3 kg fiducial volume liquid xenon detector constructed for R&D study

lead, 10 cm-thick boric acid, and 15 cm-thick polyethylene for reducing gamma rays, neutron and radon backgrounds.

Test data was taken in December 2003 and August 2004. Figure 3 shows the background distributions for the latest measurement. The large reduction of backgrounds in a smaller detector volume is observed at several hundreds keV, which demonstrates self-shielding of the detector. The reduction of backgrounds is as expected by Monte Carlo simulations.

As the internal source of backgrounds,  $^{85}\text{Kr}$  in xenon is one of potential sources. In order to purify xenon, a test distillation system was constructed which is able to process 0.6 kg Xe/hour and achieve better than 1/1000 reduction in krypton concentration. In March 2004, we processed original xenon which contains 3 ppb mol/mol krypton with this distillation system and measured krypton concentration by an API-MS detector after the process. As a result, it was found that the processed xenon contains only  $3.3 \pm 1.1$  ppt mol/mol krypton and that the 1/1000 reduction had been achieved.

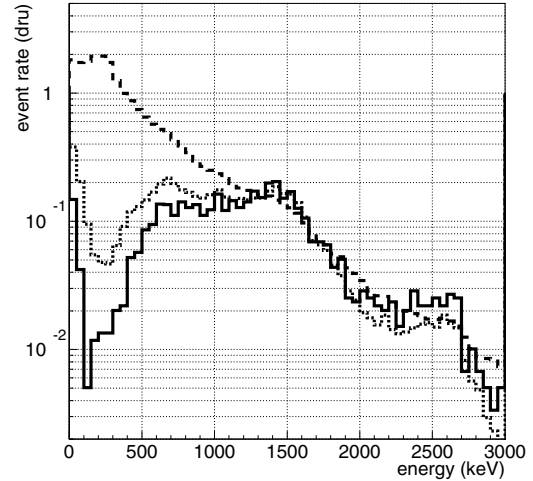


Fig. 3. Background spectrum measured by the 3 kg fiducial volume detector. The dashed, dotted and solid histograms show the rate of the events which were observed in all volume, 20 cm and 10 cm cube centered at the center of the detector, respectively.

## Bibliography

- [1] Y. Suzuki et al., "Low energy solar neutrino detection by using liquid xenon," Aug. 2000, hep-ph/0008296.
- [2] S. Moriyama, "XMASS EXPERIMENT I," proceedings of the International Workshop on Technique and Application of Xenon Detectors, Kashiwa, Japan, 3–4 Dec. 2001.
- [3] Y. Takeuchi, "Recent status of the XMASS project," presentation in the International Conference on High Energy Physics (ICHEP), Beijing, China, 16–22 Aug. 2004.
- [4] S. Moriyama, "XMASS experiment," proceedings of the International Workshop on the Identification of Dark Matter, Edinburgh, Scotland, 6–10 Sep. 2004.

# HIGH ENERGY COSMIC RAY DIVISION

## Overview

Three major research activities of the High Energy Cosmic Ray division are the study of very high energy gamma-rays by the CANGAROO group, extremely high energy cosmic rays by the Telescope Array (TA) group, and very high energy cosmic rays and gamma-rays by the Tibet AS $\gamma$  Collaboration. Other activities, such as experiments utilizing the Akeno observatory, the Norikura observatory, the Mt. Chacaltaya observatory (jointly operated with Bolivia), and the emulsion-pouring facilities are closely related to inter-university joint research programs. Also the activity for development of high resolution telescope is intensively going on.

The CANGAROO project (Collaboration of Australia and Nippon for a GAMMA-Ray Observatory in the Outback) is a set of large imaging Cherenkov telescopes to make a precise observation of high-energy air showers originated by TeV gamma-rays. It started as a single telescope with a relatively small mirror (3.8 m in diameter) in 1992. In 1999 a new telescope with a 7-m reflector has been built, and now it has a 10-m reflector with a fine pixel camera. The main purpose of this project is to explore the violent, non-thermal universe and to reveal the origin of cosmic-rays. An array of four 10-m telescopes has been completed in March 2004 so that more sensitive observation of gamma-rays is realized with its stereoscopic imaging capability of Cherenkov light. We have detected several gamma-ray sources in the southern sky and detailed study of these sources are now ongoing.

At the Akeno observatory, a series of air shower arrays of increasing geometrical sizes have been constructed and operated to observe extremely high energy cosmic rays (EHECRs). The Akeno Giant Air Shower Array (AGASA) was operated from 1991 to January 2004 and covered the ground area of 100 km<sup>2</sup> as the world largest air shower array. In 13 years of operation, AGASA observed a handful of cosmic rays exceeding the theoretical energy end point of the extragalactic cosmic rays (GZK cutoff) at 10<sup>20</sup> eV. The Telescope Array (TA), a large plastic scintillator array with air fluorescence telescopes under construction in Utah, USA, will succeed AGASA and measure the EHECRs with an order of magnitude larger aperture than that of AGASA to unveil the origin of super-GZK cosmic rays discovered by AGASA.

An air shower experiment aiming to search for celestial gamma-ray point sources started in 1990 with Chinese physicists at Yangbajing (Tibet, 4,300 m a.s.l.) and has been successful. This international collaboration is called the Tibet AS $\gamma$  Collaboration. An extension of the air shower array was completed in 1995 and an emulsion chamber has been combined with this air shower array since 1996 to study the primary cosmic rays around the knee energy region. After successive extensions carried out in 1999, 2002 and 2003, the total area of the air shower array amounts to 37,000 m<sup>2</sup>. The sun's shadow in cosmic rays affected by the solar magnetic was observed for the first time in 1992, utilizing its good an-

gular resolution at multi-TeV energy region. From this experiment with better statistics, we expect new information to be obtained on the large-scale structure of the solar and interplanetary magnetic field and its time variation due to the 11-year-period solar activities.

## CANGAROO-II & -III Project

[Spokespersons : R. W. Clay, M. Mori, and T. Tanimori]

In collaboration with the members of:

Institute for Cosmic Ray Research, University of Tokyo, Kashiwa, Chiba 277-8582, Japan: Department of Physics, Graduate School of Science, Kyoto University, Sakyo-ku, Kyoto 606-8502, Japan: RSAA, Australian National Univ., ACT 2611, Australia: Dept. of Physics, Univ. of Adelaide, SA 5005, Australia: Department of Physics, Yamagata University, Yamagata, Yamagata 990-8560, Japan: Institute of Space and Astronautical Science, Japan Aerospace Exploration Agency, Sagami-hara, Kanagawa 229-8510, Japan: Faculty of Management Information, Yamanashi Gakuin University, Kofu, Yamanashi 400-8575, Japan: Department of Physics, Tokai University, Hiratsuka, Kanagawa 259-1292, Japan: Department of Physics, Konan University, Kobe, Hyogo 658-8501, Japan: Ibaraki Prefectural University of Health Sciences, Ami, Ibaraki 300-0394, Japan: Faculty of Engineering, Shinshu University, Nagano, Nagano 480-8553, Japan: Solar-Terrestrial Environment Laboratory, Nagoya University, Nagoya, Aichi 464-8602, Japan: National Astronomical Observatory of Japan, Mitaka, Tokyo 181-8588, Japan: School of Allied Health Sciences, Kitasato University, Sagami-hara, Kanagawa 228-8555, Japan: Faculty of Science, Ibaraki University, Mito, Ibaraki 310-8512, Japan

To summarize CANGAROO-II and -III of the fiscal year 2004, three important things happened;

1. H.E.S.S.<sup>1</sup> published the confirming results to the CANGAROO-II.
2. H.E.S.S. published the conflicting results to the past CANGAROO-I.
3. The stereoscopic analysis was partially established.

We report them as follows.

### CANGAROO-II results

The result of the supernova remnant RX J1713.7-3946 [1] was confirmed by H.E.S.S. [2]. H.E.S.S. observed shell structure of this supernova remnant and the flux is consistent ( $\sim 0.7$  Crab) with our one as shown in Figure 1. The spectral index slightly differs, however, the deviation is only 2.2  $\sigma$  level. We

\*1 H.E.S.S. is the new array of four 12m-diameter Cherenkov telescopes built in Namibia by the group led by Max Planck Institute for Nuclear Physics (Germany).

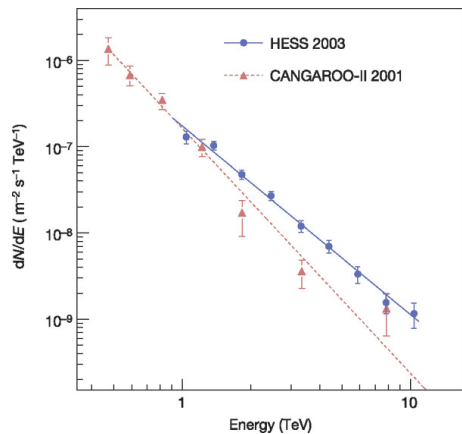


Fig. 1. Differential gamma-ray fluxes obtained by CANGAROO-II and H.E.S.S. Copied from Fig. 3 of Ref. [2].

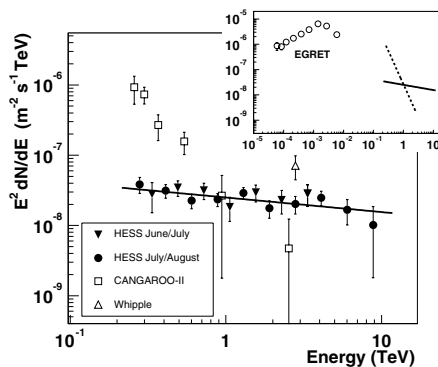


Fig. 2. Energy spectrum  $E^2 dN/dE$  of  $\gamma$ -rays from the Galactic Centre. Full circles: H.E.S.S. 'July/August 2003' data set. Full triangles: H.E.S.S. 'June/July 2003' data set. The line indicates a power-law fit to the 'July/August' spectrum. Open squares: CANGAROO-II spectrum from Summer 2001 and 2002 (Tsuchiya et al. [3]). Open triangle: Whipple flux from 1995 through 2003 (Kosack et al. [5]), converted to a differential flux at the peak detection energy assuming a Crab-like spectrum. The inset shows the EGRET flux from 1991 to 1996 (Mayer-Hasselwander et al. [6]) (circles) compared to fits to the CANGAROO-II (dashed line) and H.E.S.S. (solid line) spectra. Due to the poor angular resolution of EGRET ( $1^\circ$ ) the flux shown may include other sources. Copied from Fig. 4 of Ref. [7].

will observe this in summer of 2005 in order to investigate the spectral dependence on the shell positions using stereoscopic observation techniques.

The Galactic Center result [3, 4] was also confirmed by H.E.S.S. [7] and VERITAS [5]. The fluxes obtained by these three groups are summarized in Fig. 2. The flux level at low energy differed by one order at the lowest energy binning. We investigated our analysis, however, at present we have not found any faults in our code. The coming observation in the summer of 2005 will be awaited. Also these experimental data gave significant upper limits in the relic density of the cold dark matter of TeV mass.

The second supernova remnant RX J0852.0-4622 was revealed by CANGAROO-II [8]. The emission profile is shown in Fig. 3.

Recently and preliminary, it was confirmed by H.E.S.S. [9]. CANGAROO-III (stereoscopic system) had observed this

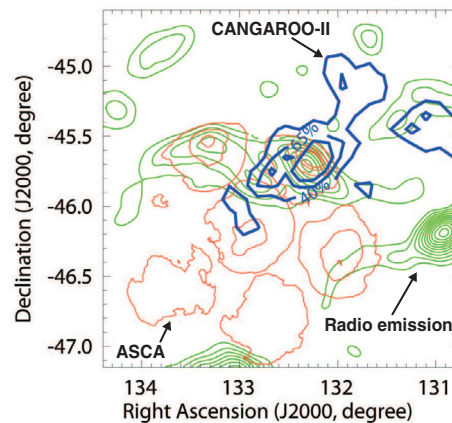


Fig. 3. The "significance map" obtained by the CANGAROO-II telescope is shown by the blue contours. The telescope tracking center is at the north-west rim of RX J0852.0-4622. The red contours with levels at 20%, 45%, 65%, and 80% are an ASCA GIS image. The green contours show the 4850 MHz radio emission.

supernova remnant in 2004 Feb. Our preliminary analysis confirmed these results. We are preparing publication on this result. The flux level is consistent with H.E.S.S.

### CANGAROO-I enigma

H.E.S.S. published two serious confictions with CANGAROO-I results [11, 10]. They are concerning with the supernova remnant SN 1006 and pulsar PSR B1706-44. The H.E.S.S.'s upper limits corresponded to 1/10 of the CANGAROO-I fluxes. CANGAROO-III had observed these two objects and obtained enough statistics. We are doing our best in order to publicize our most recent results on these two objects in the summer conferences of 2005.

### CANGAROO-III results

The CANGAROO-III stereoscopic observations started from 2003 Dec. Presently the work was concentrated on developing the calibration and analysis softwares. Also nice thing is the improvement of the camera system. By introducing the optimized-size PMT and Winston-cone light-guide, the light correction efficiency improved by a factor of two. We now can stably observe  $\mu$ 's Cherenkov rings, the radius of which is about 1.3 degrees as shown in Fig. 4. We have developed a high efficiency and clean selection of these events. After applying cuts, we can select them [12] without reducing the acceptance. These events can be used for calibration of reflectivity and spot size of mirrors. Previously, we estimated the absolute energy via using cosmic-ray rate and night sky background. With these, our measurement became more accurate and they would help in solving the differences in the absolute fluxes in between the major Cherenkov telescopes.

Using the tuned Monte-Carlo inputs, we can see the standard candle, i.e., the Crab. The angular spectrum of the Crab is shown in Fig. 5. The angular resolution is consistent with that obtained by the  $\mu$ -ring study. Also the flux is consistent with the world average. The Hillas parameter distributions are consistent with the Monte-Carlo predictions. The signal-to-noise ratio is worse compared to that of H.E.S.S. which is mainly due to the spot size deterioration of the mirror system

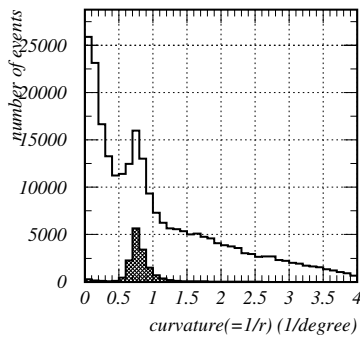


Fig. 4. Curvature (= inverse of radius) distributions for  $\mu$ -rings. The blank histogram is for all events and the hatched for the selected ones.

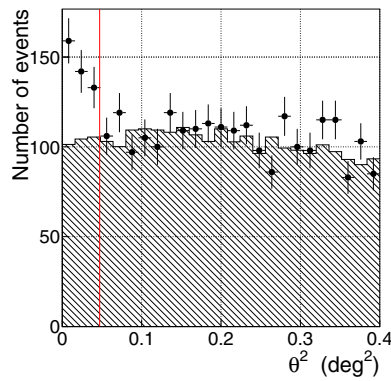


Fig. 5.  $\theta^2$  distribution for the Crab. The point with error bars are made from the signal region and the histogram from the background region. The red line is the cut position.

[13]. The alignment work is necessary in 2005.

The Galactic disk is the strongest source of gamma-rays in the GeV energy region and could be the source of TeV gamma-rays. Two regions of the Galactic disk, around  $(l, b) = (13^\circ, 0^\circ)$  and  $(-19.5^\circ, 0^\circ)$ , which are not visible by the northern telescopes, were scanned for the first time at TeV energies by the CANGAROO-III stereoscopic system. We could not find any statistically significant signals and obtained upper limits on diffuse gamma-ray flux above 600 GeV as shown in Fig. 6. We discussed the spectral index measured by EGRET using this result [14].

The giant radio galaxy Cen A, which is the nearest ( $z = 0.0018$ ) active galactic nuclei and the first claimed TeV gamma-ray source in 1975 [15], was observed by CANGAROO-III. Again we could not see any statistically significant signal and obtained upper limits as shown in Fig. 7. The limit corresponded to be 1/10 of Crab flux. These are also lower than the previous measurements by an order. The discussion of the AGN unified picture was carried out based on

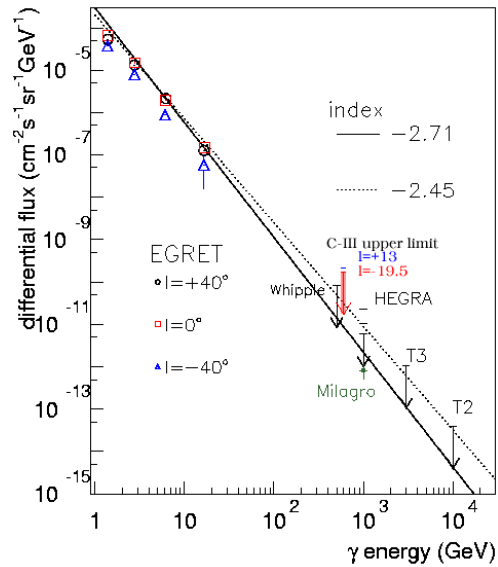


Fig. 6. Upper limit (the red arrow) for the gamma-ray emission from the Galactic Disk, together with the other wave-length data.

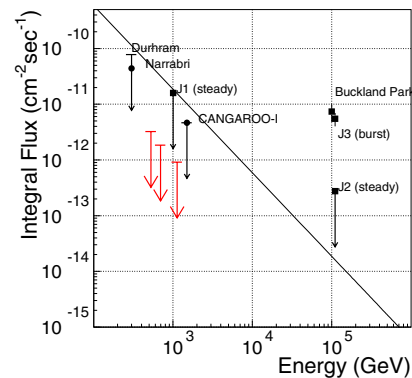


Fig. 7. Upper limits obtained for Cen-A (the red arrows), together with the previous measurements (the black). The line is the Crab flux.

this result [16].

### Prospect

We would like to publish these first results after summarizing the above-mentioned calibrations and etc. Also in the summer conference, we might open our results on SN 1006 and PSR B1706-44 based on the results of the stereo observations.

### Bibliography

[1] "The acceleration of cosmic-ray protons in the supernova remnant RX J1713.7-3946," R. Enomoto *et al.*, Nature, **416**, 823 (2002).

- [2] “High-energy particle acceleration in the shell of a supernova remnant,” F. A. Aharonian *et al.*, *Nature*, **432**, 75 (2004).
- [3] “Detection of sub-TeV Gamma-rays from the Galactic Center Direction by CANGAROO-II” K. Tsuchiya, R. Enomoto, L. T. Ksenofontov, M. Mori, and T. Naito, *et al.* [CANGAROO-II Collaboration], *Astrophys. J.* **606**, L115 (2004) [arXiv:astro-ph/0403592].
- [4] “Very High Energy Gamma-ray Observations of the Galactic Center with the CANGAROO-II Telescope,” K. Tsuchiya, Ph. D. Thesis, Univ. of Tokyo, Jan. 2005.
- [5] Kosack, K., Badran, H. M., Bond, H. I., et al. 2004, *ApJ*, 608, L97.
- [6] Mayer-Hasselwander, H. A., Bertsch, D. L., Dingus, B. L., et al., 1998, *A&A*, 335, 161.
- [7] “Very high energy gamma rays from the direction of Sagittarius A\*”, A. Aharonian *et al.*, *A&A*, **425**, L13 (2004).
- [8] “Detection of Gamma Rays around 1 TeV from RX J0852.0-4622 by CANGAROO-II,” H. Katagiri, R. Enomoto., L. T. Ksenofontov, and M. Mori *et al.* [CANGAROO Collaboration], *Astrophys. J.* **619**, L163 (2005) [arXiv:astro-ph/0412623].
- [9] “Another Shell-Type Supernova Remnant - RX J0852.0-4622,” H.E.S.S. Collaboration, <http://www.mpi-hd.mpg.de/hfm/HESS/public/som/current2.htm>
- [10] “Search for TeV emission from the region around PSR B1706-44 with the H.E.S.S. experiment,” F. Aharonian *et al.*, *A&A*, **432**, L9 (2005).
- [11] “Upper limits to the SN1006 multi-TeV gamma-ray flux from H.E.S.S. observations,” F. Aharonian *et al.*, *A&A*, in press.
- [12] Master thesis in Japanese, Y. Adachi, Univ. of Tokyo. 2005.
- [13] Master thesis in Japanese, R. Kiuchi, Univ. of Tokyo. 2005.
- [14] “Very High Energy Gamma-ray Observations of the Galactic Plane with the CANGAROO-III Telescopes,” M. Ohishi, Ph. D. Thesis, Univ. of Tokyo, Mar. 2005.
- [15] Grindlay, J. E., Helmken, H. F., Hanbury Brown, R., Davis, J., Allen, L. R. 1975, *ApJ* 201, 82.
- [16] “Observation of TeV Gamma-rays from the Active Radio Galaxy Centaurus A with CANGAROO-III Imaging Atmospheric Cherenkov Telescope,” S. Kabuki, Ph. D. Thesis, Univ. of Tokyo, Jun. 2005.

## Study of the Most Energetic Cosmic Rays — AGASA Collaboration

[Spokesperson : M. Teshima]

Max-Planck Institute for Physics, Germany

In collaboration with the members of:

Kinki University, Osaka; Yamanashi University, Kofu; Saitama University, Saitama; Musashi Institute of Technology, Tokyo; Tokyo Institute of Technology, Tokyo; Nishina Memorial Foundation, Tokyo; Hirosaki University, Hirosaki; Osaka City University, Osaka; RIKEN, Saitama; Max-Planck Institute for Physics, Germany; Ehime University, Matsuyama; Fukui University of Technology, Fukui; Communications Research Laboratory, Tokyo; National Institute of Radiological Sciences, Chiba; University of Chicago, U.S.A.; Chiba University, Chiba.

### Introduction

The AGASA is a giant air shower array covering an area of 100 km<sup>2</sup>. It has been in operation in Akeno village and its vicinity, 130 km west of Tokyo, in order to study EHECRs above 10<sup>19</sup> eV. In this energy region, distinctive features in the energy spectrum and arrival direction distribution are expected.

If the cosmic rays are of extragalactic origin, photopion production between cosmic rays and primordial microwave background photons becomes important at energies above 6 × 10<sup>19</sup> eV with a mean free path of about 6 Mpc. Therefore a cutoff in the energy spectrum is expected at around several times 10<sup>19</sup> eV, and is called Greisen-Zatsepin-Kuzmin (GZK) cutoff [3]. Cosmic rays exceeding this cutoff energy must be originated from nearby extra-galactic sources within 50 Mpc. For cosmic rays of this origin, expected arrival directions are relatively isotropic and should have some correlation with the material distribution around our galaxy; super galactic plane or clusters of galaxies.

On the other hand, if they are galactic origin, their arrival directions should have a strong correlation with the galactic structure, since the gyro-radius of protons of energy above 10<sup>19</sup> eV are comparable with the galactic scale. A study of correlations of EHECRs with the galactic structure and/or with the large scale structure of galaxies is important.

As a mechanism of producing these EHECRs, the diffusive shock acceleration is most widely accepted. Shocks at radio lobes of Active Galactic Nuclei, termination shocks in the local group of galaxies and others have been discussed to be possible sites [4]. The acceleration above 10<sup>20</sup> eV in dissipative wind models of cosmological gamma-ray burst is also proposed [5]. Since various theoretical difficulties exist in accelerating cosmic rays up to the highest observed energies, it is also discussed that these cosmic rays are possibly the decay products of some massive particles produced at the collapse and/or annihilation of cosmic topological defects which could have been formed in a symmetry-breaking phase transition in the early universe [6].

The details of the AGASA are described in Chiba et al. [1] and Ohoka et al. [2]. The array is operational since 1991, and the exposure of  $5.8 \times 10^{16} \text{ m}^2 \text{ s sr}$  above  $10^{19} \text{ eV}$  has been accumulated by the end of the AGASA operation (January 2004). Extensive air showers with zenith angles smaller than  $45^\circ$  and with core locations inside the array area were used for the analysis. In the energy range above  $10^{19} \text{ eV}$ , we only used such events that passed through an eye scan to confirm their core positions and energies.

## Energy Spectrum

In order to calculate the primary energy of giant air showers observed by AGASA, the particle density at a distance of 600 m from the shower axis ( $S(600)$ ) is used as an energy estimator, which is known to be a good parameter [7]. The conversion factor from  $S(600) [\text{m}^{-2}]$  to the primary energy  $E_0 [\text{eV}]$  is derived by simulation [8] as

$$E_0 = 2.0 \times 10^{17} \times S(600)^{1.0} \quad (1)$$

The details of determination of arrival directions and  $S(600)$  are described in Takeda et al. [10].

The differential primary energy spectrum above  $10^{18.5} \text{ eV}$  is shown in Fig. 1 [11]. The bars represent statistical errors only. The resolution of energy determination is about 25% at  $10^{20} \text{ eV}$ , which is estimated by analyzing the simulated showers. The dominant contribution of the resolution comes from the fluctuation of the shower development and the limited number of sampled particles by the scintillator. The overall systematic error in determining the energy scale of the primary cosmic ray is also analyzed by the simulation. The dominant source of the error comes from the unknown composition of the primary and the unknown cross section of the hadronic interaction at extremely high energy. It is estimated to be 18% [12].

The energy spectrum extends beyond  $10^{20} \text{ eV}$  and we observed 11 events above the GZK cutoff energy. The expected energy spectrum with the GZK cutoff is shown in Fig. 1 by the dashed curve. The expected number of events above  $10^{20} \text{ eV}$  is 1.8 taking the energy resolution of AGASA into account. The energy spectrum is therefore extending beyond  $10^{20} \text{ eV}$  without the GZK cutoff.

## Arrival Direction

### Above GZK energy

The arrival direction of the highest energy cosmic rays above  $4 \times 10^{19} \text{ eV}$  is shown in Fig. 2 [13] in the equatorial coordinates. Small circles and squares show events above  $4 \times 10^{19} \text{ eV}$  and  $10^{20} \text{ eV}$ , respectively. They appear to be distributed uniformly over the observed sky. We have carried out several tests for global anisotropy but could not find any large scale structures in this distribution. However, we found one triplet and five doublets of events clustering within  $2.5^\circ$  angular separation as indicated by shadowed circles in Fig. 2. The chance probability for creating these clustering from the uniformly distributed cosmic rays was evaluated as low as  $P_{ch} \sim 10^{-3}$ . No outstanding astronomical objects have been found in the directions of these clusters within 50 Mpc.

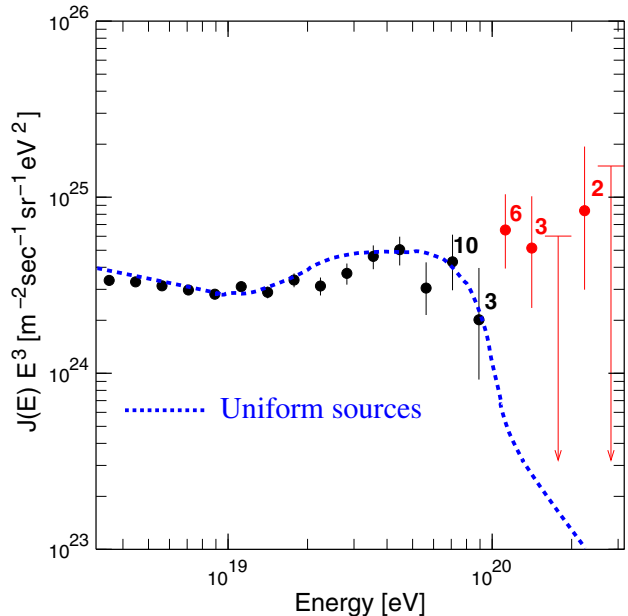


Fig. 1. The energy spectrum observed by AGASA. The vertical axis is multiplied by  $E^3$ . Error bars represent the Poisson upper and lower limits at 68% and arrows are 90% C.L. upper limits. Numbers attached to points show the number of events in each energy bin. The dashed curve represents the spectrum expected for extragalactic sources distributed uniformly in the Universe taking account of the effect of energy resolution.

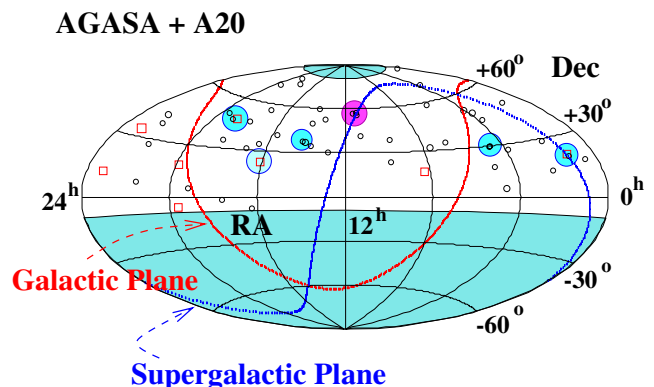


Fig. 2. The arrival direction of the highest energy cosmic rays above  $4 \times 10^{19} \text{ eV}$  in the equatorial coordinates.

In Fig. 3 [14], we show the space angle distribution between two cosmic ray events above  $4 \times 10^{19} \text{ eV}$ . We observe a clear peak at small correlation angles below  $3^\circ$ . The shape of the peak is consistent with the resolution of the angular determination of AGASA. This result suggests the existence of point like compact sources. The magnetic field in the intergalactic spaces is required to be  $\approx \text{nG}$  or less for charged particles to form these clusters.

### Anisotropy around $10^{18} \text{ eV}$

The harmonic analysis in the right ascension was carried out using about 216,000 events of cosmic rays observed by AGASA [15]. The value of  $k \sim 14$  at  $10^{18} \text{ eV}$  is seen in the

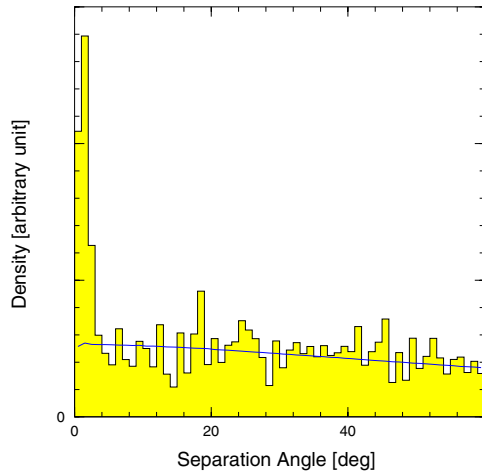


Fig. 3. The space angle distribution between two events above  $4 \times 10^{19}$  eV. We observe a clear auto-correlation within three degrees.

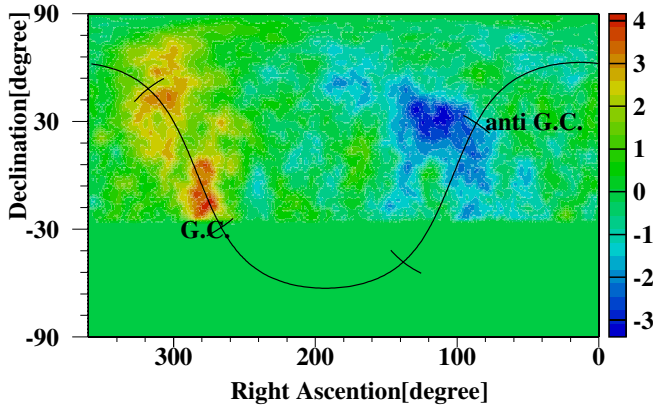


Fig. 4. The statistical significance of the deviations of the arrival direction distribution of the cosmic rays above  $10^{18}$  eV in the equatorial coordinates.

first harmonic. The phase of the maximum amplitude corresponds to 20 hr in the right ascension. The statistical significance is high, corresponding to a chance probability of  $10^{-6}$ .

In Fig. 4, the arrival direction distributions in the equatorial coordinates are shown. They show significant deviations from the expected isotropic distribution. Here, the energy region of  $10^{18}$  eV  $\sim 10^{18.4}$  eV is selected which maximize the  $k$ -value of the harmonic analysis. The AGASA is insensitive for events with declination less than  $-25^\circ$  as long as we use showers with zenith angles less than  $60^\circ$ . We have chosen a circle of  $20^\circ$  radius to evaluate the excess in Fig. 4. A  $4.5 \sigma$  excess (obs./exp. = 506/413.6) near the galactic center region can be seen in the figure. We also observe a deficit corresponding to  $-4.0 \sigma$  in the vicinity of anti-galactic center. An excess of  $3.9 \sigma$  significance (obs./exp. = 3401/3148) is seen in the Cygnus region.

## The Highest Energy Gamma Rays

The highest energy gamma ray primary is a good discriminator of EHECR origins. The top-down theories such as the decay of topological defects and super-heavy particles predict a high level of gamma ray composition whereas the bottom-up theories predict none. Since the gamma ray has less probability of generating hadronic particles, the muon content of the shower is expected to be significantly less compared to the proton or nucleus primaries. The muon density in the EHECR air showers was measured using 27 proportional counters of 2.8-10 m<sup>2</sup> area installed in the region of AGASA array. The muon density 1000 m away from the shower core was determined by fitting the lateral distribution of the muon component. The result was compared with the prediction of Monte Carlo simulations with gamma ray, proton and iron primaries. As a result, upper limits on the gamma ray fraction with 95% confidence level are determined to be 34%, 59% and 63% for cosmic rays with energies more than  $10^{19}$  eV,  $10^{19.25}$  eV and  $10^{19.5}$  eV [16].

## From AGASA to Telescope Array

AGASA had ceased taking data on January 5th, 2004 after 13 years of fruitful operation. As described in this report, its contribution to the physics of ultra-high energy cosmic ray was remarkable. The analysis using the whole data sample is now proceeding. We continue to build a succeeding experiment, Telescope Array, in order to identify the origin of cosmic rays over  $10^{20}$  eV discovered by AGASA.

## Bibliography

- [1] N. Chiba et al., *Nucl. Instrum. Methods A* **311**, 388 (1992).
- [2] H. Ohoka et al., *Nucl. Instrum. Methods A* **A372**, 527 (1997).
- [3] K. Greisen, *Phys. Rev. Lett.* **16**, 748 (1966); G. T. Zatsepin and V. A. Kuzmin, *Pisma Zh. Eksp. Teor. Fiz.* **4**, 144 (1966).
- [4] Various acceleration models are discussed in *Astrophysical Aspects of the Most Energetic Cosmic Rays*, ed. M. Nagano and F. Takahara (World Scientific, Singapore, 1990) pp. 252–334.
- [5] E. Waxman, *Phys. Rev. Lett.* **75**, 386 (1995); M. Vietri, *Ap. J.* **453**, 883 (1995); M. Milgrom and V. Usov, *Ap. J.* **449**, L37 (1995);
- [6] Recent summary and references are described in P. Bhattacharjee, *Proc. of ICRR Symp. on Extremely High Energy Cosmic Rays : Astrophysics and Future Observatories* ed. M. Nagano, (Inst. of Cosmic Ray Research, University of Tokyo., 1997) p. 125.
- [7] A. M. Hillas et al, *Proc. 12th ICRC, Hobart* **3**, 1001 (1971).
- [8] H. Y. Dai et al., *J. Phys. G: Nucl. Part. Phys.* **14**, 793 (1988).

- [9] S. Yoshida et al., *J. Phys. G: Nucl. Part. Phys.* **20**, 651 (1994).
- [10] M. Takeda et al., *Phys. Rev. Lett.* **81**, 1163 (1998).
- [11] M. Takeda et al., *Proc. 28th ICRC, Tsukuba* **1**, 381 (2003).
- [12] M. Takeda et al., *Astroparticle Phys.* **19**, 447 (2003).
- [13] M. Takeda et al., *Ap. J.* **522**, 225 (1999); *astro-ph/0008102*.
- [14] M. Teshima et al., *Proc. 28th ICRC, Tsukuba* **1**, 401 (2003).
- [15] N. Hayashida et al., *Astroparticle Phys.* **10**, 303 (1999).
- [16] K. Shinozaki et al., *Ap. J.* **571**, L117 (2002).

## Seeking for an Origin of Super-GZK Events — Telescope Array Experiment

[Spokesperson: M. Fukushima]

High Energy Cosmic Ray Div. ICRR, Univ. of Tokyo, Kashiwa, 277-8582 Chiba

In Collaboration with the members of:

Chiba University, Chiba, Japan; Communications Research Laboratory, Tokyo, Japan; Ehime University, Matsuyama, Japan; Hiroshima City University, Hiroshima, Japan; ICRR, Univ. of Tokyo, Tokyo, Japan; KEK, High Energy Accelerator Organization, Tsukuba, Japan; Kinki University, Osaka, Japan; Kanagawa University, Yokohama, Japan; Kochi University, Kochi, Japan; Montana State University, Bozeman MT, USA; Musashi Institute of Technology, Tokyo, Japan; National Institute of Radiological Sciences, Chiba, Japan; Osaka City Univ., Osaka, Japan; Rutgers University, Piscataway, New Jersey, USA; Saitama Univ., Saitama, Japan; Shibaura Institute of Technology, Saitama, Japan; Tokyo Institute of Technology, Tokyo, Japan; University of New Mexico, Albuquerque, New Mexico, USA; University of Utah, Salt Lake City, Utah, USA; Yamanashi Univ., Kofu, Japan;

## Extremely High Energy Cosmic Rays

The origin of the extremely high energy (EHE) cosmic rays is an enigma. Eleven events observed by AGASA clearly demonstrate the existence of particles above  $10^{20}$  eV in the universe. As predicted by Greisen Zatsepin and Kuzmin (GZK), such particles collide with the microwave background and quickly loses its energy by the pion photoproduction. The universe is not transparent for EHE particles, and we have to look for the origin of such particles within 50 Mpc (= GZK horizon) of our galaxy.

Powerful extragalactic objects such as the active galactic nuclei, radio galaxies and the gamma ray bursts may be suspected as the acceleration site of EHE proton or nucleus. The search for the astronomical origin in the arrival direction of the AGASA events, however, failed to find such objects within 100 Mpc of our galaxy. The origins beyond this limit may be tolerated, but only if we assume special mechanism to allow a



Fig. 1. Detector Arrangement of Phase-1 Hybrid TA.

longer propagation beyond the GZK limit, such as the violation of special relativity or the EHE neutrinos as the carrier of such energy. In addition, it is generally perceived that the astronomical acceleration above  $10^{20}$  eV is difficult to achieve.

It is fascinating to imagine that the EHE cosmic ray is generated by the decay of super-heavy elementary particles in the present universe. The energies above  $10^{20}$  eV are easily obtained if the particle mass is at the Grand Unification scale of  $10^{15}$  GeV. Such particles may be either surviving as a relic particle of the Big Bang or presently generated by the decay of topological defects. An abundant generation of EHE gamma rays and neutrinos, in place of protons and nuclei, is expected in the decay of such particles.

## Overview of the Experiment

The Telescope Array (TA) experiment is proposed to investigate the nature of super-GZK cosmic rays and draw a decisive conclusion on its origin.

In the first stage of construction, TA is a hybrid detector composed of a large plastic scintillator array and 3 sets of air fluorescence telescopes installed around the ground array and overlooking it (phase-1 Hybrid TA, see Fig. 5)[1,2,3]. The ground array will give an aperture approximately an order of magnitude larger than that of AGASA. The fluorescence telescope will cross-calibrate the shower parameters measured by the ground array by employing a direct calorimetry in the atmosphere and by imaging the shower axis and shower longitudinal development. It will also supply information on the particle species of the primary cosmic rays by measuring the depth of the shower maximum ( $X_{max}$ ). The whole detector will be installed in the West Desert of Utah, USA, about 140-mile south west of Salt Lake City.

## Hybrid TA : Ground Array

The ground detector consists of an array of 576 plastic scintillators deployed in a grid of 1.2 km spacing covering the ground area of  $\sim 760$  km<sup>2</sup> [4]. The detector acceptance is constant for cosmic rays with energies more than  $10^{19.5}$  eV entering the detector with zenith angles less than  $45^\circ$ .

The scintillation light is read out by a wave length shifter fiber of 1 mm diameter installed in a groove produced on the surface of the scintillator. One layer of the scintillation

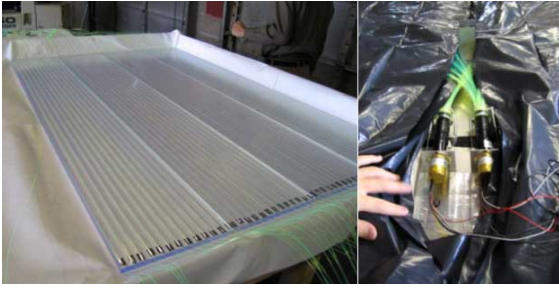


Fig. 2. Scintillation detector of TA

counter consists of two sets of 4 plates of  $150\text{ cm} \times 25\text{ cm}$  and with a thickness of  $1.2\text{ cm}$  shown in Fig. 6 and is read out by 96 fibers. The final scintillation counter is composed of two layers of  $3\text{ m}^2$ , each of which is read out by a separate PMT. A coincidence is taken between 2 layers for obtaining a stable trigger condition against environmental background and PMT noise.

The signal from the PMT will be continuously digitized with a 12-bit flash ADC with 50 MHz sampling. For a PMT signal exceeding  $1/3$  of the muon peak, a complete wave form of  $\sim 4\ \mu\text{s}$  is stored locally in a memory with a time stamp supplied by the Global Positioning System (GPS). This rate of local buffering is expected to be less than 1 kHz for the  $3\text{ m}^2$  counter. The relative timing between remotely separated counters should be maintained within  $\pm 20\text{ ns}$  by the GPS for the good resolution of arrival direction. A list of triggered events containing the pulse height and timing information of the hits is sent to a central DAQ system every second. If a trigger condition of 3 or more muons is adopted, the trigger list would contain  $\sim 100$  events. An air shower event is identified by the central DAQ software by requiring clustered hits of counters with a good timing of coincidence. The air shower event rate will be significantly less than 1 Hz when we require at least 3 counters are hit at the same time.

The data acquisition system will be composed of a wireless local area network (LAN) using 2.4 GHz spread spectrum technology. Considering a limited reach of the presently available models, two stages of data concentration will be necessary to reach the central DAQ from individual counters. The speed of less than 1 Mbps is, however, sufficient for the expected trigger rate and DAQ throughput even when 2 or more stages of data collection are necessary. Five communication towers would be needed: three for nearby telescope stations and two for the places where communication may be difficult by only three towers.

The total electrical power consumed by the PMT, ADC, GPS and LAN will be of  $\sim 5\text{ W}$ . The scintillation detector is locally generated by the solar panel of  $\sim 120\text{ W}$ , installed on top of the platform at a 60 degree angle. Behind and below the panel will be a metal enclosure containing the storage battery and electronics. A 10-foot antenna would be attached to each platform. A simple and robust counter design together with an independent GPS, wireless-LAN and local power generator will make the system easy to deploy and maintain in the



Fig. 3. A view of a TA fluorescence station in Utah.

desert.

### Hybrid TA : Fluorescence Telescope

The fluorescence measurement is made at 3 stations surrounding the ground array[5]. The stations form a triangle with a length of sides 30–40 km. Twelve reflecting telescopes are installed at each station and cover the sky of  $3^\circ - 34^\circ$  in elevation and  $108^\circ$  in azimuth looking toward the center of the ground array (see Figures 5 and 7). The stereo acceptance of the detector is  $\sim 670\text{ km}^2\text{ sr}$  for  $E > 10^{20}\text{ eV}$  by requiring at least one station is within 45 km from the shower center. The acceptance is 4 times larger than that of AGASA even assuming 10% duty factor. Approximately 60% of the events for  $E > 10^{20}\text{ eV}$  are observed by all 3 stations.

The field of view of each telescope is  $18.0^\circ$  in azimuth and  $15.5^\circ$  in elevation. The telescope has a spherical dish of 3.3 m diameter composed of 18 hexagonal segment mirrors (see Fig. 8). The focal length is 2960 mm and the spot size on the focal plane is less than the specification (20 mm) in the full width for which 90% of light is concentrated according to the measurement of the mirrors for the first telescope station. The air shower image is recorded by a camera composed of  $16 \times 16$  2-inch PMTs placed on the imaging plane (see Fig. 9). Each PMT pixel covers  $1.1^\circ \times 1.0^\circ$  patch of the night sky. The shape of the photocathode is made hexagonal for the maximum light collection efficiency. The PMT high voltage is supplied by a bleeder with zener diodes to ensure a stable gain ( $< 2\%$ ) under the variation of the night sky background, and a good linearity ( $< 5\%$ ) up to 16 k photoelectrons in 200 ns. The 8-stage PMT (Hamamatsu R6234) is operated at  $-800\text{ Volt}$  with a gain of  $\sim 10^5$ .

A signal from the PMT is amplified by a factor of 4 with a pre-amplifier and is sent to a Stretcher Amplifier by a factor of 2 and a 12-bit ADC with 40 MHz sampling in a Signal Digitizer and Finder (SDF) module. The digitized four successive signals are summed and sent to a data buffer, which is adopted to cover a dynamic range corresponding to  $\sim 32\text{ K}$  photoelectrons with the aid of an analog sum of 16 channels with the gain of  $1/16$ . The digitized signal is further fed to a Signal Finder part to search for a fluorescence signal in  $25.6\ \mu\text{s}$  time



Fig. 4. Telescope installed in the telescope building in Utah

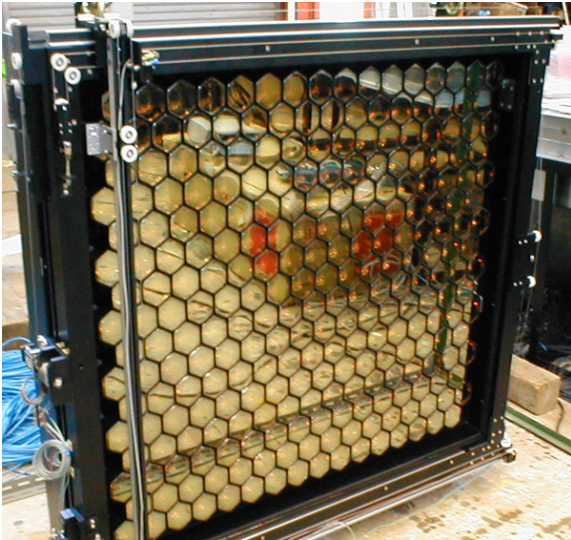


Fig. 5. Prototype Camera of TA

window. The timing and pulse height of all PMTs are collected for one camera and a shower track is searched from hit pattern in a Track Finder (TF) module. Test setup of the readout and trigger system is shown in Fig. 10. The information of a trigger is broadcasted to all cameras in the station through a Central Trigger Decision (CTD) module and data are collected via Ethernet to build a complete event.



Fig. 6. Test setup of readout and trigger for the fluorescence telescope.

For the precise measurement of energy, the absolute calibration of the telescope sensitivity is important. We have to understand the efficiency of telescope optics, mirror reflectivity, filter transmission, PMT quantum efficiency and the electronics sensitivity. Each component will be calibrated piece by piece at the production stage and will be monitored in situ by various light emitting pulser system such as a diffused Xenon lamp, a blue LED and a tiny YAP ( $\text{YAlO}_3:\text{Ce}$ ) scintillator with  $^{241}\text{Am}$  source. The present uncertainty of the PMT quantum efficiency (QE) and the dinode collection efficiency (CE) of produced photoelectrons is each  $\sim 10\%$  and the systematic uncertainty of PMT sensitivity reaches to  $\sim 14\%$  in total according to the producer. We made a simple pulsed UV light calibration source with 5% absolute intensity error by using a Rayleigh scattering of nitrogen laser light by pure nitrogen gas molecules. We checked the value of company supplied PMT efficiency by using this system. The preliminary result shows that the combined error of QE+CE can be made at 5% level and the actual error of the company supplied QE and CE values are smaller than quoted by the company.

The ultra-violet fluorescence light generated by the air shower in the atmosphere is scattered and lost along the path of transmission to the telescope. The responsible processes are Rayleigh scattering by the air molecule and Mie scattering by the aerosol. The Rayleigh scattering is elementary and the loss can be calculated and corrected with an accuracy better than 5% knowing the density distribution of the atmosphere. The amount of Mie scattering differs from place to place and changes with time reflecting the aerosol distribution in the air. The primary task of the atmospheric monitoring is to determine the loss by the Mie scattering with an accuracy better than 10%. It is particularly important for cosmic rays dropping in the region of the ground array. These events will be measured by the telescope and the ground array independently, and are important means to cross-calibrate energies measured by both systems. The atmospheric monitoring will be made by the lidar system located near each



Fig. 7. Lidar system located near the telescope station in Utah.

station. It consists of a pulsed Nd:YAG laser and a light receiver attached on an alt-azimuth mount (See Fig. 11). Using this system, we can shoot laser at any direction and measure the 3-dimensional distribution of atmospheric extinction coefficients within 10 km of each station[6]. An infra-red CCD camera is mounted on the same alt-azimuth and monitors the existence of low clouds in the night sky. A few more additional laser guns will be located in the center of the ground array area. The analysis of the side scattered light from these guns will be made by using the absolute calibration of the laser power and the light receiver. Field tests of prototype monitoring system have been made since 1997 in Utah and Akeno.

The most critical work of the air shower experiment as a calorimeter is to calibrate absolute energy scale of the detector at the energies of our concern, namely at  $\sim 10^{20}$  eV. One such possibility of end-to-end absolute energy calibration is to inject an electron beam of energy 10–100 MeV from the linac vertically up in the atmosphere. If we take 40 MeV electron beam with  $10^9$  particles per bunch, the total energy is equivalent to  $\sim 10^{17}$  eV. Such amount of fluorescence lights generated 100 m away is clearly detectable by the fluorescence telescope. The energy of the linac beam is deposited in the air by the low energy electrons and gammas. Note that the situation is similar to the actual air shower; a large part of the air shower energy is deposited in the air by the low energy electrons and positrons below the critical energy. We are in the process of designing such calibration device for the hybrid TA experiment.

Power for these fluorescence detectors will be supplied by diesel generators. Fuel for the generators will be stored on-site in large tanks.

## Construction

The phase-1 Hybrid Telescope Array will be built by the collaboration of Japanese and American physicists. The group consists of cosmic ray physicists who have been working in AGASA and HiRes experiments, and high energy physicists who worked in the accelerator experiments in US and Japan. The construction of TA started in the summer of 2003 by the Grants-in-Aid for Scientific Research (Kakenhi).

On December in 2004, 20 scintillation ground detectors were deployed by helicopter for the engineering test. Figure 12 shows one of the detectors deployed in the field. Data transfer was successful between the detector and the temporary communication tower. The timing distributions of sig-



Fig. 8. A scintillator ground detector deployed in the field.

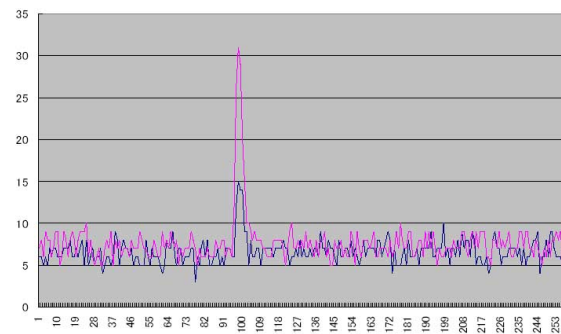


Fig. 9. The timing distributions of signals from the scintillator detector by a cosmic ray muon.

nals from the scintillator detector by a cosmic ray muon are shown in Fig. 13.

On October 2004, the construction of one of the three telescope buildings was completed. The structure of twelve telescopes were installed early in 2005 and attached two composite mirrors as shown in Fig. 7. The test observation of air shower using this ground array and the telescopes will be performed in 2005. The full deployment of scintillator ground detectors will begin in mid-to late 2005. The construction of the 2nd telescope station will also start in 2005. The full detector will be completed and operational in 2007.

## Bibliography

- [1] The Telescope Array Project: Design Report. July, 2000, available by the web <http://www-ta.icrr.u-tokyo.ac.jp/index.html>.
- [2] M. Fukushima, Proc. of APPI2003 workshop, KEK Proceedings 2003-6.
- [3] M. Fukushima et al., Proc. of 28th International Cosmic

Ray Conference, Vol. 2,1025(2003).

- [4] S. Kawakami et al., Proc. of 28th International Cosmic Ray Conference, Vol. 2,1033(2003).
- [5] F. Kakimoto et al., Proc. of 28th International Cosmic Ray Conference, Vol. 2, 1029(2003).
- [6] T. Yamamoto et al., Nucl. Instr. and Methods **A488**, 191(2002).

## Experimental Study of High-energy Cosmic Rays by the Tibet Air Shower Array in the Tibetan Highlands (The Tibet AS $\gamma$ Collaboration)

[Spokesperson : Masato Takita]

ICRR, Univ. of Tokyo, Kashiwa, Chiba 277-8582

In collaboration with the members of:

Hirosaki Univ., Hirosaki; Utsunomiya Univ., Utsunomiya; Saitama Univ., Urawa; Kanagawa Univ., Yokohama; Yokohama National Univ., Yokohama; Shonan Inst. of Technology, Fujisawa ; Tokyo Metropolitan Coll. of Aeronautical Eng., Tokyo ; NACSIS, Monbukagakusho, Tokyo ; Konan Univ., Kobe, Shibaura Inst. of Technology, Tokyo; China

Since 1990, the Tibet air shower array has been successfully operated at Yangbajing (4 300 m above sea level) in Tibet. Some results obtained from this experiment have been reported elsewhere. The first air shower array (Tibet-I) was updated in late 1994 by increasing the number of scintillation detectors from 65 to 221, and then this array (called Tibet-II) has been fully operating. The Tibet-II array consists of 185 first-timing (FT) plastic scintillation detectors of 0.5 m<sup>2</sup> each. With a FT detector, equipped is a plastic scintillator plate in 3 cm thickness each viewed by a 2'' $\phi$  PMT (HPK H1161). They are placed at a grid point with 15 m spacing, as in Tibet-I. Among these, each of the 52 FT detectors also contains a 1.5'' $\phi$  PMT (HPK H3178) for a wide dynamic-range measurement of the particle density. The FT array is also surrounded by 32 density detectors of 0.5 m<sup>2</sup> each to obtain a good core location for an individual air shower event. The effective area for detecting an contained air shower event is about 8 times as large as Tibet-I. The air shower events have been accumulated at a rate of about 150 Hz to efficiently detect air showers with energies around 10 TeV. In 1996, a high-density array was constructed near the center of the Tibet-II array. This array (HD-array) consists of 110 plastic scintillation detectors, each of which was deployed at a grid point with 7.5 m spacing. The HD array is sensitive to air showers with energies around a few TeV. The trigger rate of the HD array has been set to about 150 Hz. Using this HD array, in 1999, we succeeded in observing multi-TeV  $\gamma$  ray signals from the Crab Nebula at 5.5  $\sigma$  confidence level. This was the first detection of multi-TeV  $\gamma$ -ray signals by a conventional air shower array. Subsequently, we also detected multi-TeV  $\gamma$  rays successfully at 3.7  $\sigma$  level from Mrk501 which was in a highly flaring state between March 1997 and August 1997.

In the late fall of 1999, the area of the HD array was enlarged up to 22000 m<sup>2</sup> (Tibet-III). It is equipped with 533 plastic scintillation counters (497 FT + 36 density PMTs) in total.

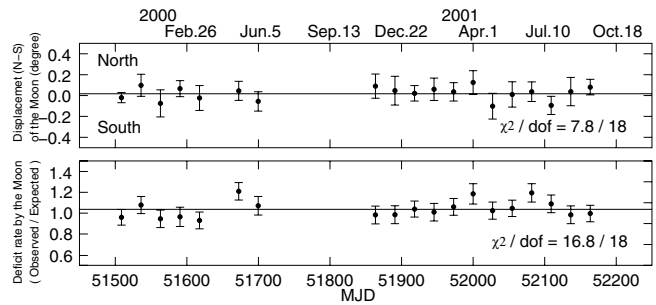


Fig. 1. Tibet-III long-term stability in pointing accuracy and angular resolution.

The trigger rate has been set approximately to 680 Hz.

The performance of the Tibet air shower array has been well examined by observing the moon's shadow in cosmic rays, and the deficit map of cosmic rays around the moon demonstrates the angular resolution to be around 0.9° at a few TeV for the Tibet-III array. The long-term stability in pointing accuracy (less than 0.02°) and angular resolution is demonstrated in Fig. 1.

Multi-TeV  $\gamma$ -ray signal was successfully detected at  $\sim 5\sigma$  level from the Crab (the standard candle in  $\gamma$ -ray astronomy) by the Tibet-III array. We also succeeded in observing multi-TeV gamma-ray flares at 5.1 $\sigma$  level from Markarian 421 which was in a very active phase during the year 2000 and 2001. We observed a clear long-term positive correlation between X-ray data (RXTE satellite) and our TeV  $\gamma$ -ray data from Mrk421 in the active period.

We also searched for multi-TeV diffuse  $\gamma$  rays from the galactic plane. As there was no significant signal, flux upper limits were obtained from the inner galaxy ( $20^\circ < l < 55^\circ$ ,  $-2^\circ < b < 2^\circ$ ) and the outer galaxy ( $140^\circ < l < 225^\circ$ ,  $-2^\circ < b < 2^\circ$ ).

Then, autumn 2002, the Tibet-III array was further extended to 37000 m<sup>2</sup> with 733 plastic scintillation counters by adding 200 more FT counters (i.e., 697 FT + 36 density PMTs in total), as is shown in Fig. 2. The trigger rate has been set to 1500 Hz at a few TeV energy threshold. In 2003, 56 FT detectors were further added in the outer region of the array in order to expand the effective high-density area up to 37000 m<sup>2</sup>. The 37000 m<sup>2</sup> Tibet-III with 789 counters are in continuous operation. The trigger rate is 1700 H.z We are now accumulating Tibet-III data to obtain a standard TeV  $\gamma$ -ray flux from the Crab and to search for unknown constant/transient TeV  $\gamma$ -ray sources.

A hybrid experiment of emulsion chambers (EC) and air shower array started in 1996 to obtain the energy spectrum of the primary cosmic-ray proton flux around the knee energy region. The total area of EC, each having the size of 40 cm  $\times$  50 cm, is 80 m<sup>2</sup> and the total thickness of lead plates is 14 r.l. High-sensitivity X-ray films were interleaved between the 14 r.l. lead plates at every 2 r.l. to detect  $\gamma$ -ray families. Just below the emulsion chambers, the burst detectors (BD) with the same area as EC were set up to locate the air shower cores of the family events to be observed in EC. This detector complex was set up near the center of the Tibet-II array (AS) to get on the information on air showers accompanied with the family events. The first EC exposure was terminated in August



Fig. 2. 37000  $m^2$  Tibet-III array operating at Yangbajing.

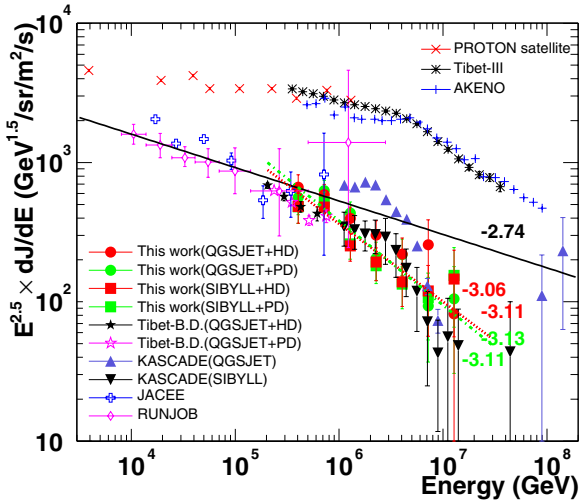


Fig. 3. Primay proton energy spectrum in the knee energy region.

of 1997 and X-ray films inserted in EC were developed for analysis. A high-energy family event of about 500 TeV was observed in this exposure and its primary energy is estimated to be about  $10^{16}$  eV from the size of the accompanying AS data. This hybrid experiment continued until 1999. Using the BD + AS data, we obtained the energy spectrum of primary protons (820 proton-induced events during 690-day detector live time) with its primary energies 200–1000 TeV by a neural network method. The differential energy spectrum obtained in this energy range can be fit by a power law with the spectral index of  $-2.97 \pm 0.06$ , which is steeper than that obtained by direct measurements at lower energies. We also obtained the energy spectrum of helium nuclei. All of the features of BD events are wholly compatible the heavy enriched composition in the knee region. In 2003, we finished the analysis of all the EC data by means of an automatic analysis program based on track information read out by the image scanners. The primary proton spectrum including the EC + BD + AS data around the knee region, being inaccessible by any direct observations, are being analyzed with the 3-year data obtained by the hybrid experiment and a preliminary result is shown in Fig. 3.

We also obtained a preliminary result on the primary cosmic-ray all-particle energy spectrum, as shown in Fig. 4,

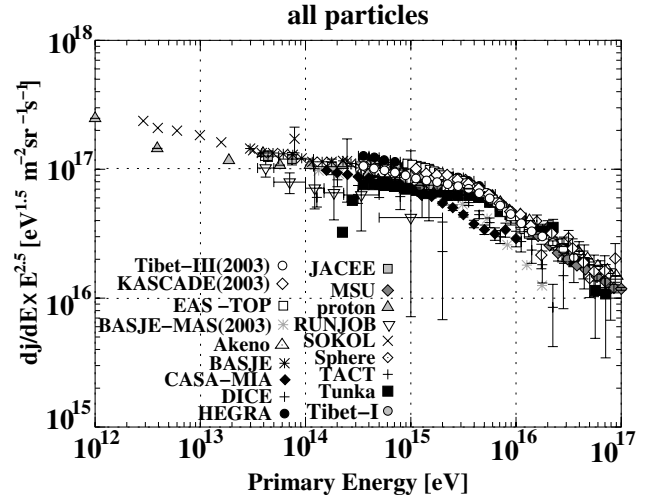


Fig. 4. Primay all-particle energy spectrum in the knee energy region.

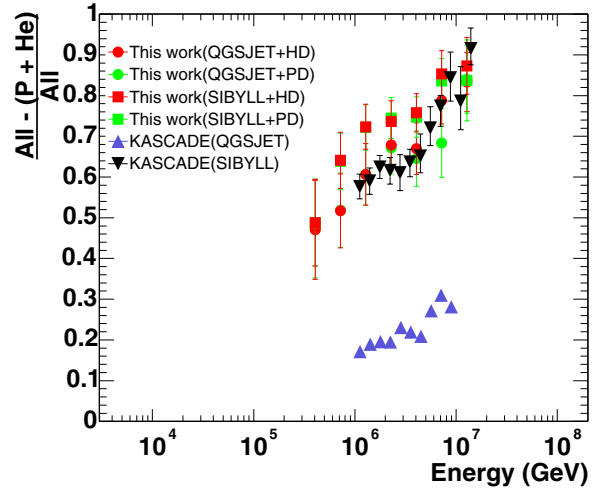


Fig. 5. Primay (all-particle-(proton+helium))/all-particle flux ratio in the knee energy region.

which is consistent with the one obtained by the Tibet-I experiment. The (all-particle - (proton+He))/all-particle flux ratio is shown in Fig. 5, indicating that the knee is composed of nuclei heavier than helium. It should be noted that the flux ratio largely cancels out the systematic energy scale uncertainty in the airshower energy determination.

Based on the Tibet-III data from 1999 and 2003, we succeeded in observation of the multi-TeV galactic cosmic-ray anisotropy at solar time frame due to the terrestrial orbital motion around the Sun, i.e. Compton-Getting (C-G) effect. As shown in Fig. 5, we observed a clear C-G anisotropy in the 6.2 and 12 TeV data samples, while the anisotropy observed in the 4 TeV data sample deviates from the expected C-G anisotropy. This suggests an additional anisotropy superposed at the multi-TeV energies, e.g., the solar modulation effect.

As discussed elsewhere, the Tibet air shower array is very powerful to get new information on the relation between time variation of the large-scale structure of the solar and inter-

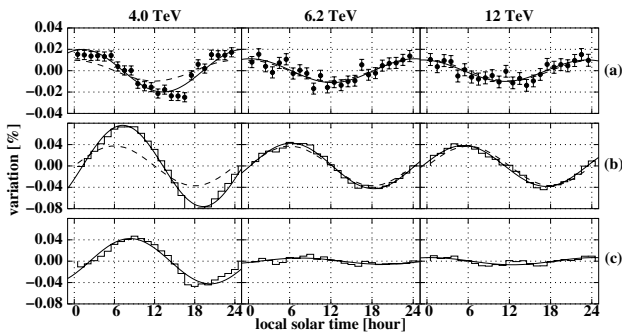


Fig. 6. Multi-TeV cosmic-ray anisotropy at solar time frame obtained by Tibet-III.

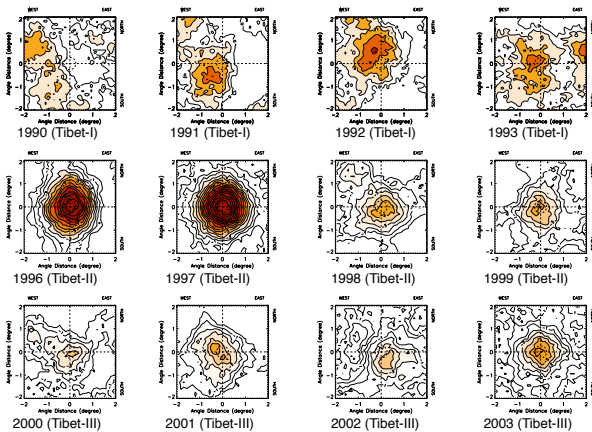


Fig. 7. Yearly variation of the Sun's shadow observed by the Tibet air shower array from 1990 to 2003. Mode energies are 10 TeV.

planetary magnetic fields and the solar activities, since high-statistics data taken by the Tibet air shower array can follow up the movement of the sun's shadow at every one-two months. The sun's shadow was observed in the direction significantly away from the optically observed sun's position during the period from 1990 through 1993. Note that this period corresponded to the near-maximum or at the decreasing phase in the solar cycle 22. In 1996 and 1997, however, we found that the sun's shadow was observed in the direction close to the optically observed sun's direction, since the solar cycle was in a quiet phase then. Since 1998, the sun's shadow began to be obscure shown in Fig. 6, as the solar activities were back in an active phase. We expected that the sun's shadow would change its position again, according to the solar activities as the next solar cycle (Cycle 23) goes toward its maximum around the year of 2001 or 2002. As the maximum showed a double-peak structure and the solar activities were still in high states in 2002, we have not observed a clear sun's shadow yet, although the sun starts exhibiting a darker shadow in cosmic rays in 2003. Thus, the results will contribute considerably to the study of solar terrestrial physics.

This group has developed and completed several automatic measuring systems that are powerful for analyzing cosmic ray tracks or air shower spots, that is, automatic microdensitometers and precise coordinate-measuring systems controlled by a computer. Enormous data recorded on nuclear

emulsion plates or X-ray films are rapidly and precisely measured by the use of these measuring systems. At present, five workstations are introduced to improve data-processing capacity.

The emulsion-pouring facilities can meet the demands for making any kind of nuclear emulsion plates which are used for cosmic ray or accelerator experiments. The thermostatic emulsion-processing facilities are operated in order to develop nuclear emulsion plates or X-ray films. Using these facilities, it is also possible to make and develop emulsion pellicles in 600-micron thickness each. In this way, these facilities are open to all the qualified scientists who want to carry out joint research program successfully.

A scintillation-fiber calorimeter has been developed to be loaded on satellites/balloons in the future for the observation of GeV - TeV  $\gamma$  rays/electrons.

### List of Other Inter-University Research Programs

Code No.: 8

Title: Sidereal daily variation of  $\sim 10$  TeV galactic cosmic-ray intensity observed by the Tibet air shower array.

Spokesperson: K. Munakata (Shinshu University)

Participating Institutions: Shinshu Univ.

Code No.: 9

Title: Observation of High-Energy Electrons and Gamma Rays with a Balloon-borne Instrument

Spokesperson: Shouji Torii (Kanagawa University)

Participating Institutions: Kanagawa Univ., ISAS, Rikkyo Univ.,

ICRR Univ. of Tokyo, and Shibaura Inst. of Technology.

Code No.: 10

Title: Observation of high-energy primary electrons and atmospheric gamma rays by emulsion chambers.

Spokesperson: T. Kobayashi (Aoyama Gakuin University)

Participating Institutions: Utsunomiya Univ., Kanagawa Univ., ICRR Univ. of Tokyo, Univ. of Tokyo.

### Development of Wide Angle High Resolution Detector

[Spokesperson : M. Sasaki]

ICRR, Univ. of Tokyo, Kashiwa, Chiba 277-8582

ICRR, Univ. Tokyo; IfA, Univ. Hawaii; Ibaraki Univ.; KEK; National Astronomical Observatory; National Taiwan Univ.; National United Univ.; Toho Univ.; Tohoku Univ.; Tokyo Institute of Technology; Univ. Hawaii Hilo; Univ. Hawaii Manoa.

### Ashra Project Summary

The activities herein contribute to the technology development and demonstration of the All-sky Survey High Resolution Air-shower detector (Ashra; <http://www.icrr.u-tokyo.ac.jp/~ashra>) for the advancement of particle astrophysics. Ashra records images in unprecedented arc-minute

detail of high-energy cosmic particle interactions in the atmosphere using new CMOS technology. Tracks of nitrogen fluorescence and beams of Cherenkov radiation reveal the arrival direction, energy, and identity of cosmic rays (neutrinos, nuclei and gamma rays) over an energy range of 7 orders of magnitude, from TeV to EeV scale and beyond. Ashra sees not only near horizontal air showers due to neutrinos, but those showers exiting the nearby mountains due to conversion of traversing tau neutrinos, and includes a view of the Galactic Center region. Moreover, the detector can be used to seek optical flashes from Gamma Ray Bursts, providing early alert to telescopes for more detailed observation, particularly those located nearby.

Ashra consists of three high-altitude (3 km) stations to be incrementally installed at Mauna Loa, Hualalai, and Mauna Kea on the island of Hawaii. Each station, separated by 30–40 km, observes the entire moonless night sky with 12 detectors. A detector utilizes four 2.2 m projected diameter spherical reflectors for viewing a  $50^\circ$ -circle (0.5 sr) region of sky. Detector images pass through a photoelectric pipeline for trigger processing and recording on 4 mega-pixel CMOS sensors. Covering the sky with 48 M pixels, roughly a thousand-fold improvement over presently employed technology, represents resolution measured in arc minutes rather than degrees (as achieved with photomultipliers). This unprecedented pixelization provides shower reconstruction with better pointing accuracy (arc-minutes), improved energy determination, and an extension of the range to which distant high energy showers can be detected (because of being able to resolve shorter tracks on the sky).

The increased pixelization will pay off in energy, particle type discrimination, origin direction and effective volume. The most unique feature of Ashra however is the ability to serve as simultaneous detector for both the long duration (100  $\mu$ s) fluorescent events and short (few ns) air Cherenkov events, not possible with earlier instruments. The problem of integrating background light over long times is solved by an image delay system to the CMOS sensors, and a moving electronic shutter driven from a parallel multi-anode photomultiplier trigger.

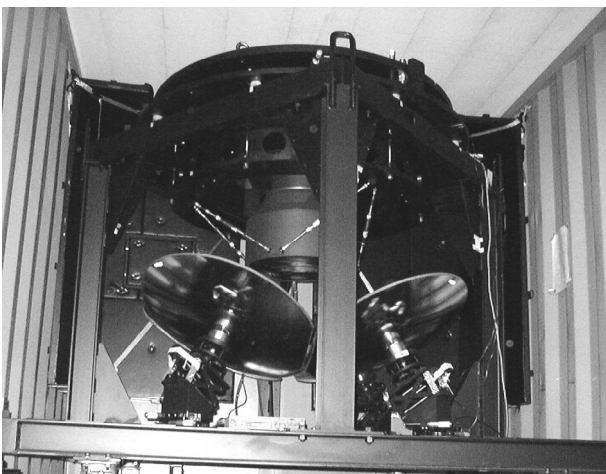


Fig. 1. The 2/3 scale Ashra prototype telescope operated on Haleakala.

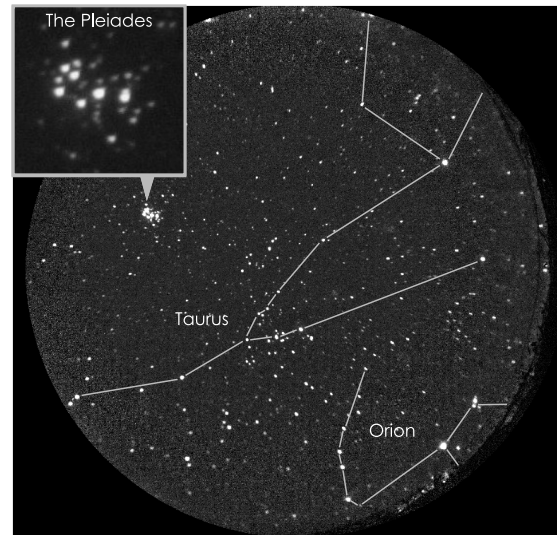


Fig. 2. Example of a 50-degree FOV image in which the constellation of Taurus and Orion can be clearly identified. The inset of a 2-degree square window shows a close-up view of the Pleiades.

The major gain here is the ability to monitor the whole sky continuously for extended (dark) periods, making an unprecedented search for new point (and time varying) sources such as the numerous gamma ray bursts, soft gamma ray repeaters, unidentified EGRET sources and so on. Note that the effective area of Ashra for such a search is much larger than water Cherenkov based detectors.

All Ashra systems now exist in the prototype stage and first versions have been assembled on Haleakala since Fall 2004 (Fig. 1). Land acquisition on Mauna Loa via the University of Hawaii is well underway. It is planned to install the first station on Mauna Loa beginning in 2005 and completed in 2006. Major detector components include optics, image pipeline, trigger, imaging sensors, and data acquisition hardware. In the Ashra optics, photons from air showers are collected using modified Baker-Nunn optics (Sasaki et al., 2002). The fine resolution (arcminutes) in the wide field of view (0.5 sr) has been already demonstrated (Fig. 2). Adding those, we successfully made a cross-observation of the field covering the HETE-2 WXM error box of GRB041211 continuously between the time 1h7m before GRB041211 and that 1h41m after GRB041211 taking 2000 images covering the WXM error box every 5 s with 4 s exposure time. We detected no new objects in the WXM error box resulting the 3-sigma limiting magnitudes are stringently derived (GCN Report #2846, see also <http://www.icrr.u-tokyo.ac.jp/~ashra/GRB041211/>). A demonstration alt-az mounted air Cherenkov detector on Haleakala is in place and has also been collecting data with the image pipeline and the self-trigger system.

## Chacaltaya Observatory of Cosmic Physics

[Spokespersons : H. Yoshii and F. Kakimoto]

In collaboration with the members of:

Ehime Univ., Matsuyama; Tokyo Inst. of Tech., Tokyo; The Inst. of Phys. and Chem. Res., Saitama; IIF, UMSA, La Paz, Bolivia; Okayama Univ., Okayama; Nagoya Univ., Nagoya; National Astronomical Observatory, Tokyo; Kobe Univ., Kobe; Musashi Inst. of Tech., Tokyo; MPI fur Physik, Muncen, Germany.

The air shower experiment of BASJE (Bolivian Air Shower Joint Experiment) group has been continued from 1962 at Mt. Chacaltaya in Bolivia (Fig. 1). The main theme of the present experiment is to investigate the origin of primary cosmic rays around the knee region. For this study we measure the energy spectrum, the chemical composition and the arrival distribution of primary cosmic rays using the MAS (Minimum Air Shower) array (Fig. 2).

The information of the chemical composition is also important for derivation of the energy spectrum, which is estimated from the observed air shower size spectrum by using a Monte-Carlo simulation. In our experiment, the chemical composition is determined with three different experiments. First we measured arrival time distributions of air Cherenkov light for cosmic rays from  $10^{15}$  to  $10^{16.5}$  eV. Since this method has a better mass resolution, we could determine the mixing ratios of p, He, CNO group, Ne-S group, and Fe as a function of the primary energy [1]. However, since the energy range is so limited in this method, second we observed lateral distributions of air Cherenkov light. Then we estimated the mixing ratios of p-He, medium heavy group and Fe in the energy range from  $10^{14.5}$  to  $10^{16}$  eV [2]. These results are consistent with each other at the overlapping energy range and the result at the lowest energy range is consistent with that of the direct observations as shown in Fig. 3. Notably these two experiments measure the longitudinal developments of air showers at their early stages. So third we examined the observed equi-intensity curves to estimate the chemical composition using the information of the longitudinal developments at the deeper atmosphere [3]. This result is also shown in Fig. 3 at the energy range from  $10^{14}$  to  $10^{16}$  eV and is also consistent with



Fig. 1. The Laboratory of Cosmic Ray Physics at Mt. Chacaltaya.

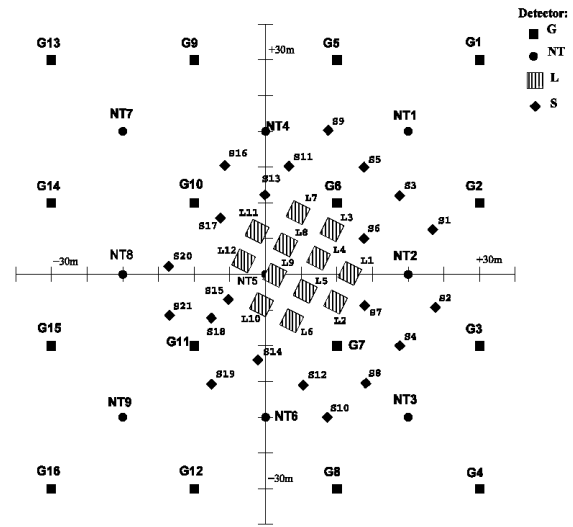


Fig. 2. The MAS array.

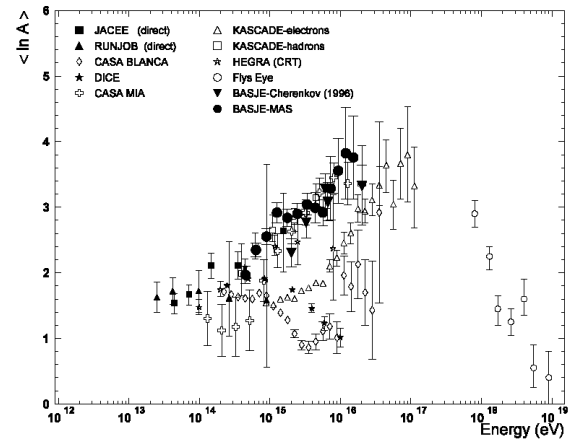


Fig. 3. The averaged  $\ln A$  of primary cosmic rays.

the previous two results. As a result, the chemical composition becomes gradually heavy from  $10^{14}$  eV to the knee region and the main component at and above the knee is Fe. Taking account of this result, we estimated the primary energy spectrum converting from the observed air shower size spectrum as shown in Fig. 4. This spectrum shows the knee structure around  $10^{15.5}$  eV and the power index changes from 2.66 to 3.19 at the knee. Then we examined models of the cosmic ray origin comparing with our results. At present, Biermann's model [4], in which the cosmic rays are accelerated at Wolf-Rayet stars, is the most promising one and alternatively we proposed a model. In our model the primary energy spectra for each components are extrapolated linearly using the direct observation data but assuming the existence of leakage from the galactic disc at a constant rigidity of  $10^{14.5}$  V [5].

Anisotropy in the arrival distribution of primary cosmic rays is very small especially in the energy range below the knee due to their gyro motion in the galactic magnetic field. However if there is a powerful source of primary cosmic rays near the solar system, we can expect the existence of cosmic

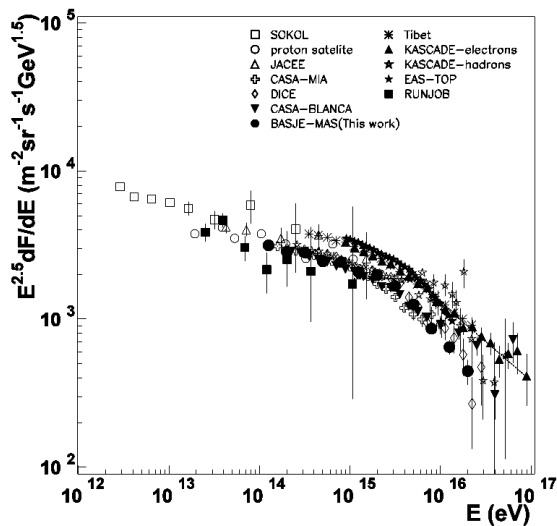


Fig. 4. The energy spectrum of primary cosmic rays.

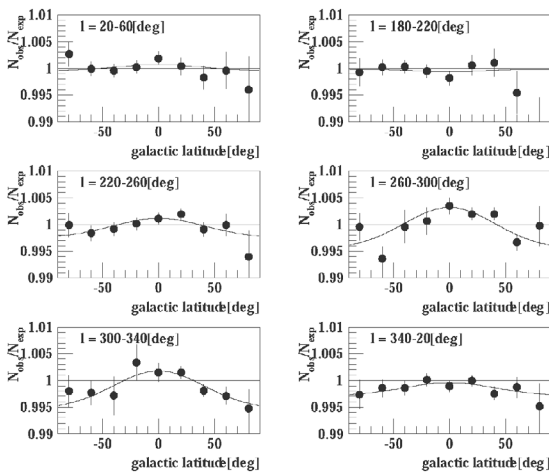


Fig. 5.  $N_{\text{obs}}/N_{\text{exp}}$  against the galactic latitude for each galactic longitude bin.

ray flow from the direction of the source. For example Ptuskin calculated the anisotropy amplitude as a function of the diffusion coefficient for several sources [6]. These amplitudes are about the order of 0.1% and so that we must analyze data with extreme caution. Then we derived the ratio of  $N_{\text{obs}}$  (the number of observed showers) to  $N_{\text{exp}}$  (that of expected ones) as a function of the galactic longitude for each galactic latitude bin using our observed data of air showers with primary energies above  $3 \times 10^{13}$  eV [7]. This result is shown in Fig. 5 and shows that there is enhancement of primary cosmic rays at regions with the galactic longitude from 220 to 340 degrees and with the galactic latitude around 0 degree. This result is very interesting because this region includes the Vela SNR.

For the next step we start the construction of a new array to observe air showers with the primary energies above  $10^{16}$  eV. The arrangement of the detectors is shown in Fig. 6. The new experiment will be started in 2006.

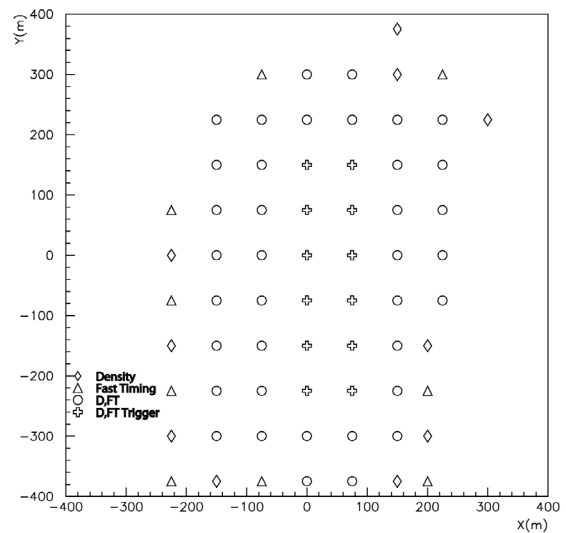


Fig. 6. The arrangement of detectors of a new array at Mt. Chacaltaya.

## Bibliography

- [1] Y. Shirasaki et al., *Astroparticle Physics*, 15, 357–381 (2001)
- [2] H. Tokuno et al., in preparation for the submission.
- [3] S. Ogio et al., *Astrophys. J.*, 612, 268–275 (2004)
- [4] P. L. Biermann, *Astron. Astrophys.*, 271, 649 (1993)
- [5] S. Ogio and F. Kakimoto, *Proc. of 28th ICRC at Tsukuba, HE*, 315–318 (2003)
- [6] V. S. Ptuskin, in *Astrophysics of cosmic rays* ed. by V. S. Berezinskii et al., North-Holland (1990)
- [7] S. Ogio et al., *Il Nuovo Cimento*, 24C, 625–630 (2001)

# ASTROPHYSICS and GRAVITY DIVISION

## Overview

Astrophysics and Gravity Division consists of Gravitational Wave Group, The Sloan Digital Sky Survey Group and Theory Group. The Gravitational Wave Group conducts TAMA project jointly with researchers of gravitational wave experiment and theory in Japan. The Group also conducts a CLIO project that aims to practically test the cryogenic laser interferometer system underground in Kamioka as one of R&Ds for LCGT project to detect gravitational wave events. The Sloan Digital Sky Survey Group continues accumulating data of images and spectroscopic observation of galaxies and publishing papers in collaboration with worldwide researchers. Theory Group introduced a new professor who conducts theoretical study of the Universe in addition to the existing research group of astroparticle physics.

## TAMA Project

[Spokesperson : Kazuaki Kuroda]

ICRR, Univ. of Tokyo, Kashiwa, Chiba 277-8582

In collaboration with the members of: TAMA collaboration NAOJ, Tokyo; KEK, Tsukuba; UEC, Tokyo; Osaka City Univ., Osaka; Kyoto Univ., Kyoto; Osaka Univ., Osaka; Niigata Univ., Niigata)

## Overview

A gravitational wave is a physical entity in space-time predicted by Einstein's theory of general relativity. Its existence was indirectly proven by the observation of PSR1913+16 by Taylor and Hulse [1], who won the Nobel prize in 1993. However, nobody has succeeded to directly detect gravitational waves. The theory of gravitation can be tested by the detection of gravitational waves. A gravitational wave detector is the last eye of mankind to inspect the universe. In order to directly observe gravitational waves, we have been developing a sensitive interferometric gravitational wave detector. We succeeded in operating TAMA for 558 hours with a sensitivity by which we could make observations of the coalescence of double neutron stars occurring within a range of 73 kpc with a signal-to-noise ratio of 10 (DT9 in 2004). Since the first data-taking run (DT1), we have accumulated data of more than 3100 hours in total. A facility for data analysis was made at ICRR, Kashiwa in 2003, and the first approach on TAMA data analysis was completed.

After DT9, the observational operation was stopped for almost one year for noise hunting so as to attain the objective sensitivity. We will be able to report the limiting factor at around the frequency of the best sensitivity.

Table 1. TAMA data-taking runs including long-term observations

Run	Term	Year	Length (Hour)
DT1	6-Aug → 7-Aug	1999	7
DT2	17-Sept → 20-Sept	1999	31
DT3	20-Apr → 23-Apr	2000	13
DT4	21-Aug → 4-Sept	2000	161
DT5	2-Mar → 8-Mar	2001	111
DT6	15-Aug → 20-Sept	2001	1038
DT7	31-Aug → 2-Sept	2002	25
DT8	14-Feb → 14-Apr	2003	1158
DT9	28-Nov → 10-Jan	2004	558

## Status of TAMA Project

TAMA is a gravitational wave project to construct a 300 m baseline laser interferometer at the Mitaka campus of the National Astronomical Observatory of Japan (NAOJ) and to conduct observations. TAMA is a five-year project, started in April, 1995, and is organized by researchers belonging to universities and national laboratories. We regard the TAMA interferometer as a step toward the final scale interferometer in the sense of technology and construction budget. We have so far achieved nine data-taking runs that span from two to four weeks (Table 1). In the former half runs, its sensitivity improvement was the first priority. Nonetheless, both the stability and reliability had to be improved to check the sensitivity, itself. In the latter half runs, the operation became easier after installing an automatic control system.

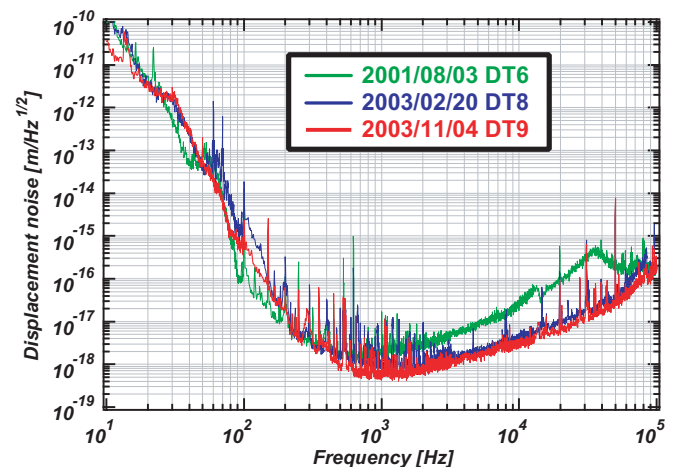


Fig. 1. Before operation stop for noise-hunting in 2004 the sensitivity was improved after the power recycling mirror installation. The sensitivity was physically limited by the photon shot noise at frequencies of more than 1 kHz. Since seismic noise in lower frequencies than 30 Hz disturbed the stable operation of the interferometer, a tighter feedback gain of the mirror alignment control loop was adopted, which resulted in an actuator force noise.

During the course of this project, we established techniques necessary for constructing a large-scale and highly sensitive interferometer. From analyses of DT8 and DT9, no traces of gravitational waves were detected. The previous result was published, and its stable operation was reported [2] [3]. The sensitivity at DT9 is shown in Fig. 1. At the time of DT6, we had analyzed several noise sources that limited the sensitivity, and almost all sources were identified, except for the noise that limits the sensitivity at frequencies around 600 Hz. After DT6, TAMA entered the Phase II stage, where a power recycling mirror was installed to reduce the shot noise. The recycling mirror was installed between the beam splitter and the mode cleaner (in Fig. 2). The role of this mirror is to recycle the laser power returning from the beam splitter by making the phase coincident with the input laser beam from the entrance. At this stage, the power-recycling gain was set at three, but would be finally set at 10. We could observe the coalescence of neutron-star binaries occurring within 73 kpc with a signal-to-noise ratio of 10 at the time of DT9. The range depends on the mass of the target, as shown in Fig. 3. As far as the coalescence of the binary neutron stars with the nominal mass of  $1.4 M_{\odot}$  is concerned, the distance range does not become larger by improving the sensitivity at lower frequency, such as 100 Hz. A sensitivity improvement at lower frequencies is effective for the detection of coalescences involving heavier compact stars, like black holes. After DT9, we stopped the observational operation of TAMA and entered a work phase of noise-hunting to attain the final sensitivity. Since noise-hunting is meaningful only when the temporal best sensitivity is obtained, almost all adjustments must be done at quiet times in a sense of seismic vibration. The sensitivity in a frequency range of less than 300 Hz was limited by the alignment control noise, which arose from the actuator force noise on the main mirror. For observation data-taking runs, the feedback gain was set rather high to maintain stable operation against any irregular disturbance of the seismic motions. This gain needs to be decreased to reduce this force noise. Electric circuits demodulating the signal from the photodiode were checked and revised. The oscillator noises were checked and confirmed to be safe by a simulation of the modulation-demodulation procedure.

The most effort was applied to reduce scattering light noise. Almost all reflections were captured by light-absorbing cells that were made of a highly light-absorbing material. However, some reflections were not correctly captured due to limited space for mounting absorbers. For example, the reflection point from the outer surface of the near mirror of the Fabry-Perot cavity is quite close to the reflection from the inner surface of the near mirror, even at the position of the photodiode, which means that the absorber cell blocks the output beam of the interferometer. If the wedge angle of the near mirror was designed much larger, this would be avoided. Among many reflective surfaces inside the vacuum chamber around the optical system of the interferometer, the reflection from the surface of the photodiode was regarded as the most harmful one because the photodiode is placed on an optical bench outside the vacuum. The reflection light is heavily contaminated by the vibration of the photodiode due to seismic noise.

In order to estimate how much light-scattering noise

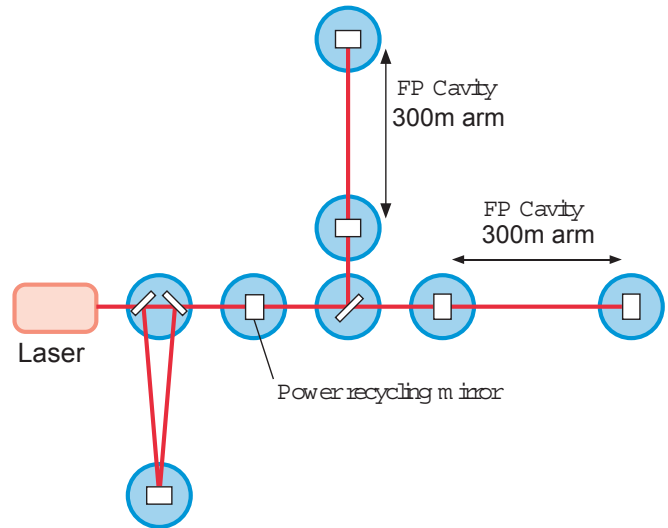


Fig. 2. Optical configuration of TAMA300 as the final stage (DT7-DT9). The reflectance of the recycling mirror was chosen to obtain a power recycling gain of 3 at this moment.

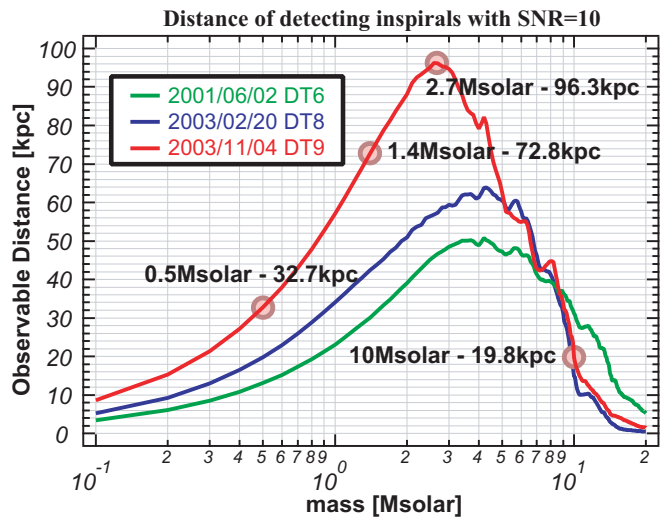


Fig. 3. Detectable range in DT9 for each mass of a neutron star binary system by a signal-to-noise (SN) ratio of 10. The coalescence of the nominal binary system ( $1.4 M_{\odot}$  of each mass) can be detected up to 73 kpc.

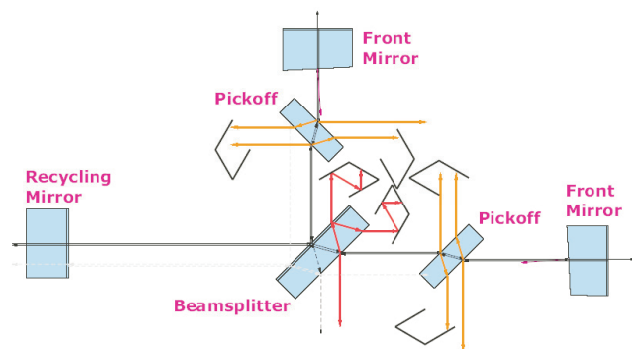


Fig. 4. For noise-hunting, the central part of the interferometer (Michelson part) was inspected with appropriate stray-light absorbers consisting of boxes made of a highly reflective material.

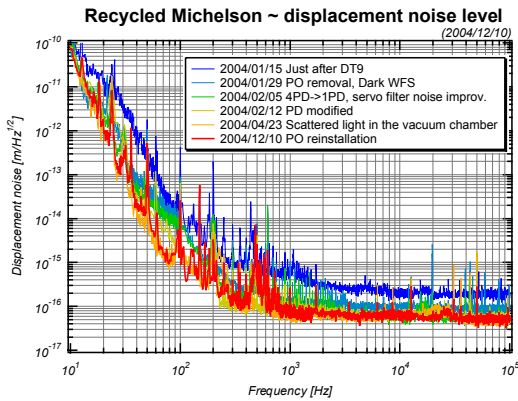


Fig. 5. Improvement of the sensitivity of the Michelson part without Fabry-Perot cavities to find the ultimate limiting factor of the sensitivity.

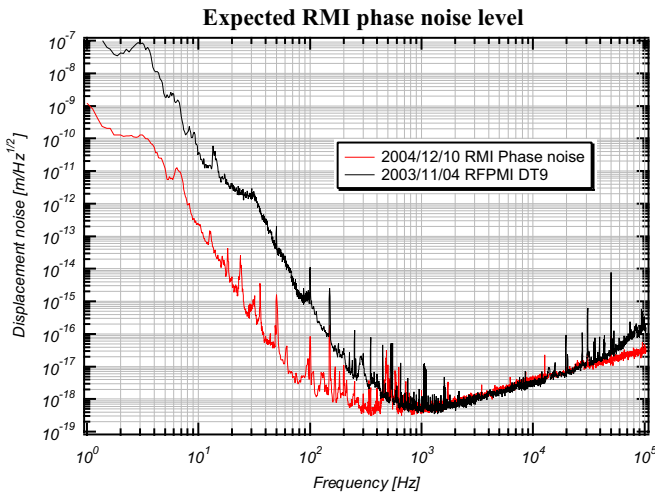


Fig. 6. If the present sensitivity limit arises only from the light scattering, the improvement of the Michelson part will result in increasing the sensitivity.

is produced in the interferometer, the central part of the interferometer (Michelson part) was checked. Absorbers were mounted as shown in Fig. 4 to kill stray light beams. Figure 5 shows the history of improving the sensitivity of the Michelson part without Fabry-Perot cavities. By using stray light-beam absorbers, one and a half orders of the noise magnitude were reduced. If the sensitivity limit arises only from this stray light, a one and half order improvement of the sensitivity is expected by restoring Fabry-Perot cavities (Fig. 6).

## LCGT Project

[Spokesperson : Kazuaki Kuroda]

ICRR, Univ. of Tokyo, Kashiwa, Chiba 277-8582

In collaboration with the members of: LCGT collaboration NAOJ, Tokyo; KEK, Tsukuba; UEC, Tokyo; Osaka City Univ., Osaka; Kyoto Univ., Kyoto; Osaka Univ., Osaka; Ni-

igata Univ., Niigata)

## Overview

Although the recent discovery of the binary neutron star system [4] has increased the birth rate of the coalescence, it is not easy to observe such gravitational wave events during a short observation time. This is because the birth rate of the coalescence of double neutron stars is  $10^{-5} - 10^{-6}$  a year in a galaxy as big as our Galaxy [5]. This means that we need to wait for long time to detect a gravitational wave from the coalescence of binary neutron stars by the present detector. This is the reason why we have to plan LCGT (Large-scale Cryogenic Gravitational wave Telescope) [6]. There are many other possible gravitational wave sources in the universe other than the coalescence of binary neutron stars. However, the coalescence of binary neutron stars differs completely from other sources in the sense that its wave form is precisely predicted, and its existence has certainly been confirmed.

## Current status of LCGT Project

The target sensitivity of LCGT is to observe binary neutron star coalescence events occurring at 252 Mpc with  $S/N=10$  in its optimum configuration. This is ten-times more sensitive than that of the LIGO (I), and by two orders more than that of TAMA at their most sensitive frequencies. This will be attained by dual interferometers located underground, using a three-kilometer length baseline, cooling mirrors at cryogenic temperature, and a high-power laser source employing 150 W output. The optical configuration is a power recycled Fabry-Perot-Michelson interferometer with the resonant-sideband-extraction (RSE) scheme (in Fig. 7). The detailed design of the control system is under consideration.

Table 2 lists the important parameters of LCGT, which were revised two times from the original design. The ultimate sensitivity of a laser interferometer is determined by seismic noise at low frequencies (10-30 Hz) (which is reduced by improving the vibrational isolation system), and it is limited by photon shot noise at higher frequencies (more than 300 Hz), which can be improved only by increasing the light power in the main cavities. The sensitivity of middle frequencies (30-300 Hz) is limited by the photon recoil force noise. This requires that thermal noise is reduced both by decreasing the temperature and by decreasing the internal mechanical loss (*i.e.*, increasing the mechanical Q of vibration modes). The source of thermal noise comes from both mirror internal vibration, mechanical loss of the optical coating and swing noise of the pendulum suspending the mirror. The reduction of thermal noise is attained by cooling down both the mirror, itself, and the suspension system that suspends the mirror.

The main effort on the research and development for LCGT has been placed on cryogenic mirrors for the past years. The implementation of cryogenic mirrors is one of the most straight-forward solutions to improve the sensitivity. A conceptual design of the cryogenic mirror system is shown in Fig. 8, where only a part of the end-mirror chamber is focused.

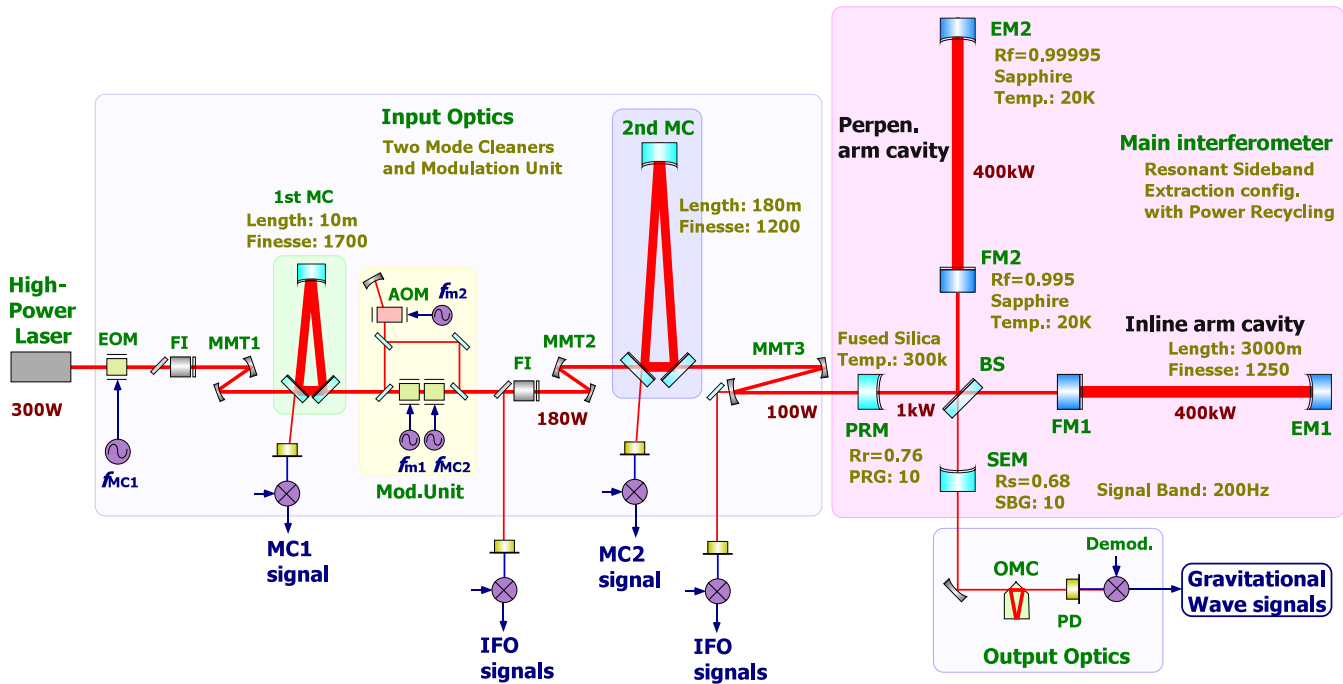


Fig. 7. Optical design of LCGT. The optical configuration is a power recycled Fabry-Perot-Michelson interferometer with the resonant-sideband-extraction (RSE) scheme.

Table 2. LCGT design parameters to detect binary neutron-star coalescence events in 252 Mpc.

Item	Parameter
Baseline Length	3 km
Interferometers	Two set
Optical Power	Power recycled Fabry-Perot-Michelson with RSE Laser: 150 W; Finesse: 2000 Input power at BS: 750 W Cavity power 770 kW
Beam radius at End Main Mirror	3 cm Sapphire 30 kg, 20 K Diameter 25 cm Mechanical Q: $10^8$
Suspension pendulum	Frequency: 1 Hz; Q: $1 \times 10^8$ 10 K
Vacuum	$\leq 10^{-7}$ Pa

1. Removal of heat produced by high-power laser illumination.
2. Holding the high Qs of the mirror internal modes and suspension pendulum.
3. Reducing the contamination of mirror surfaces.
4. Estimating heat production by optical loss in the mirror.
5. Alignment control of mirrors in a cryogenic environment
6. Low mechanical loss of the optical coating.

The mirror is suspended by one or two loops of sapphire fibers connected to an alignment control platform that has a heat link to the heat anchor (4 K) inside the vacuum located just above the platform. This platform is suspended with an insulator rod connected through the center holes of the radiation shields to an isolation table suspended by a low-frequency vibration isolator, which is placed at room temperature. Both the cryogenic system and the vibration isolator are put inside a common high-vacuum chamber.

To realize this concept, the following research subjects were considered:

We had already reported on experimental results of the first two items in the annual report (1997–1998) [7]. In regard to the third and fourth items, the results were reported in the annual report (2000–2001) and published in papers [8]. As for item 5, we confirmed that a superconducting film could be used for the receptor of the magnetic force in place of permanent bar magnets that are normally used in the existing detectors. The film can be easily sputtered on the mirror surface without harmfully degrading the mechanical Q of the mirror. The basic behaviour of this method was reported in a paper [9].

With respect to the last item, we reported on a measurement of the bulk substrate of the mirror at cryogenic temperature in the annual report (2003–2004). We can now cor-

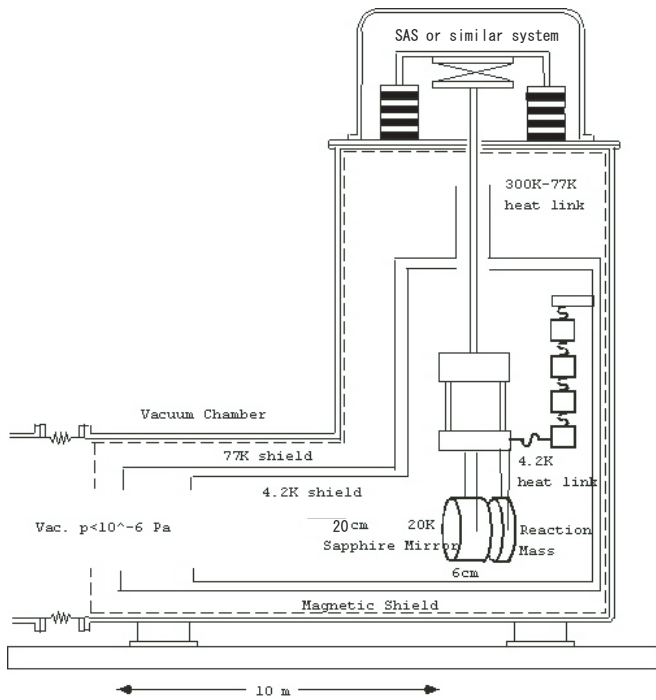


Fig. 8. Schematic design of the cryogenic suspension system. The mirror is suspended by sapphire fibers connected to a platform that has a heat link to a 4 K heat anchor inside the vacuum. The platform is also suspended with an insulator rod connected through the holes of radiation shields to an isolation table suspended by a low frequency anti-vibration system placed at room temperature in the common high vacuum.

directly estimate the thermal vibration noise of the optical coating while considering the inhomogeneous loss that had been neglected at an early stage of interferometer development. The substrate of the cryogenic mirror is sapphire, which has a large thermo-elastic thermal noise at room temperature. However, since the thermal-expansion ratio of sapphire at cryogenic temperature goes down to nearly 0 and the heat conductivity becomes greater, the thermo-elastic noise is drastically reduced at the cryogenic temperature. Thermal noise estimated from the result of coating was well below the design sensitivity of LCGT, which means that this coating noise does not limit the sensitivity, whereas, the sensitivity of a room-temperature mirror is limited by this effect. This is the significant merit of the cryogenic mirror system [10].

All of the above R&D confirmed the feasibility of reducing the thermal noise of the interferometer in the middle-frequency region. This research underlines the basis of LCGT. However, for a practical cryogenic detector, much practical R&D is needed for the installation of cryogenic mirrors. One of the earliest R&D activities was the Kashiwa cryogenic interferometer system reported in the annual report (2000–2001; 2002–2003; 2003–2004). By this Kashiwa cryogenic interferometer, we learned the necessity of several practical R&D activities and began to construct the CLIO interferometer in Kamioka to establish techniques for the cryogenic interferometer. Some of these practical studies are described here.

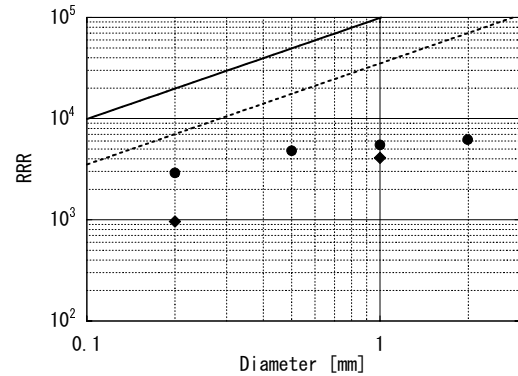


Fig. 9. Size dependence of the thermal conductivity of pure metal fibers. RRR (see text) represents thermal conductivity in this measurement. The solid line shows the calculated upper limit of aluminum (round plots), and the broken line corresponds to that of copper (diamond plots). This result supports that the thermal conductivity of the wire is approximately proportional to its cross-sectional area in these diameters.

### Practical R&Ds: Dependence of the thermal conductivity on the thickness of fiber

The mirror is cooled by sapphire crystalline fibers that suspend a main mirror at the final stage of the anti-vibration system. The thermal conductivity of the sapphire fiber was measured (and reported in the previous annual report (2001–2002)) using  $250 \mu\text{m}$  diameter sapphire fibers. Also, the thermal conductivity of the heat links was measured. The platform that suspends the main mirror is supported through holes of radiation shields from a room-temperature base, which means that some heat links are needed to connect the platform with a thermal anchor inside the cryostat system. Since the platform is close to the final stage of the anti-vibration system, such mechanical links might produce mechanical disturbances onto the main mirror. To prevent such a disturbing force, the mechanical rigidity of the heat links must be as low as possible while maintaining high heat conductivity. This is realized by dividing the heat link to many thin and long links. Imagine that one thick fiber is divided into  $N$  identical thin fibers while leaving the total cross-sectional area unchanged. Since the diameter is reduced in proportion to the square root of  $N$ , the total rigidity is reduced according to  $\frac{1}{N}$ , because each rigidity changes in proportion to the fourth power of the diameter. In this context, the thermal conductivity is supposed to be proportional to the cross-sectional area. However, the thermal conductivity of sapphire fiber is not subject to this law, but changes differently in proportion to the cube of the diameter, as reported in the previous annual report (2001–2002).

The design material of the heat links used in LCGT is pure aluminum. Although copper is possible, the heavier mass density introduces a demerit of low-frequency resonances in the heat links. According to the measurement, the size dependence of the thermal conductivity was not found for diameters ranging from 0.2 mm to 2 mm, as shown in Fig. 9, where RRR is shown in place of the conductivity, because RRR represents

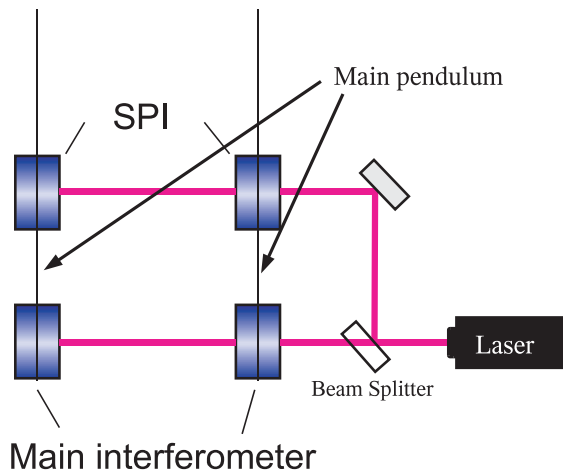


Fig. 10. Mirror suspension system adopts SPI (see text) to reject the introduction of mechanical vibration through heat links. The auxiliary mirror (SPI mirror) behaves as a heat anchor for the main mirror. The SPI mirror is suspended by an insulator wire from an upper platform placed in a room-temperature vacuum chamber through holes in the radiation shields.

the thermal conductivity in this temperature region for metals. RRR is defined as the ratio of the relative electrical resistance at 4.2 K and 300 K,  $\frac{\rho_{300K}}{\rho_{4.2K}}$ . This confirms that the design of LCGT is not affected by this size effect [11].

### Practical R&Ds: Isolation from refrigerator vibration

Since the mechanical vibration of a refrigerator is large enough to excite the suspension system of the main mirror through heat links, both efforts to reduce the vibration of the refrigerator, itself, and that to isolate the vibration from entering to the mirror suspension system were taken. The latter was accomplished by the fine and soft heat-link material described in the previous subsection. The development of a quiet refrigerator was conducted at a cryogenic science center of KEK at Tsukuba. Some important techniques were submitted as patents. Along with these R&D efforts, we plan to introduce a system of suspension-point-interferometer (SPI) in order to eliminate vibration introduced through heat links, which was originally proposed by R. Drever a long time ago, and was recently tested by Y. Aso in the physics department of the School of Science, the University of Tokyo. The main mirrors are suspended from points where auxiliary mirrors form another Fabry-Perot cavity, which will be fixed in an accuracy of a light wavelength by a feedback loop. Even if a disturbing force is applied to one or both of the auxiliary mirrors, the feedback system tries to make the cavity length constant, resulting in high rejection of the introduction of vibration. In order to guarantee the design isolation, the SPI is arranged as shown in Fig. 10, including the main mirror suspension system.

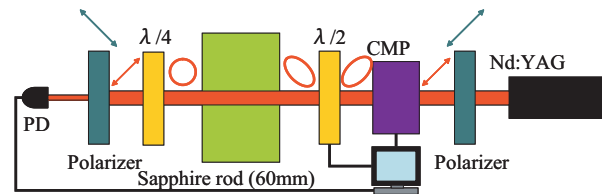


Fig. 11. Optical phase retardance caused by some imperfection is compensated by the Babinet-Soleil compensator (CMP), which is measured by determining two independent angles.

### Practical R&Ds: Measurement of the optical qualities of sapphire

The substrate of the main mirrors in the cryogenic interferometer (LCGT) is sapphire, because it has ultra-low mechanical loss and high heat conductivity at cryogenic temperature. Only fluorite is a possible substitute of sapphire, with some difficulties that should be removed if we have to utilize fluorite in place of sapphire. However, sapphire has birefringence, which is not a defect if the laser beam axis is aligned along its c-axis, which is the so-called optical axis. Also, sapphire has a rather high optical scattering loss compared with that of fused silica. A measurement of the birefringence of sapphire was scheduled both for inspecting the crystal quality of sapphire substrates that were purchased from companies producing sapphire, and for estimating the optical quality of each substrate. The measurement principle is shown in Fig. 11. Suppose that there is some imperfection of the crystal that causes an optical phase retardance between two orthogonal polarizations. Through a half-wave plate we introduce linearly polarized light that coincides with one of principle refractive axes. The retardance caused when traveling inside the sapphire substrate is compensated by a compensator (CMP), the condition of which is measured by knowing an angle position of a polarizer to extinguish the output light. Without the substrate the angle of this polarizer is orthogonally set with the input polarization angle. The fluctuation of the magnitude of the retardance is represented as the indices of the magnitude of the crystal imperfections. In this measurement, for a typical point of the substrate, the angle of the polarizer and the compensated angle were recorded. Practically, the polarizer angle was determined by knowing the optimum point. Figure 12 shows an example of mapping the measured optical phase shift caused by the substrate, which should be zero if there is no birefringence. A measurement of four sapphire rods was completed, and we confirmed that there were no apparent defects inside, and that the magnitudes of the imperfection were negligibly small in the sense of the fluctuated birefringence.

In order to measure the optical scattering loss of those sample rods, we brought two sapphire rods to Australia, and made measurements in collaboration with a gravitational wave group in the Physics department, University of Western Australia, where a measuring device of Rayleigh scattering had been developed. We successfully measured the scattering loss of the samples. Figure 13 shows a strong scattering region on the substrate, the origin of which is believed to have resulted from a remnant of the polishing powder (carbon particle). By this knowledge, we could request the procedure of manufac-

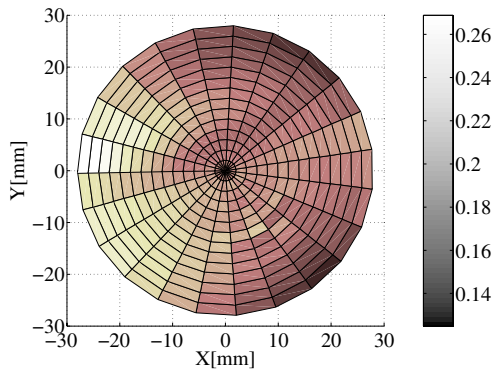


Fig. 12. Measured birefringence fluctuation in terms of the retarded angle. The fluctuation of the magnitude of the retardance represents the magnitude of the crystal imperfections, which is negligibly small for the mirror substrate. Note that a lighter color shows a worse retardance as in the right-hand side column. The unit of numbers is radians.

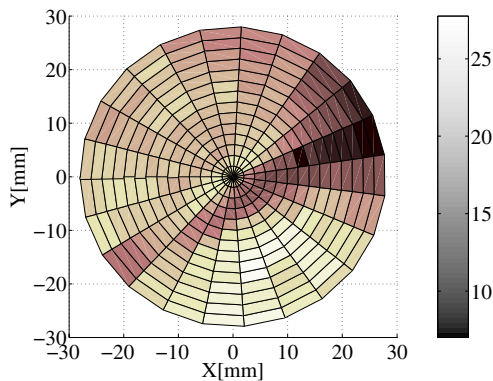


Fig. 13. Mapping of the measured scattering amplitude in terms of power loss. Note that lighter color shows stronger loss, as in the right-hand side column. The unit of numbers is ppm/cm.

turing sapphire.

Apart from the above R&D issues, researchers at the National Astronomical Observatory developed control techniques for the RSE scheme. Also, researchers at KEK tested the mechanical strength of bonded pieces made of sapphire, besides quiet refrigerators. We could not find any correlation between the birefringence and the scattering light loss.

We steadily advance towards the realization of LCGT by these R&D activities. The next step in R&D for cryogenic mirrors is to show a reduction of the noise amplitude, itself, which needs a more realistic interferometer other than the prototype with a shorter baseline. For this sake, the CLIO interferometer at Kamioka is being constructed.

## Construction of CLIO at Kamioka

[Spokesperson : Kazuaki Kuroda]

ICRR, Univ. of Tokyo, Kashiwa, Chiba 277-8582

In collaboration with members of: KEK, Tsukuba; Kyoto-U, Kyoto; Physics Department of UT, Tokyo; ERI of UT, Tokyo

CLIO is a project to construct a 100 m-baseline underground cryogenic interferometer at Kamioka. A tunnel housing the vacuum tubes with chambers has been constructed. The CLIO forms a bridge connecting the CLIK(7 m prototype cryogenic interferometer at Kashiwa campus) and the planned LCGT(3 km cryogenic interferometer at Kamioka).

The objective of CLIO is to present the validity of cryogenic interferometers in an intermediate baseline scale (100 m). We focus attention on the decrease of thermal noise by lowering the temperature by this practical interferometer system. For this reason, the interferometer optical system is designed to be as simple as possible in order to make sophisticated control techniques unnecessary during operation. This involves a locked Fabry-Perot configuration with ring mode cleaners (Fig. 14). The main mirrors are cooled at 20 K by refrigerators. The lowest noise level of CLIO is designed to be  $10^{-19} \text{ m}/\sqrt{\text{Hz}}$  around 100 Hz, which would be  $10^{-18} \text{ m}/\sqrt{\text{Hz}}$ , which results from thermoelastic noise of sapphire mirrors if cryogenics is not applied [12].

Once the objective is attained, the CLIO interferometer is used to observe gravitational wave events in parallel with the TAMA interferometer until completion of the construction of LCGT. The merits of the underground site are lower seismic noise and temperature stability. The former characteristic makes interferometer locking easily controlled, and the latter assures long-term stable operation [13]. The site of CLIO, near the Super-Kamiokande neutrino detector, is shown in Fig. 15. The tunnel was dug in 2002, and a strain meter for geophysics was installed in 2003. The construction of CLIO began in late 2003, and installation of the mode cleaner vacuum system was reported in the annual report (2003–2004). By early this year, three sets of cryostats had been installed, and its cryogenic test was finished for one cryostat (Fig. 16) and one-arm vacuum system with cryostats of both ends had been constructed (vacuum leak test was almost finished). Vacuum chambers for the input optics in the center room were fully installed.

## Bibliography

- [1] J. H. Taylor and J. M. Weisberg, *Astrophysical J.*, **345** (1989) 434.
- [2] N. Kanda, *et al.*, *Class. Quantum Grav.* **20** (2003) S761.
- [3] K. Soida, *et al.*, *Class. Quantum Grav.* **20** (2003) S645.
- [4] M. Burgay, *et al.*, *Nature*, **426** (2003) 531.
- [5] C. Kim, V. Kalogera and D. R. Lorimer, *Astrophysical J.* **584** (2003) 985.
- [6] K. Kuroda, *et al.*, *Int. J. Mod. Phys. D* **8** (1999) 557; K. Kuroda, *et al.*, *Class. Quantum Grav.* **19** (2002) 1237; T. Uchiyama, *et al.*, *Class. Quantum Grav.* **21** (2004) S1161.
- [7] T. Uchiyama, *et al.*, *Phys. Lett. A* **242** (1998) 211; T. Uchiyama, *et al.*, *Phys. Lett. A* **273** (2000) 310.
- [8] S. Miyoki, *et al.*, *Cryogenics* **40** (2000) 61; S. Miyoki, *et al.*, *Cryogenics* **41** (2001) 415; T. Tomaru, *et al.*, *Phys. Lett. A* **283** (2001) 80.

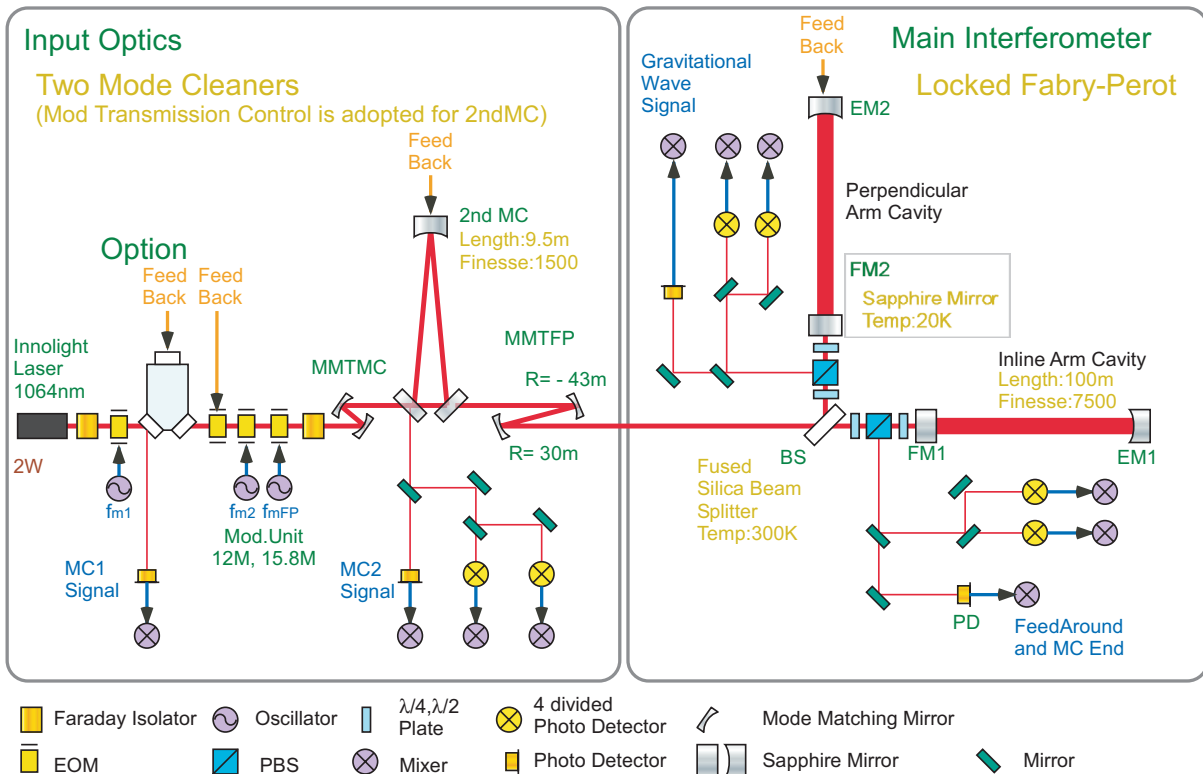


Fig. 14. Optical design of the CLIO interferometer. This is a locked Fabry-Perot configuration with ring mode cleaners.

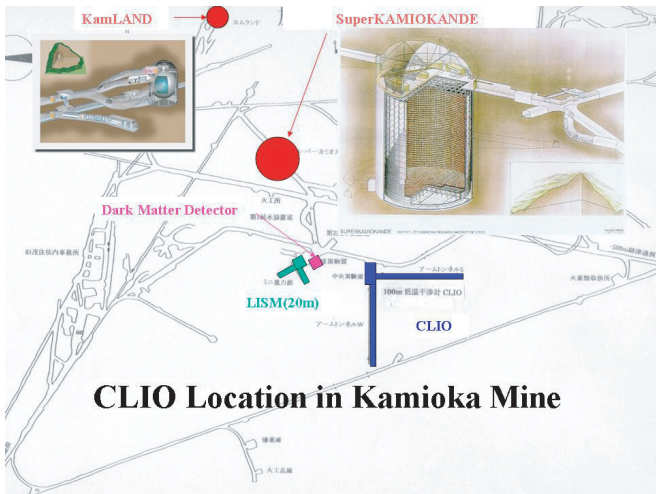


Fig. 15. Location of the CLIO interferometer.



Fig. 16. This cryostat was installed in 2004 and its cryogenic test has been successfully finished. One-arm of the vacuum system was constructed and vacuum chambers for the input optics were fully installed.

[9] N. Sato, *et al.*, *Cryogenics* **43** (2003) 425.  
 [10] K. Yamamoto, *et al.*, *Class. Quantum Grav.* **21** (2004) S1075.  
 [11] K. Kasahara, *et al.*, *TEION KOHGAKU* **39** (2004) 25 (in Japanese).  
 [12] M. Ohashi, *et al.*, *Class. Quantum Grav.* **20** (2003) S599.  
 [13] S. Sato, *et al.*, *Phys. Rev. D* **69** (2004) 102005.

## Sloan Digital Sky Survey

[Spokesperson : Michael Strauss]

Princeton Univ., Princeton, New Jersey 08544 USA

In collaboration with the members of:

University of Tokyo, 7-3-1 Hongo, Bunkyo-ku, Tokyo 113-0033, Japan; Nagoya University, Chikusa, Nagoya 464-8602, Japan; National Astronomical Observatory of Japan, 2-21-1 Osawa, Mitaka, Tokyo 181-8588, Japan; Tohoku University, Aramaki, Aoba, Sendai 980-8578, Japan; Japan Women's University, 2-8-1, Mejirodai, Bunkyo-ku, Tokyo, 112-8681, Japan; The University of Chicago, 5640, South Ellis Ave., Chicago, IL 60637, USA; Fermi National Accelerator Laboratory, P.O. Box 500, Batavia, IL 60510, USA; Institute for Advanced Study, Einstein Drive, Princeton, NJ 08540, USA; Johns Hopkins University, Baltimore, MD 21218, USA; Los Alamos National Laboratory, Los Alamos, NM 87545, USA; Max-Planck-Institute for Astronomy, Königstuhl 17, D-69117 Heidelberg, Germany; Max-Planck-Institute for Astrophysics, Karl Schwarzschildstrasse 1, D-85748 Garching, Germany; New Mexico State University, P.O. Box 30001, Dept 4500, Las Cruces, NM 88003, USA; University of Pittsburgh, 3941 O'Hara St., Pittsburgh, PA 15260, USA; Princeton University, Princeton, NJ 08544, USA; United States Naval Observatory, P.O. Box 1149, Flagstaff, AZ 86002-1149; University of Washington, Box 351580, Seattle, WA 98195, USA

Four years of operation were completed since the commencement of the production run early in the year 2000. The initial goal of the *Sloan Digital Sky Survey* (SDSS) was to cover 10000 square degrees of sky for both imaging and spectroscopic observations, but at the time the production survey began, the Five Year Baseline was developed to provide a more realistic metric against which the progress was evaluated. This decreased the target area to 8550 square degrees (7800 square degrees in the northern sky and 750 square degrees in the southern sky). The imaging carried out over 4 years has sustained nearly the planned pace. At the end of the fourth year 84 % of the northern-sky baseline and 100% of southern-sky baseline were completed. Spectroscopic surveys, however, are significantly behind the schedule. Only 40% of the baseline area were observed for the north (70% for the south). This is due to unusually poor weather conditions in the spring of 2003 and in the winter of 2004. The time-consuming spectroscopic runs were severely affected. (The overall fraction of time available for observing in January 2004, for instance, was only 16%, compared with the baseline value of 60%.) Otherwise, all the operations have been working smoothly (98% is the uptime fraction), producing the data as expected. Software has undergone extensive fine tunings and all the data were re-reduced, which are now made public as *The Second Data Release of the Sloan Digital Sky Survey*, comprising 3300 square degrees of imaging and 2600 square degrees of spectroscopic surveys done to 1 July 2002. This data base contains 88 million objects including 370000 objects with spectroscopic information.

The prime scientific goals of the SDSS are focused on extragalactic themes, including the large-scale structure of galaxies over very large volume of the Universe, and detailed

characterisations of the galaxy properties and those of quasars. As the survey proceeds, these goals have gradually been satisfied. The clustering of galaxies mapped in the three dimensional space looks very similar to what is expected in the model of the Universe dominated by cold dark matter with density fluctuations starting from nearly scale-invariant adiabatic perturbations, as predicted in the model of inflation. As a quantitative measure this density field is characterised by the statistic called the power spectrum, the squared amplitude of the Fourier modes of fluctuations as a function of scale. One of the important results is an accurate derivation of this power spectrum from galaxy clustering over the scale from 10 to 200 Mpc, and the demonstration that it joins smoothly the spectrum derived from the temperature field imprinted on the cosmic microwave background measured by Wilkinson Microwave Anisotropy Probe (WMAP) (see Figure 1). Combined with WMAP that explores the Universe at  $z \approx 1000$ , this lends the most convincing support to the standard model of structure formation in the Universe. The combined data of WMAP and SDSS yield the cosmological parameters  $\Omega_m = 0.30 \pm 0.04$ ,  $\Omega_\Lambda = 0.70 \pm 0.04$  and  $H_0 = 70 \pm 4 \text{ km s}^{-1} \text{ Mpc}^{-1}$ .

Given a few hundred thousands of galaxies with accurate multicolour photometry and spectroscopic information, many studies have been conducted to establish statistical properties of galaxies. To mention a typical result, an accurate determination was made on the average stellar mass (together with the average age and the heavy element abundance) contained in galaxies. Combined with the accurate luminosity function of galaxies, obtained also from the SDSS, this tells us that baryons in stars are  $6 \pm 1\%$  of the total. Another direction is studies of the properties of galaxies in more detail, taking the advantage of accurate photometry and spectroscopy. One such project conducts visual classification of galaxies into Hubble types. For this is a laborious process, the initial sample contains only 2000 nearby galaxies, notwithstanding this is the largest homogeneous sample of morphologically-classified galaxies ever produced. This 'small' sample already clarified a number of aspects that were not known or confusing. One example is a discovery of actively 'star forming elliptical galaxies' (Figure 2), which contrasts with the conventional wisdom that elliptical galaxies are those that have long lost star formation activity, consisting only of old stars. We find the fraction of such elliptical galaxies on the order of 0.1%, hardly discernible in samples available before the SDSS.

Gravitational lensing is also a subject to which the SDSS is making a significant contribution in a number of ways. The SDSS is one of the first few that observed a weak effect of gravitational lensing of galaxy images by foreground galaxies. The lensing effect appears as distorted images of galaxies due to the gravitational shear field, but it is only on the order of a few percent, compared with the order of unity effect of randomly oriented galaxies that have intrinsically different shapes. Millions of galaxies are needed to extract this small signal from noise of the order of unity. With the SDSS galaxy sample, this distortion was unambiguously detected, showing that the mass concentration around galaxies behaves as  $r^{-0.8}$  as a function of distance  $r$ , consistently with the famous

$r^{-1.8}$  law of the galaxy-galaxy correlation. The uniqueness of the SDSS observation over similar weak lensing projects rests in the fact that the distances to foreground galaxies are known, which in turn allows the estimate of the dark mass associated with galaxies. The analysis showed that galaxies are surrounded by the dark mass which amounts to 200 times the light in solar units. This large mass to light ratio had been inferred from a few observations in the past under some assumptions, but this time is derived without resorting to any assumptions. The large quasar sample of the SDSS also provides an excellent platform to search for classical strong gravitational lenses of quasar images, i.e., splitting of images. Among the novel cases that deserve special scientific discussion, we quote a lens of four images with their maximum separation being 14.4 arcsec, 2.5 times larger than has ever been found (Figure 3). The creation of statistical sample of strong lenses is eagerly awaited, since it will provide a new tool to study dynamical states of galaxies and their evolution.

From the commissioning phase, the SDSS project has made unrivalled contributions to our understanding of high redshift quasars. By now the project has found 6 quasars with redshift higher than 6 out of 4600 square degrees — There are no  $z > 6$  quasars reported from other existing projects. The highest redshift is 6.42, which means that the light was emitted only 0.84 Gyr after the Big Bang. Our finding shows the abundance of luminous quasars declining exponentially with redshift from  $z \approx 3$ . This sets a limit on the model of quasars at high redshifts. Also interesting with high redshift quasars is that they allow a study of the ionisation state of the intergalactic medium (IGM). We know that free electron and proton recombine and neutral hydrogen is formed at  $z \approx 1500$ , but it was again highly reionised before  $z \approx 3$ . When and how this reionisation took place is a matter of significant interest from a view of galaxy formation. The spectrum shows a flux of high redshift quasars shortwards the Lyman  $\alpha$  line nearly vanishing for  $z \approx 6$  (called Gunn-Peterson trough), indicating the change of states of the IGM at this redshift. This contrasts with the reionisation epoch of  $z \approx 17$  inferred from WMAP. How these findings will be reconciled will be followed with interest. Besides high redshift quasars, a large number of quasars are assembled and their properties are being studied, including the search for gravitational lenses and for quasars with peculiar features. Our second catalogue of quasars, containing 17000 quasars in 1400 square degrees was published.

After data taking started, it has been recognised that the excellent quality of multicolour photometry and enormous volume of the data produced by SDSS are also useful to make progress for understanding the Galactic structure and the low mass end of stars. The most interesting finding for the former perhaps is the discovery of tidal debris which were left behind when dwarf galaxies travel through the Galactic halo. The first evidence was a conspicuous enhancement in the number density of stars in a small area when it was studied as a function of radius. It was soon identified as the tidal leftover of the Sagittarius dwarf galaxy orbiting around the Galaxy. Another tidal track was then discovered for disruption of a globular cluster, Palomar 5. The tidal tail contains a comparable mass as does the cluster. The third case is the Monoceros stream. These pieces of evidence indicate a view that the Galaxy is still be-

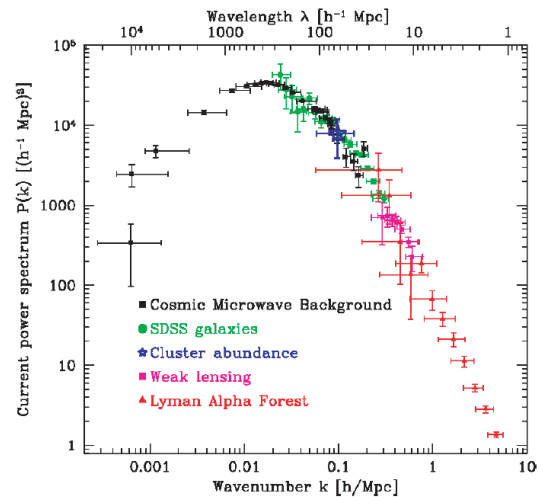


Fig. 1. The power spectrum of galaxy clustering scaled to the present epoch (SDSS galaxies) plotted with four other independent measures, extending four decades on spatial resolution, and demonstrating remarkable consistency. These data provide fundamental constraints on cosmological models. Figure is taken from Tegmark et al. Phys. Rev. D69, 103501 (2004).

ing built up in the halo. The perturbations on the tidal tracks tell us that the Galactic halo is appreciably non-spherical and lumpy. The other notable contribution from the SDSS is to the stellar science proper. A substantial number of low temperature stars found are on the extension of the M dwarf, named the L and T dwarfs, the latter dominated by methane and water features in their spectrum just as with Jupiter. Despite the discontinuous behaviour in colour space it was clarified that these stars are on a single temperature sequence. The sample allows detailed studies of low temperature stellar atmosphere. The mass contained in these low mass stars is no more than a few percent of the total star mass: therefore they cannot be a dominant component of the Galaxy mass.

To date 400 scientific papers have been written for regular journals and conference proceedings (about 150 include Japanese team members). The number of papers using the SDSS data by authors outside the SDSS is also rapidly increasing. Nevertheless, we feel that the state of analyses is still quite premature, far from exploitation of the data we produced.



## Bibliography

- [1] J. Hisano, S. Matsumoto, M. M. Nojiri and O. Saito, hep-ph/0412403 (to be published in Phys. Rev. D).
- [2] J. Hisano, S. Matsumoto, M. M. Nojiri and O. Saito, Phys. Rev. D **71** (2005) 015007.

## Significant Effects of the Second KK Particles on LKP Dark Matter Physics

[Spokesperson : M. Senami]

ICRR, Univ. of Tokyo, Kashiwa, Chiba 277-8582

In collaboration with the members of ICRR and Saitama Univ..

Kakizaki, Matsumoto, Sato and Senami investigated Kaluza-Klein (KK) dark matter physics is drastically affected by the second KK particles. Various intriguing phenomena caused by the second KK modes were discussed. In particular, we reevaluated the annihilation cross section and thermal relic density of the KK dark matter quantitatively in universal extra dimensions, in which all the standard model particles propagate. We demonstrate that the KK dark matter annihilation cross section can be enhanced, compared with the tree level cross section mediated only by first KK particles. The dark matter mass consistent with the WMAP observation is increased.

## Bibliography

- [1] M. Kakizaki, Sh. Matsumoto, Y. Sato and M. Senami, hep-ph/0502059.

## Hadronic Electric Dipole Moments in Supersymmetric Grand Unified Theories

[Spokesperson : M. Kakizaki]

ICRR, Univ. of Tokyo, Kashiwa, Chiba 277-8582

In collaboration with the members of ICRR and Tohoku Univ..

After the discovery of successful agreement of the three extrapolated gauge couplings at a higher energy scale, supersymmetric grand unified theories (SUSY GUTs) have been considered as ones of the most excellent candidates for a theory beyond the standard model. Meanwhile, it was recently pointed out that null results of hadronic electric dipole moment (EDM) experiments severely constrain CP-violating squark generation mixings in SUSY models. Bearing this situation in mind, we investigated hadronic EDM constraints on SUSY GUT models which predict sizable sfermion mixings. In the SUSY SU(5) GUT with the right-handed neutrinos, the hadronic EDMs are sensitive to the right-handed down-type squark mixings, especially between the second and third generations and between the first and third ones, compared with the other low-energy hadronic observables, and the flavor mixings are induced by the neutrino Yukawa interaction. We find that the current experimental bound of the neutron EDM may imply that the right-handed tau neutrino mass is smaller than about  $10^{14}$  GeV given the minimal supergravity boundary condition. In orbifold GUT models where the

GUT symmetry and supersymmetry are broken by boundary conditions in extra spatial dimensions, the appropriate choice of a field configuration yields rich flavor structure in the fermion and sfermion sector. We point out that a marginal chromoelectric dipole moment of the up quark is induced by the misalignment between the CP violating left- and right-handed up-type squark mixings together with the large top quark mass in contrast to the conventional four-dimensional SUSY GUTs. The sensitivity reach of hadronic EDMs is expected to be improved furthermore in future experiments, such as the deuteron EDM measurement. The interplay between future EDM and lepton flavor violation searches will probe the structure of GUT and SUSY breaking mediation mechanism.

## Bibliography

- [1] J. Hisano, M. Kakizaki, M. Nagai and Y. Shimizu, Phys. Lett. B **604** (2004) 216.
- [2] J. Hisano, M. Kakizaki and M. Nagai, in preparation.

## Big-Bang Nucleosynthesis and Hadronic Decay of Long-Lived Massive Particles

[Spokesperson : M. Kawasaki]

ICRR, Univ. of Tokyo, Kashiwa, Chiba 277-8582

In collaboration with the members of ICRR, Osaka Univ. and Tohoku Univ..

We study the big-bang nucleosynthesis (BBN) with the long-lived exotic particle, called  $X$ . If the lifetime of  $X$  is longer than  $\sim 0.1$  sec, its decay may cause non-thermal nuclear reactions during or after the BBN, altering the predictions of the standard BBN scenario. We pay particular attention to its hadronic decay modes and calculate the primordial abundances of the light elements. Using the result, we derive constraints on the primordial abundance of  $X$ .

Compared to the previous studies, we have improved the following points in our analysis: The JETSET 7.4 Monte Carlo event generator is used to calculate the spectrum of hadrons produced by the decay of  $X$ ; The evolution of the hadronic shower is studied taking account of the details of the energy-loss processes of the nuclei in the thermal bath; We have used the most recent observational constraints on the primordial abundances of the light elements; In order to estimate the uncertainties, we have performed the Monte Carlo simulation which includes the experimental errors of the cross sections and transferred energies.

We will see that the non-thermal productions of  $D$ ,  ${}^3\text{He}$ ,  ${}^4\text{He}$  and  ${}^6\text{Li}$  provide stringent upper bounds on the primordial abundance of late-decaying particle, in particular when the hadronic branching ratio of  $X$  is sizable. We apply our results to the gravitino problem, and obtain upper bound on the reheating temperature after inflation.

## Bibliography

- [1] M. Kawasaki, K. Kohri and T. Moroi  
Physical Review **D** in press.

# OBSERVATORIES and A RESEARCH CENTER

## Location of the Institute and the Observatories in Japan



### Norikura Observatory

Location: Nyukawa-mura, Ohno-gun, Gifu Prefecture 506-2100  
 g N 36°06', E 137°33', 2770 m a.s.l.  
 Telephone (Fax): +263-33-7456  
 Telephone (satellite): 090-7721-5674  
 Telephone (car): 090-7408-6224

### Akeno Observatory

Location: Akeno-mura, Kitakoma-gun, Yamanashi Prefecture 407-0201  
 N 35°47', E 138°30', 900 m a.s.l.  
 Telephone / Fax: +551-25-2301 / +551-25-2303

### Kamioka Observatory

Location: 456 Higashi-mozumi, Kamioka-cho, Hida-shi, Gifu Prefecture 506-1205  
 N 36°25'26", E 137°19'11", 357.5 m a.s.l.  
 Telephone / Fax: +578-5-2116 / +578-5-2121

### Research Center for Cosmic Neutrinos

Location: 5-1-5 Kashiwanoha, Kashiwa, Chiba Prefecture 277-8582  
 Telephone / Fax: +4-7136-3138 / +4-7136-3115

# NORIKURA OBSERVATORY

Norikura Observatory (36.10°N and 137.55°E) was founded in 1953 and attached to ICRR in 1976. It is located at 2770 m above sea level, and is the highest altitude manned laboratory in Japan maintained all the year. Experimental facilities of the laboratory are made available to all the qualified scientists in the field of cosmic ray research and associated subjects. The AC electric power is generated by the dynamo and supplied throughout the observatory. In 1996, two dynamos of 70 KVA each were replaced with the new ones. The observatory can be accessed easily by the car in summer (June–October) but an aid of snowmobile is necessary in winter time.

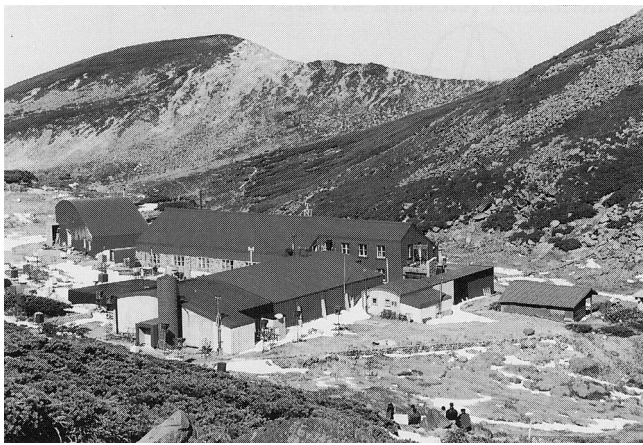


Fig. 1. Norikura Observatory.

Present academic interests of the laboratory is focused on the modulation of high energy cosmic rays in the interplanetary space associated with the solar activity and the generation of energetic particles by the solar flares.

For the modulation study, two small experiments have been operated continuously for a long time. One is a neutron monitor operated to study the correlation of solar activity and the cosmic ray flux. The other is a high counting meson telescope consisting of 36 m<sup>2</sup> scintillation counters to study the time variation of cosmic rays with energies of 10–100 TeV.

The Sun is the nearest site to the Earth capable of accelerating particles up to high energies. When the Sun becomes active, flares are frequently observed on its surface. The flare accelerates the proton and ion to high energy and they are detected on the Earth soon after the flare. Among the particles generated by the flare, high energy neutrons provide the most direct information about the acceleration mechanism as they come straight from the flare position to the Earth without being affected by the magnetic field.

The detection of solar flare particles has been very active in the Norikura observatory for the last 10 years. The muon telescope of the observatory successfully detected flare particles in association with a large flare occurred on the 29th of September, 1989. The data suggested that protons could be

accelerated at least up to 50 GeV in a large solar flare considering the geomagnetic cut-off rigidity of the proton is estimated to be 11.5 GeV at Mt. Norikura. The high altitude of the observatory is essential for detecting the flare particles without significant attenuation.

In 1990, Nagoya group constructed a solar neutron telescope consisting of scintillators and lead plates, which measures the kinetic energies of incoming neutrons up to several hundred MeV. This telescope observed high energy neutrons associated with a large flare occurred on the 4th of June, 1991. The same event was simultaneously detected by the neutron monitor and the high counting meson telescope of the Norikura observatory. This is the most clear observation of solar neutrons at the ground level in almost ten years since the first observation at Jungfrauoch in 1982.

A new type of large solar neutron telescope (64 m<sup>2</sup> sensitive area) was constructed by Nagoya group in 1996. It consists of scintillators, proportional counters and wood absorbers piled up alternately. This takes a pivotal role among a worldwide network of ground based solar neutron telescopes of the same type in Yangbajing in Tibet, Aragatz in Armenia, Gornergrat in Switzerland, Chacaltaya in Bolivia and Mauna Kea in Hawaii. The Sun is being watched for 24 hours using this network.



Fig. 2. New Solar-Neutron Telescope of Nagoya Group.

The Sun is reaching the maximum activity in 2001 and the active phase will continue for next few years. All the telescopes in the Norikura observatory, neutron, meson and muon telescopes, will be operated continuously through this solar cycle (Cycle 23) in order to obtain comprehensive information on the solar flare phenomena. Important hints for understanding the mechanism of cosmic ray acceleration will be obtained by this measurement.

In addition to the long-term cosmic-ray observations mentioned above, various kinds of short-dated experiments are carried out every year taking an advantage of the high altitude of the observatory. As a few examples, following experiments

have been performed; a search for super heavy particles with plastic plates, a precise measurement of atmospheric gamma rays and muons, collection of cosmic dusts contained in the snow and the performance study of the balloon borne cosmic ray experiments. A part of the facility has been open for the environmental study at high altitude such as the aerosol removal mechanism in the atmosphere.

The 50th anniversary of the Norikura Observatory was celebrated in 2003. The feasibility of the automatic operation of the Norikura Observatory during winter period has been tested since winter 2004.

# AKENO OBSERVATORY

The Akeno Observatory has evolved into a complex scientific center for studying ultra-high-energy cosmic rays through extensive air showers in the energy range  $10^{15}$  eV  $\sim$   $10^{20}$  eV, and is being used by many universities. The observatory is in Akeno-chou, Hokuto-shi, located about 20 km west of Kofu and about 130 km west of central Tokyo. Its altitude is 900 m above sea level, and the location is at longitude  $138.5^{\circ}$ E and latitude  $35.5^{\circ}$ N. An aerial view of the 1 km<sup>2</sup> array area is shown in Fig. 1.

The following seven experiments were performed in Akeno Observatory.

- a) Observation of Ultra-High Energy Cosmic Rays (N. Hayashida, ICRR)
- b) Prototype Test of Telescope Array (TA) Detectors (M. Fukushima, ICRR)
- c) Atmospheric Monitoring Experiments with LIDAR System (M. Chikawa, Kinki Univ.)
- d) Observation of Galactic Cosmic Ray Intensity with Large Area Muon Telescopes (S. Kawakami, Osaka City Univ.)
- e) Observation Test for High Energy Cosmic Ray Using Very Wide Field Refractive Optics (S. Ebisuzaki, Riken)
- f) Multicolor Imaging Telescopes for Survey and Monstrous Explosions (N. Kawai, Tokyo Inst. Tech.)
- g) Wide Field Telescope for Hunting Gamma-Ray Burst Optical Flashes (T. Tamagawa, Riken)

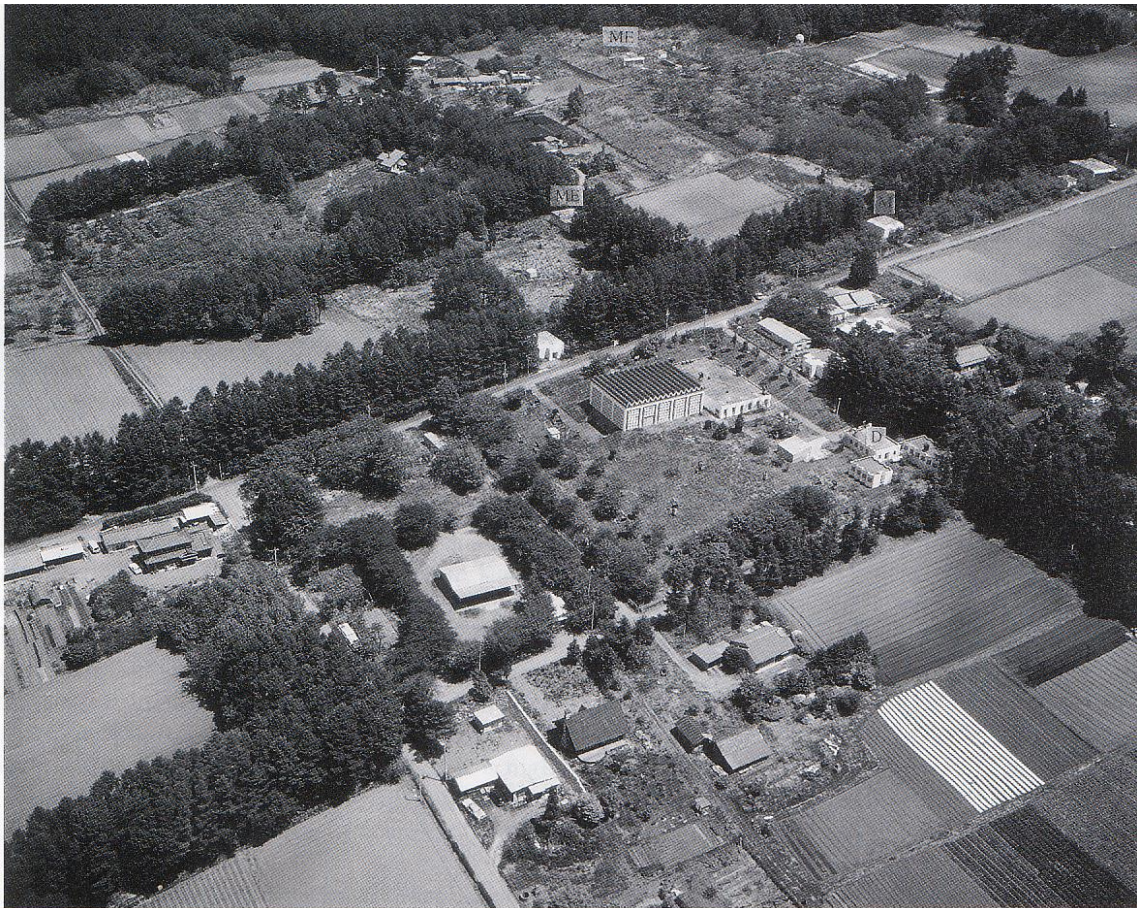


Fig. 1. Akeno central campus and 1 km<sup>2</sup> array area.

- |                              |                           |
|------------------------------|---------------------------|
| C: Central laboratory        | D: Dormitory              |
| S: Sub-electronics stations  | M: Muon detectors (1 GeV) |
| ME: Muon detectors (0.5 GeV) |                           |



Fig. 2. TA surface detector prototype

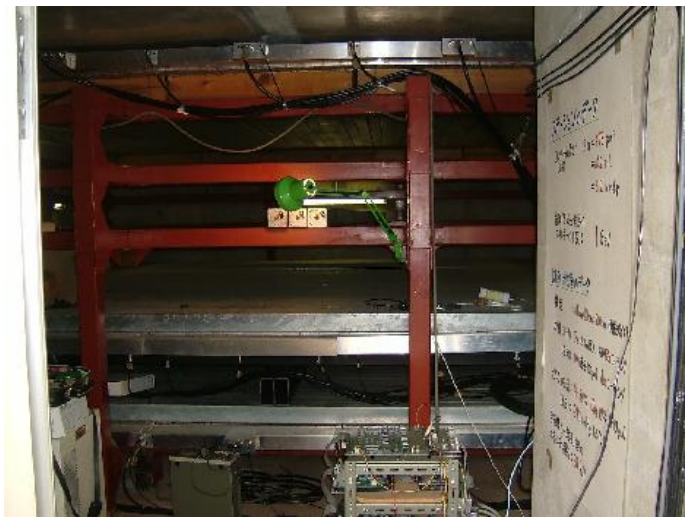


Fig. 5. Large area muon telescope

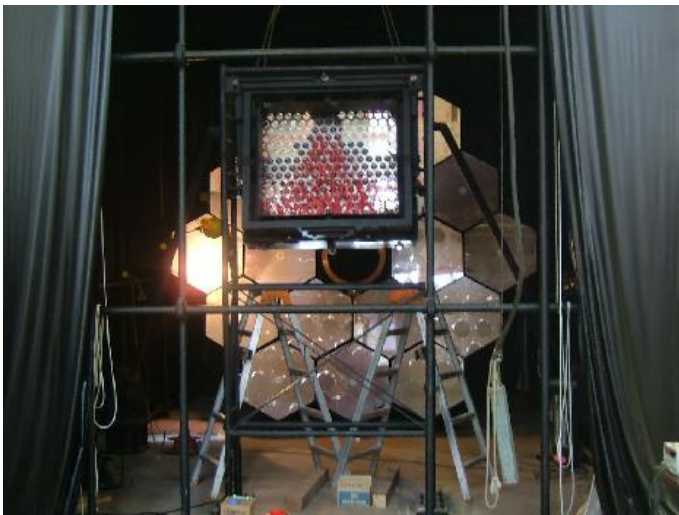


Fig. 3. TA fluorescence detector prototype



Fig. 6. Telescopes for gamma-ray burst observation



Fig. 4. LIDAR system for atmospheric monitoring experiment

# KAMIOKA OBSERVATORY

The observatory operates a 50,000 ton water Cherenkov detector, Super-Kamiokande, which is located 1000 m underground in Kamioka Mine. The purpose of Super-Kamiokande is to study elementary particle physics and astrophysics through neutrino detection and nucleon decay searches. Super-Kamiokande discovered evidence for neutrino oscillations using atmospheric neutrinos in 1998. Solar neutrino oscillation was established in 2001 by comparing results from the SNO experiment in Canada. In 2002, neutrino oscillation was confirmed using artificial neutrinos produced by a proton accelerator at KEK.

There are also 100 m long laser interferometers in Kamioka Mine which are aiming to study gravitational waves and geophysics. Using the low background environment in Kamioka Mine, dark matter search experiments are also being constructed.

There are research offices, a computer facility and a dormitory for researchers located outside of Kamioka Mine and easy access to the detectors in the mine.

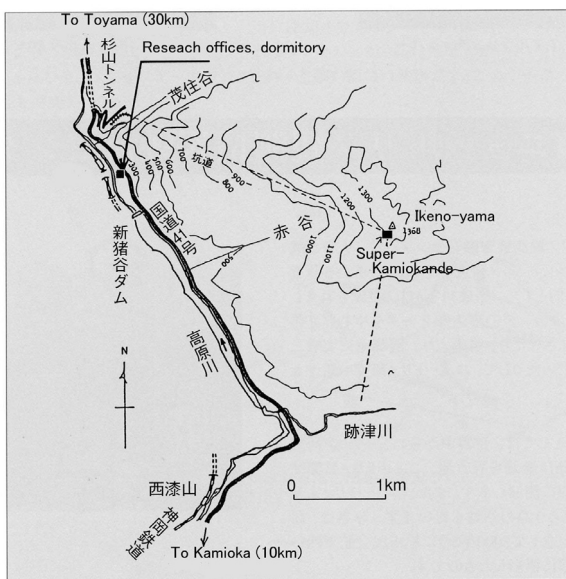


Fig. 1. Map of Kamioka observatory.

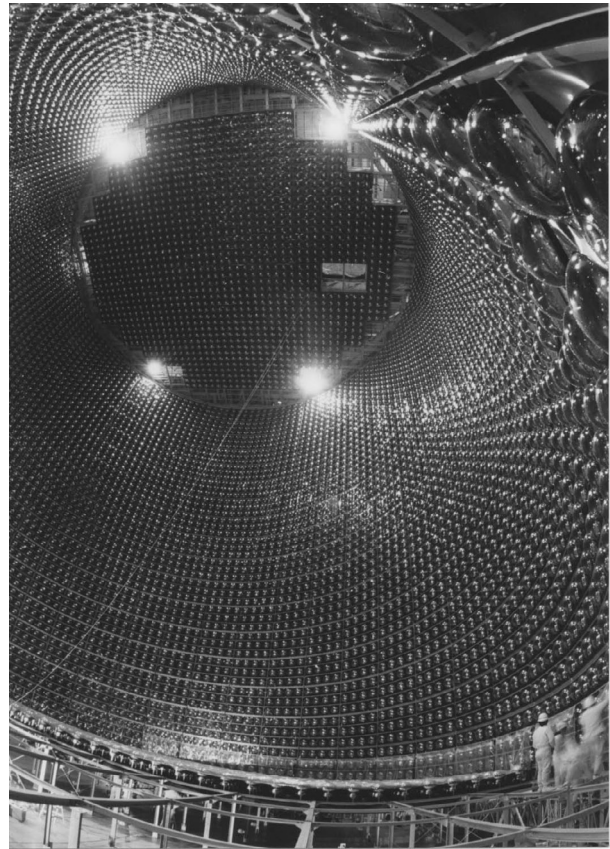


Fig. 2. Super-Kamiokande detector.



Fig. 3. 100 m baseline laser interferometers for gravitational wave and geophysics in Kamioka mine.



Fig. 4. Mt. Ikeno-yama in which Kamioka Mine is there.



Fig. 5. Research offices and computer facility.



Fig. 6. Dormitory for researchers.

# RESEARCH CENTER FOR COSMIC NEUTRINOS

Research Center for Cosmic Neutrinos was established in April 1999. The main objective of this center is to study neutrinos based on data from various observations and experiments.

In order to promote the studies of neutrino physics, it is important to provide the opportunity for discussions on theoretical ideas and experimental results on neutrino physics. Therefore, one of the most important, practical jobs of this center is the organization of neutrino related meetings. In the fiscal year 2004, we organized one international workshop and two local neutrino meetings. The topic of the international workshop was on the sub-dominant oscillation effects in atmospheric neutrino experiments. About 30 researchers working in neutrino oscillation phenomenology, neutrino experiments, cosmic ray measurements, atmospheric neutrino flux calculation and neutrino interaction discussed details on the possible observation of the sub-dominant oscillation effect, such as the effect of the solar neutrino oscillations on atmospheric neutrino experiments.

In the local meetings, we have discussed topics such as, atmospheric neutrinos, solar neutrinos, accelerator neutrino experiments, reactor neutrino experiments, high energy neutrino astronomy, models of neutrino mass, and unified theories. In each meeting, about 40 researchers participated.

Atmospheric neutrino data from Super-Kamiokande give the most precise information on neutrino oscillations. With the increased data, it is more important to have better predictions of the neutrino flux. Therefore, we work on the prediction of the atmospheric neutrino flux. In order to predict the flux accurately, it is important to know the details of the data on the measurements of primary and secondary cosmic ray fluxes. For this reason, we have a close collaboration with researchers working in the cosmic ray flux measurements.

We worked for the basic study of the possibility of the intermediate detector on J-PARC long baseline neutrino experiment. This study is also related to the future 1 Mton water Cherenkov detector (Hyper-Kamiokande), which should be able to measure various important quantities such as leptonic CP violation, proton decay and supernova neutrinos.

It is important that the general public knows the achievements of the present science. Because of this reason, we had a public lecture at Kashiwa. Two active scientists related to neutrino physics lectured on various aspects of neutrino physics.

Finally, we mention that scientific staffs in this center are actively working in the Super-Kamiokande and K2K experiments.



Fig. 1. RCCN International Workshop on sub-dominant oscillation effects in atmospheric neutrino experiments, Kashiwa, Dec. 2004.

# APPENDICES

## **A. ICRR International Workshops**

## **B. ICRR Seminars**

## **C. List of Publications**

- (a) **Papers Published in Journals**
- (b) **Conference Papers**
- (c) **ICCR Report**

## **D. Doctoral Theses**

## **E. Public Relations**

- (a) **ICCR News**
- (b) **Public Lectures**
- (c) **Visitors**

## **F. Inter-University Researches**

## **G. List of Committee Members**

- (a) **Board of Councillors**
- (b) **Executive Committee**
- (c) **Advisory Committee**

## **H. List of Personnel**

## A. ICRR International Workshops

### RCCN International Workshop “sub-dominant oscillation effects in atmospheric neutrino experiments”

Date: 9–11 December, 2004

Place: Institute of Cosmic Ray Research, Kashiwa, Japan.

#### Outline

Atmospheric neutrino experiments have been studying  $\nu_\mu \rightarrow \nu_\tau$  oscillations extensively. The zenith angle and energy dependent deficit, or more recently the  $L/E$  dependent deficit, of atmospheric muon neutrinos has been used to constrain the neutrino oscillation parameters:  $\sin^2 2\theta_{23} > 0.9$  and  $1.9 < \Delta m_{23}^2 < 3.0 \times 10^{-3} \text{ eV}^2$

As a natural extension of the present  $\nu_\mu \rightarrow \nu_\tau$  oscillation studies, atmospheric neutrino experiments should study three flavor oscillation effects. One is the effects driven by  $\theta_{13}$  and the other is the ones driven by the solar oscillation terms ( $\theta_{12}$  and  $\Delta m_{12}^2$ ). Especially, thanks to the diameter of the Earth, atmospheric neutrino experiments are, in principle, sensitive to the solar neutrino oscillation terms. If the solar neutrino oscillation effect is observed, it is possible to get unique information, such as a discrimination of  $\theta_{23}$  larger or smaller than 45 degree for non-maximal  $\sin^2 2\theta_{23}$ .

It is predicted that the effect of solar neutrino oscillations on atmospheric neutrino experiments is relatively a small effect, and improvements of the accuracy of our understanding of the flux and the neutrino interaction cross sections are required. In addition, very careful evaluations of the systematic uncertainties are required. These topics will be discussed in detail in this workshop.

#### Participants

20 from Japan, 3 from U.S.A., 2 from Italy, 2 from Russia, 2 from Spain, 1 from U.K., 1 from Germany, 1 from Rep. of Korea

### Toward Very High Energy Particle Astronomy 5 (VHEPA-5)

Date: 7–8 March, 2005

Place: Institute of Cosmic Ray Research, Kashiwa, Japan.

#### Outline

The 5th annual meeting on High Energy Particle Astronomy, “Toward Very High Energy Particle Astronomy 5” aimed to explore and understand recent rapid progress on very high energy particle astronomy/astrophysics both in observational and theoretical sides. We had twelve invited talks on various subjects. The highlights of this year’s meeting were two topics. First one was the latest results of H.E.S.S. presented by Dr. S. Funk from Max-Planck Institute fuer Kernphysik. In particular the discovery of 8 new TeV sources on the Galactic plane, among which 6 are unknown from optical, radio or X-ray’s observations, was astonishing. This is the first time ever new astronomical sources are found by the Cherenkov telescope. Cangaroo team too showed their results after this talk. Second excitement of the meeting was recent gigantic gamma-ray flare of SGR 1806-20. Dr. N. Kawai presented a review on this hottest subject. There were also a couple of related talks on this giant flare event, mostly from the theoretical point of view.

#### Participants

40 from Japan, 1 from Germany, 1 from Swiss

## B. ICRR Seminars

Date	Lecturer	Title
April 19, 2004	KAKIZAKI Mitsuru (ICRR, University of Tokyo)	“Flavor structure in super-symmetric models”
April 22, 2004	ASAOKA Yoichi (ICRR, University of Tokyo)	“Ashra Experiment : The status of the detector development”
April 23, 2004	Alexei Yu Smirnov (Tokyo Metropolitan Univ. International Center for Theoretical Phys., Trieste Institute for Nuclear Research of Russian Academy of Sciences)	“Toward precision measurements in solar neutrino”
April 26, 2004	SENAMI Daishi (ICRR, University of Tokyo)	“Neutrino mass and Leptogenesis via multi-scalar field evolution”
May 10, 2004	TAKAHASHI Satoshi (ICRR, University of Tokyo)	“Toward Understanding the Dark Side of the Universe”
May 13, 2004	Dr. Ralph Engel (Institute of Nuclear Phys., Forschungszentrum Karlsruhe)	“Status and Prospect of the Pierre Auger Project”
May 17, 2004	HARADA Junpei (ICRR, University of Tokyo)	“Hypercharge and baryon minus lepton number in E-6 GUTcd ht rs”
May 24, 2004	MATSUMOTO Shigeki (ICRR, University of Tokyo)	“Explosive Dark Matter Annihilation”
June 9, 2004	KANEYUKI Kenji (ICRR, University of Tokyo)	“New result of K2K”
June 14, 2004	KITANO Ryuichiro (Princeton University)	“Anomaly mediation, electroweak symmetry breaking and baryo/lepton genesis”
July 5, 2004	YAMAMOTO Tokonatsu (Chicago University)	“Observation of urtra-high energy cosmic ray by Pierre Auger Project”
October 18, 2004	Yoshimura Motohiko (Okayama University)	“Towards resolution of the mass hierarchy problem in a cosmological context”
October 27, 2004	TANAHASHI Seiji (Tohoku University)	“The Structure of Corrections to Electroweak Interactions in Deconstructed Higgsless Models”
November 18, 2004	J. J. Gomez Cadenas (Valencia and KEK)	“Effect of correlations and degeneracies in future neutrino oscillation experiments”
November 18, 2004	NISHIMURA Jun (Emeritus Professor in the University of Tokyo and ISAS)	“Cosmic Ray Electrons and Supernova Acceleration”
November 25, 2004	TANAKA Reizaburo (Okayama University)	“Prospects for TeV Scale New Physics at LHC”

Date	Lecturer	Title
December 9, 2004	TAKAYAMA Humihiro (University of California)	“SuperWIMP dark matter and the related topics”
January 5, 2005	MURAKI Yasushi (Nagoya University)	“Cosmic ray acceleration in thundercloud and effect on climate”

## C. List of Publications — 2004 fiscal year

### (a) Papers Published in Journals

1. “Search for Dark Matter WIMPs using Upward Through-going Muons in Super-Kamiokande,” S. Desai *et al.* (Super-Kamiokande collaboration), Phys. Rev. D70 (2004) 083523; D70 (2004) 109901.
2. “Atmospheric neutrinos,” T. Kajita, New Jour. Phys. 6 (2004) 194.
3. “A measurement of atmospheric neutrino oscillation parameters by Super-Kamiokande-I,” Y. Ashie *et al.* (Super-Kamiokande collaboration), Submitted to Phys. Rev. D, hep-ex/0501064.
4. “Search for nucleon decay via modes favored by supersymmetric grand unification models in Super-Kamiokande-I,” K. Kobayashi *et al.* (Super-Kamiokande collaboration), Submitted to Phys. Rev. D, hep-ex/0502026.
5. “Measurement of single  $\pi^0$  production in neutral current neutrino interactions with water by a 1.3 GeV wide band muon neutrino beam,” S. Nakayama *et al.* (K2K collaboration), Submitted to Phys. Lett. B, hep-ex/0408134.
6. “The K2K SciBar detector,” K. Nitta *et al.*, Nucl. Inst. Meth. A535 (2004) 147.
7. “Evidence for muon neutrino oscillation in an accelerator-based experiment,” E. Aliu *et al.* (K2K collaboration), Phys. Rev. Lett. 94 (2005) 081802.
8. “A new calculation of the atmospheric neutrino flux in a 3 dimensional scheme,” M. Honda *et al.*, Phys. Rev. D, 70 (2004) 043008.
9. “Atmospheric Neutrinos,” T. Kajita, New J. of Phys., 6 (2004) 194.
10. “Detection of Gamma Rays around 1 TeV from RX J0852.0-4622 by CANGAROO-II,” H. Katagiri, R. Enomoto., L. T. Ksenofontov and M. Mori *et al* [CANGAROO Collaboration], Astrophys. J. **619**, L163 (2005) [arXiv:astro-ph/0412623].
11. “Detection of sub-TeV Gamma-rays from the Galactic Center Direction by CANGAROO-II,” K. Tsuchiya, R. Enomoto, L. T. Ksenofontov, M. Mori and T. Naito, *et al.* [CANGAROO-II Collaboration], Astrophys. J. **606**, L115 (2004) [arXiv:astro-ph/0403592].
12. “A Search for TeV Gamma-ray Emission from the PSR B1259-63/SS2883 Binary System with the CANGAROO-II 10-m Telescope,” A. Kawachi, Y. Naito, J. R. Patterson, and P. G. Edward *et al.* [The CANGAROO-II Collaboration], Astrophys. J. **607**, 949 (2004) [arXiv:astro-ph/0402214].
13. “The naissance of high energy particle astronomy with ASHRA,” M. Sasaki, High Energy particle News, Volume23, Number 2 (July/August, September 2004) 63–69.
14. “Observation by an Air-Shower Array in Tibet of the Multi-TeV Cosmic-Ray Anisotropy due to Terrestrial Orbital Motion Around the Sun,” M. Amenomori *et al.*, Phys. Rev. Lett., 93 (2004)061101-1-4.
15. “Automatic analysis of the emulsion chamber using the image scanner applied to the Tibet hybrid experiment,” S. Ozawa *et al.*, NIM, A523 (2004) 193–205.
16. “Ultrastable performance of an underground-based interferometer observatory for gravitational waves,” S. Sato, *et al.*, Physical Review D, 69(2004) 102005-1-102005-7.
17. “Coincidence analysis to search for inspiraling compact binaries using TAMA300 and LISM data,” H. Takahashi, *et al.*, Physical Review D, 70(2004) 042003-1-042003-17.

18. "Manufacturing of a 10-km-scale radius-of-curvature surface using a thin-film coating technique," S. Miyoki, M. Ohashi, K. Waseda, H. Karochi, T. Tomaru, to be published in *Optics Letters*.

## (b) Conference Papers

1. M. Nakahata, "Super-Kamiokande and Solar Neutrinos," Carolina Neutrino Workshop 2004, University of South Carolina, USA, April 16–17, 2004. (to be published)
2. Y. Suzuki, "Future Experiments on Sub-MeV Solar Neutrinos," Solar Neutrino Physics after 50 years, Workshop in honor of John Bahcall, University of Milano, Milano, Italy, May 6th, 2004. (to be published)
3. M. Nakahata, "Super-Kamiokande's Solar Neutrino Results," XXIst International Conference on Neutrino Physics and Astrophysics (Neutrino 2004), Paris, France, June 14–19, 2004. (to be published)
4. Y. Suzuki, "Future Solar Neutrino Experiments," XXIst International Conference on Neutrino Physics and Astrophysics (Neutrino 2004), Paris, France, June 14–19, 2004. (to be published)
5. Y. Koshio, "XMASS," The 12th International Conference on Supersymmetry and Unification of Fundamental Interactions (SUSY04), Tsukuba, Japan, June 17–23, 2004. (to be published)
6. S. Nakayama, "K2K NC  $\pi^0$  production," 6th International Workshop on Neutrino Factories and Superbeams (NuFact04), Osaka, Japan, July 26–August 1, 2004. (to be published)
7. Y. Takeuchi, "SuperK: solar neutrino physics," 6th International Workshop on Neutrino Factories and Superbeams (NuFact04), Osaka, Japan, July 26–August 1, 2004. (to be published)
8. C. Saji, "Recent results from Super-Kamiokande on atmospheric neutrino measurements," 32nd International Conference on High Energy Physics (ICHEP 2004), Beijing, China, August 16–22, 2004.
9. K. Ishihara, "Solar Neutrino Measurement at Super-Kamiokande," 32nd International Conference on High Energy Physics (ICHEP 2004), Beijing, China, August 16–22, 2004. (to be published)
10. Y. Takeuchi, "Recent Status of the XMASS Project," 32nd International Conference on High Energy Physics (ICHEP 2004), Beijing, China, August 16–22, 2004. (to be published)
11. Y. Suzuki, "Super-Kamiokande Results (Neutrino Oscillations)," Nobel Symposium on Neutrino Physics, Haga Slott, Sweden, August 19–24, 2004. (to be published)
12. Y. Koshio, "Day/Night asymmetry in SK and in larger detectors," International Workshop on "Neutrino Oscillation Workshop 2004" (NOW2004), Otranto, Italy, September 11–17, 2004. (to be published)
13. M. Nakahata, "Future solar neutrino experiments," International Workshop on "Neutrino Oscillation Workshop 2004" (NOW2004), Otranto, Italy, September 11–17, 2004. (to be published)
14. S. Moriyama, "Super-Kamiokande atmospheric neutrinos," International Workshop on "Neutrino Oscillation Workshop 2004" (NOW2004), Otranto, Italy, September 11–17, 2004. (to be published)
15. S. Moriyama, "XMASS," 5th International Workshop on the Identification of Dark Matter (IDM2004), Edinburgh, Scotland, September 6–10, 2004. (to be published)
16. C. Mitsuda, "Recent Status of the XMASS Project," 5th International Heidelberg Conference on DARK MATTER IN ASTRO AND PARTICLE PHYSICS (DARK 2004), Texas, USA, October 3–9, 2004. (to be published)
17. S. Moriyama, "XMASS," The Future of Dark Matter Detection, Chigago, USA, December 9–10, 2004. (to be published)
18. S. Nakayama, "Effect of solar terms to  $\theta_{23}$  determination in Super-Kamiokande and important systematic errors for future improvements," RCCN International Workshop sub-dominant oscillation effects in atmospheric neutrino experiments, Kashiwa, Japan, December 9–11, 2004. (to be published)
19. M. Nakahata, "Japanese and eastern facilities," Topical Workshop in Low Radioactivity Techniques (LRT2004), Sudbury, Canada, December 12–14, 2004. (to be published)
20. Y. Takeuchi, "Distillation purification of liquid xenon," Topical Workshop in Low Radioactivity Techniques (LRT2004), Sudbury, Canada, December 12–14, 2004. (to be published)

21. S. Moriyama, "Self-shielding effect for liquid xenon," Topical Workshop in Low Radioactivity Techniques (LRT2004), Sudbury, Canada, December 12–14, 2004. (to be published)
22. A. Minamino, "XMASS experiment : Dark matter search with liquid Xe detector," KEKPH meeting, KEK, Japan, March 03–05, 2005. (to be published)
23. Y. Koshio, "The current status of XMASS using 100 kg detector," Applications of Rare Gas Xenon to Science and Technology (XeSAT2005), Waseda, Japan, March 8–10, 2005. (to be published)
24. Y. Takeuchi, "Distillation purification of xenon for krypton and measurement of radon contamination in liquid xenon," Applications of Rare Gas Xenon to Science and Technology (XeSAT2005), Waseda, Japan, March 8–10, 2005. (to be published)
25. T. Kajita *et al.*, "Future atmospheric neutrino experiments - the case of water Cherenkov detectors," The 5th workshop on "Neutrino Oscillations and their Origin" (NOON2004), (11–15 February 2004, Odaiba, Tokyo, Japan) to be published.
26. T. Kajita, "Atmospheric neutrinos - past, present and future," 7th International Conference on Heavy Quarks and Leptons, (1–5 June 2004, San Juan, Puerto Rico) to be published.
27. T. Kajita, "Atmospheric neutrinos - present and future," 6th International Workshop on Neutrino Factories and Superbeams, (26 July–1 August 2004, Osaka, Japan) to be published.
28. T. Kajita, "Super-Kamiokande atmospheric neutrino results and long baseline experiments in Japan," Neutrino Oscillation Workshop (NOW2004), (11–17 September 2004, Otranto, Italy) to be published.
29. K. Okumura, "SK atmospheric Neutrino Results," Second NO–VE International Workshop on NEUTRINO OSCILLATION IN VENICE, (3–5 December, 2003 Venice Italy) 129–133.
30. L. T. Ksenofontov, R. Enomoto, H. Katagiri and K. Tsuchiya *et al.* [CANGAROO Collaboration], "Search for TeV Gamma-rays from the Remnant of SN 1987A," 2nd VERITAS Symposium on TeV Astrophysics of Extragalactic Sources, Chicago, Illinois, 24–26 Apr. 2003, *New Astron. Rev.* **48**, 485 (2004).
31. H. Kubo *et al.* [CANGAROO Collaboration], "Status of the CANGAROO-III Project," 2nd VERITAS Symposium on TeV Astrophysics of Extragalactic Sources, Chicago, Illinois, 24–26 Apr. 2003, *New Astron. Rev.* **48**, 323 (2004).
32. M. Mori, "Recent Topics from Very High Energy Gamma-ray Astrophysics," 6th RESCEU Symposium "Frontier in Astroparticle Physics and Cosmology," Sanjo hall, Univ. Tokyo (November 04–07, 2003), "Frontier in Astroparticle Physics and Cosmology" (eds. K. Sato and S. Nagataki, Universal Academy Press, Tokyo, 2004)
33. A. Kawachi, T. Naito and S. Nagataki, "High Energy Emissions from the PSR1259-63/SS2883 Binary System," Proceeding of the International Symposium on High Energy Gamma-Ray Astronomy Heidelberg, Germany (July 26–30, 2004) (*to be published*)
34. M. Mori [CANGAROO Collaboration], "Recent Results from CANGAROO-II & CANGAROO-III," *ibid.*
35. Ken'ichi Tsuchiya [CANGAROO Collaboration], "Detection of Sub-TeV Gamma-rays from the Galactic Center with the CANGAROO-II Telescope," *ibid.*
36. M. Ohishi, M. Mori and M. Walker, "Gamma-Ray Spectra due to Cosmic-Ray Interactions with Dense Gas Clouds," *ibid.*
37. K. Tsuchiya, "Status of an Atmospheric Cherenkov Imaging Camera for the CANGAROO-III Experiment and Perspectives of the Field," Fourth International Conference on Physics Beyond the Standard Model "BEYOND THE DESERT" '03 (June 9–14, 2003, Castle Ringberg, Tegernsee, Germany) published as "Beyond the Desert 2003" (ed. Klapdor-Kleingrothaus, H.-V., Springer, Heidelberg, 2004), pp. 819–830.
38. I. Kouga *et al.*, "The simulation for the aerosol analysis using imaging rider," 23th laser sensing symposium (16–17 September 2004, Tsukuba, Japan) 107–108.
39. M. Sasaki *et al.*, GRB041211: Ashra Prototype optical observation, GCN report (2846).
40. M. Takita, "Extensive Air Shower Observation for Energy  $< 10^{17}$  eV and Related Topics," the 28th International Cosmic Ray Conference, (31 July–7 August 2003, Tukuba, Japan), vol. 8, 277–297.
41. S. Miyoki and LCGT Collaborations. "Large scale cryogenic gravitational wave telescope," (5–9, Sep., Seattle, Washington, USA) Nuclear Physics B - Proceedings Supplements, Volume 138, January 2005, Pages 439–442.

42. T. Akutsu *et al.*, “Burst wave analysis of TAMA300 data with the ALF filter,” The 9th annual Gravitational Wave Data Analysis Workshop (GWDAW-9), (15–18 December 2004, Annecy, France) to be published.
43. T. Uchiyama *et al.*, “Present status of CLIO in 2004,” 19th European Cosmic Ray Symposium (Aug. 29–Sep. 5, 2004, Firenze, Italy) to be published.
44. M. Ohashi *et al.*, LCGT Project, 19th European Cosmic Ray Symposium (Aug. 29–Sep. 5, 2004, Firenze, Italy) to be published.
45. N. Sato *et al.*, “Underground Interferometers in Japan,” 2005 Aspen Winter Conference on Gravitational Waves Gravitational Wave Advanced Detectors (GWADW) (16–22 January 2005, Aspen, Colorado, USA).
46. N. Sato *et al.*, “Making a data analysis processor with FPGA for a gravitational-wave event search,” 19th European Cosmic Ray Symposium (Aug. 29–Sep. 5, 2004, Firenze, Italy).

### (c) ICRR Report

1. ICRR-Report-507-2004-5 (August 23, 2004)  
“Unstable state decay without exponential Law-small Q value s-wave (sQs) decay,”  
T. Jittoh, S. Matsumoto, J. Sato, Y. Saito and K. Takeda
2. ICRR-Report-508-2004-6 (August, 2004)  
“Big-bang nucleosynthesis and harmonic decay of low-lived massive particles,”  
M. Kawasaki, K. Kohri and T. Moroi
3. ICRR-Report-509-2004-7 (July, 2004)  
“making waves on CMB power spectrum and inflation dynamics,”  
M. Kawasaki, F. Takahashi and T. Takahashi
4. ICRR-Report-510-2004-8 (September, 2004)  
“Early reionization by decaying particles and cosmic microwave background radiation,”  
S. Kasuya and M. Kawasaki
5. ICRR-Report-511-2004-9 (October 18, 2004)  
“Life-time entropy production due to the decay of domain walls,”  
M. Kawasaki and F. Takahashi
6. ICRR-Report-512-2004-10 (October 1, 2004)  
“Constraining neutrino masses by CMB experiments alone,”  
K. Ichikawa, M. Fukugida and M. Kawasaki
7. ICRR-Report-513-2004-11 (December 29, 2004)  
“Non-perturbative effect on dark matter annihilation and gamma ray signature from galactic center,”  
J. Hisano, S. Matsumoto, M.M. Nojiri and S. Saito
8. ICRR-Report-513-2004-12  
“Significant effects of second KK particles on LKP dark matter physics,”  
M. Kakizaki, S. Matsumoto, Y. Sato and M. Senami
9. ICRR-Report-515-2004-13 (March, 2005) “Detection of TeV gamma-rays from the supernova remnant RX J0852.0-4622,”  
H. Katagiri
10. ICRR-Report-516-2004-14 (March, 2005) “Very high energy gamma-ray observations of the Galactic Center with the CANGAROO-II telescope,”  
K. Tsuchiya
11. ICRR-Report-517-2004-15 (March, 2005) “Very high energy gamma-ray observations of the Galactic plane with the CANGAROO-III telescope,”  
M. Ohishi

## D. Doctoral Theses

1. "Very High Energy Gamma-ray Observations of the Galactic Center with the CANGAROO-II Telescope," Ken-ichi Tsuchiya, Ph. D. Thesis, University of Tokyo, Mar. 2005
2. "Very High Energy Gamma-ray Observations of the Galactic Plane with the CANGAROO-III Telescopes," Michiko Ohishi, Ph. D. Thesis, University of Tokyo, Mar. 2005
3. "Observation of TeV Gamma-rays from the Active Radio Galaxy Centaurus A with CANGAROO-III Imaging Atmospheric Cherenkov Telescope," Shigeto Kabuki, Ph. D. Thesis, University of Tokyo, Jun. 2005
4. "The sub-hundred GeV  $\gamma$ -ray astronomy by MAGIC," Keiichi Mase, PhD Thesis, University of Tokyo, Feb. 2005
5. "Study of coincidence analysis to search for gravitational waves from inspiraling compact binaries using interferometer data," Hiroyuki Takahashi, PhD Thesis, Niigata University, Mar. 2005
6. "Exploring Clusters of Galaxies," Hiroshi Ohno, PhD Thesis, University of Tokyo, Mar. 2005
7. "Cosmic Microwave Background Constraint on Neutrino Mass," Kazuhide Ichikawa, PhD Thesis, University of Tokyo, Mar. 2005
8. "Origin and Evolution of Large Lepton Asymmetry," Hiromitsu Takahashi PhD Thesis, University of Tokyo, Mar. 2005

## E. Public Relations

### (a) ICRR News

ICRR News is a newspaper published quarterly in Japanese to inform the Institute's activities. This year's editors were K. Okumura and M. Ohashi. It includes : (1) reports on investigations by the staff of the Institute or made at the facilities of the Institute, (2) reports of international conferences on topics relevant to the Institute's research activities, (3) topics discussed at the Institute Committees, (4) list of publications published by the Institute [ICRR-Report, ICRR-Houkoku(in Japanese)], (5) list of seminars held at the Institute, (6) announcements, (7) and other items of relevance. The main topics in the issues in 2004 fiscal year were :

#### No. 54 (May 10, 2004)

- Statements from old and new directors (Y. Suzuki and M. Yoshimura)

#### No. 55 (July 22, 2004)

- Emperor and Empress visiting to Super-Kamiokande
- Completion of CANGAROO-III telescope (M. Mori)
- K2K new result (K. Kaneyuki)
- Report on Neutrino 2004 conference (S. Moriyama)

#### No. 56 (March 18, 2005)

- Report on Kyodo-riyo workshop (M. Shiozawa)
- ICRR open house (H. Sagawa)

**(b) Public Lectures**

- “ICRR public lecture on Neutrino,” May 15 2004, Kashiwa.  
“Opening address,” Takaaki Kajita, ICRR, “Supernova explosion and neutrinos - how the black holes and neutron stars are formed,” Katsuhiko Sato, University of Tokyo, “IceCube - a neutrino telescope in the south pole -,” Shigeru Yoshida, Chiba University,
- “JPS public lecture on Neutrino,” November 6 2004, Chuo University.  
“Measuring the neutrino mass using the earth,” Takaaki Kajita, ICRR, “Solving the solar neutrino problem by KamLAND,” Kunio Inoue, Tohoku University, “Unified theories of particle physics - message from neutrinos -,” Masako Bando, Aichi University,

**(c) Visitors****Visitors to Kamioka Observatory. (Total: 210 groups, 4380 people)**

- Masayuki Hara (Vice Governor of Gifu prefecture) [May 21, 2004]
- Yutaka Nakaoki (Governor of Toyama prefecture) [June 29, 2004]
- Emperor Akihito and Empress Michiko; Yamato Inaba (Vice-Minister of MEXT); Masatoshi Koshihara (Professor emeritus, Univ. of Tokyo); Takeshi Sasaki (President of Univ. of Tokyo); Toshitsugu Fujii (Vice-President of Univ. of Tokyo); Taku Kajiwara (Governor of Gifu prefecture); Toyotaro Iwai (Chairperson of Gifu prefectural assembly); Katsumi Funasaka (Mayor of Hida city); Takashi Ishida (Chairperson of Hida city council) [July 13, 2004]
- Eiichi Yamashita (Upper House member) [August 24, 2004]
- Financial committee members in Lower House [September 8, 2004]
- Norihisa Tamura (Parliamentary Secretary of MEXT) [September 28, 2004]
- Kanji Fujiki (Counselor, Personnel Division, Secretariat of MEXT) [November 25, 2004]
- Ikuo Shirokane (General Manager, Tokai Office, Japan Post) [December 7, 2004]
- Kouichi Matsushita (President, Fujitsu Chubu Systems) [January 18, 2005]
- Naoto Kan (Lower House member) [February 6, 2005]
- MEXT Super Science High-school (SSH): total 8 schools

**Visitors to International Astrophysical Observatory, Woomera, Australia.**

- Mr. Satoshi Shinki (Ministry of Education, Science and Culture); Mr. Toshihito Suzuki, Mr. Naoki Saito, Mr. Toshiharu Oki (Administration section, University of Tokyo) [January 18–19, 2004]
- Mr. Keikichi Koike, Mr. Toru Nishimura, Mr. Ryoji Shigeta (Shingei Film Co. Ltd.) [December 14–15, 2004]

## F. Inter-University Researches

	Applications	Adoptions	Researchers
<b>Facility Uses</b>			
Kamioka Observatory	20	20	446
Norikura Observatory	11	11	91
Akeno Observatory	11	11	193
Research Center for Cosmic neutrinos	2	2	13
Emulsion and Air Shower Facilities in Kashiwa	3	3	66
Low-level Radio-isotope Measurement Facilities in Kashiwa	4	4	28
Others	1	1	22
<b>Collaborative Researches</b>			
High Energy Cosmic Ray Researches in the Underground and Deep Sea	3	3	12
High Energy Cosmic Ray Researches in Flyers and at High Altitude and Ground	11	9	71
High Energy Gamma Ray Source Researches	8	8	83
Chemical Composition and Isotope Measurement	2	2	13
Development of Observational Methods and Instruments	3	3	80
Theoretical Researches or Rudimental Researches	2	1	8
<b>Others</b>			
Conferences	5	4	29
Special Activity on Abroad	4	4	79

## G. List of Committee Members

### (a) Board of Councillors

SUZUKI, Yoichiro	ICRR, The University of Tokyo
KURODA, Kazuaki	ICRR, The University of Tokyo
KAJITA, Takaaki	ICRR, The University of Tokyo
FUKUSHIMA, Masaki	ICRR, The University of Tokyo
OKAMURA, Sadanori	The University of Tokyo
KOMIYAMA, Hiroshi	The University of Tokyo
KOBAYASHI, Makoto	KEK
KUGO, Taichi	Kyoto University
KAIFU, Norio	National Astronomical Observatory
SATO, Humitaka	Konan University
TOKI, Hiroshi	Osaka University
SUZUKI, Atsuto	Tohoku University
OHTA, Itaru	Utsunomiya University
INOUE, Hajime	Institute of Space and Astronautical Science
ITO, Nobuo	Osaka City University

### (b) Executive Committee

SUZUKI, Yoichiro	ICRR, The University of Tokyo
TORII, Shoji	Kanagawa University
MURAKI, Yasushi	Nagoya University
TANIMORI, Toru	Kyoto University
KAJINO, Fumiyoshi	Konan University
SAKAI, Norisuke	Tokyo Institute for Technology
ENYO, Hideto	RIKEN
WATANABE, Yasushi	Tokyo Institute for Technology
NAKAMURA, Takashi	Kyoto University
MINOWA, Makoto	The University of Tokyo
KURODA, Kazuaki	ICRR, The University of Tokyo
FUKUGITA, Masataka	ICRR, The University of Tokyo
FUKUSHIMA, Masaki	ICRR, The University of Tokyo
NAKAHATA, Masayuki	ICRR, The University of Tokyo
TAKITA, Masato	ICRR, The University of Tokyo

### (c) Advisory Committee

KAJINO, Fumiyoshi	Konan University
MURAKI, Yasushi	Nagoya University
TORII, Shoji	Kanagawa University
TANIMORI, Toru	Kyoto University
KAWAKAMI, Saburo	Osaka City University
YANAGITA, Shohei	Ibaraki University
MUNAKATA, Kazuki	Sinshu University
SHIBATA, Makio	Yokohama National University
MATSUBARA, Yutaka	Nagoya University
HOTTA, Naoki	Utsunomiya University
OGIO, Shoichi	Tokyo Institute for Technology
SAKURAI, Takahisa	Yamagata University
SHIOZAWA, Makoto	ICRR, The University of Tokyo
MORI, Masaki	ICRR, The University of Tokyo
OHASHI, Masataka	ICRR, The University of Tokyo
KANEYUKI, Kenji	ICRR, The University of Tokyo
TAKITA, Masato	ICRR, The University of Tokyo
HISANO, Junji	ICRR, The University of Tokyo

## H. List of Personnel

**Director** SUZUKI Yoichiro

**Vice Director** KURODA Kazuaki

### Neutrino and Astroparticle Division

#### Kamioka Observatory

Professor	SUZUKI Yoichiro,	NAKAHATA Masayuki	
Associate Professor	TAKEUCHI Yasuo,	SHIOZAWA Masato,	MORIYAMA Shigetaka
Research Associate	KOSHIO Yusuke,	OBAYASHI Yoshihisa,	MIURA Makoto,
	KAMEDA Jun,	TAKEDA Atsushi,	ISHIHARA Kenji
Technical Staff	MIZUHATA Minoru,	FURUTA Takashi	
Research Fellows	NAMBA Toshio,	mitsuda Chikaori,	OGAWA Hiroshi
Administrative Chief	AKIMOTO, Masatoshi,	GOTO Shohachiro	
Secretary	OKURA Yoko,	MURAKI Yasuko,	MAEDA Yukari,
	OKADA Eri		

#### Research Center for Cosmic Neutrinos

Professor	KAJITA Takaaki		
Associate Professor	KANEYUKI Kenji		
Research Associate	OKUMURA Kimihiro		
Technical Staff	SHINOHARA Masanobu		
Research Fellows	SAJI Choji,	NAKAYAMA Shoei,	HIGUCHI Itaru,
	HONDA Morihiro,	ISHITSUKA Masaki	
Secretary	FUKUDA Yoko,	KITSUGI Atsuko	

### High Energy Cosmic Ray Division

Professor	FUKUSHIMA Masaki,	MORI Masaki	
Associate Professor	ENOMOTO Ryoji,	YOSHIKOSHI Takanori,	TAKITA Masato,
	SASAKI Makoto		
Research Associate	HAYASHIDA Naoaki,	HATANNO Yoshikazu,	KAWACHI Akiko,
	OHNISHI Munehiro,	ASAOKA Yoichi,	TAKEDA Masahiro
Technical Staff	AOKI Toshifumi,	TOYODA Setsuko,	KOBAYASHI Takahide
Research Fellows	OZAWA Shunsuke,	UDO Shigeharu,	TOKUNOU Hisao,
	MIYAMOTO Tomoko,	KOBAYASHI Noriko,	TSUCHIYA Kenichi,
	HARA Satoshi,	SHIOMI Atsushi,	TSUCHIYA Harufumi,
	KAWATA Kazumasa,	HUANG Jing,	TANAKA Akiko,
	SAWANO Sumiko,	HATSUMI Ryoichi,	KANAZAWA Shuji,
	SOMENO Hidemasa,	FUKUDA Hisahe	
Secretary	KOBAYASHI Noriko,	TANAKA Akiko,	SAWANO Sumiko

#### AKENO Observatory

Associate Professor	SAGAWA Hiroyuki		
Technical Staff	TORII Reiko,	OHOKA Hideyuki,	KAWAGUCHI Masami
	SUDA Takayuki		

#### NORIKURA Observatory

Technical Staff	YAMAMOTO Kuniyuki,	AGEMATSU Yoshiaki,	USHIMARU Tsukasa,
	YOKOYAMA Chiaki,	SHIMODAIRA Hideaki,	YOSHIDA Takeji

## Astrophysics and Gravity Division

Professor	FUKUGITA Masataka,	KURODA Kazuaki,	KAWASAKI Masahiro
Associate Professor	OHASHI Masatake,	YASUDA Naoki,	HISANO Junji
Research Associate	MIYOKI Shinji,	UCHIYAMA Takahasi	
Technical Staff	ISHITSUKA Hideki		
Research Fellows	YAMAMOTO Kazuhiro,	HAYAKAWA Hideaki,	OKADA Atsushi,
	SENAMI Masato,	MATSUMOTO Shigeki,	TAKAHASHI Tomo
	HARADA Junpei,	KAKIZAKI Mitsuru,	

## Administration Division

### Project Division

Head NAKATSUKA Kazuo

### General Affairs Section

Head MATSUZAKI Hiroshi  
 Staff HAMANO Teruko, YAMAGUCHI Yoshiyuki, TASHIRO Megumi,  
 AKIYAMA Makiko

### Public Relations and Project Section

Head FUJIEDA Yuichi  
 Secretary KOKUBUN Yayoi, TAKAHASHI Junko, KITA Aiko

### Library Office

Staff SAITO Akiko

## Graduate Students

MASE Keiichi(D3),	TAKETA Akimichi(M1),	ADACHI, Yuki(M2),
OHISHI, Michiko(D3),	KABUKI, Shigeto(D3),	YUASA Midori(M1),
KIUCHI Ryuta(M2),	KAWASAKI Sho(M1),	
YUKAWA Ryohei(M1),	SAITO Takayuki(M1),	
MANAGO, Naohiro(D3),	JOBASHI Masashi(D3),	MASUDA, Masataka(D3),
AITA Yuichi(M2),	OKUMURA Akira(M2),	NODA Koji(M1),
MINAMINO Akihiro (D1),	HOSAKA Junya (M2),	TAKENAGA Yumiko(M2),
MITSUKA Gaku (M1),	NISHINO Haruki (M1),	
KONDO, Kazuhiro(D3),	KASAHARA Kunihiro(D2),	OKUTOMI Akira(D2),
TOKUNARI Masao(D1),	AKUTSU, Tomomi (M2),	KAMAGASAKO Shogo(M1),
KAMAGASAKO Shogo(M1),	OGURO Kei (M2),	SAITO Osamu(M2),
TAKAHASHI Huminobu(D3),	ICHIKAWA Kazuhide(D3),	NAGAI Minoru(M2),
KONYA Kenichiro(M2),	TAKAHASHI Hiroyuki(M1),	TAKAYAMA Tsutomu(M1),
KANZAKI Toru(M1),	NISHIHARA Tatsuo(M1).	